

Electronic Supplementary Information

Synthesis and investigation of donor-porphyrin-acceptor triads with long-lived photo-induced charge-separate states

Julien B. Kelber, Naitik A. Panjwani, Di Wu, Rafael Gómez-Bombarelli, Brendon W. Lovett, John J. L. Morton and Harry L. Anderson

TABLE OF CONTENTS

	<u>page</u>
1) General information	S2
2) Characterization of reaction intermediates and new compounds	S3
(a) 2-(4-Nitrophenyl)isoindoline-1,3-dione-5-benzoic acid (1)	S3
(b) (2-(4-Nitrophenyl)isoindolin-5-yl)methanol (2)	S5
(c) (2-(4-Nitrophenyl)isoindoline-5-carbaldheyde (3)	S7
(d) 5-Bromo-2-(4-(diethylamino)phenyl)isoindoline-1,3-dione (6)	S9
(e) 5-Bromo-2-(4-(diethylamino)phenyl)-4H-isoindoline (7)	S11
(f) 5-(4,4,5,5-Tetramethyl-1,3,2-dioxaborolan-2-yl)-2-(4-(diethylamino)phenyl)-4H-isoindoline (8)	S13
(g) 2-Bromoanthraquinone	S15
(h) 2-Bromoanthracene (mixture with anthracene) (9)	S15
(i) 2-Bromo-5,12-[1,2]benzenotetracene-6,11(5H,12H)-dione	S16
(j) 2-(4,4,5,5-Tetramethyl-1,3,2-dioxaborolan-2-yl)-5,12-[1,2]benzenotetracene-6,11(5H,12H)-dione (10)	S17
(k) Bromoporphyrin 12	S19
(l) TNQ-ZnP _{Ar} -TAPD	S22
(m) Porphyrin aldehyde 14	S30
(n) Porphyrin aldehyde 15	S31
(o) C ₆₀ -ZnP _{Ar} -TAPD	S33
3) Synthesis of reference and known compounds	S37
(a) Porphyrin boronic acids 13 and S1	S37
(b) 2-((3,4-Bis(dodecyloxy)benzyl)amino)acetic acid (S3)	S39
(c) Porphyrins S4 and S5	S41
4) Assignment of the TAPD-ZnP _{Ar} -TNQ triad ¹ H NMR spectrum using reference compounds	S43
5) Frontier orbitals energies of triads	S44
6) Frontier orbitals distribution of triads	S45
7) Ionization potential and electron affinities of moieties	S47
8) Inner-sphere reorganization energies	S48
9) Predicted recombination rates	S49
10) Analysis of the influence of conformational factors on electronic coupling	S50
11) Cambridge database analysis of the dihedral angles between meso-phenyls and porphyrin planes	S52
12) Methods and kinetic modeling of the Electronic Paramagnetic Resonance (EPR) experiments	S53
13) References	S56

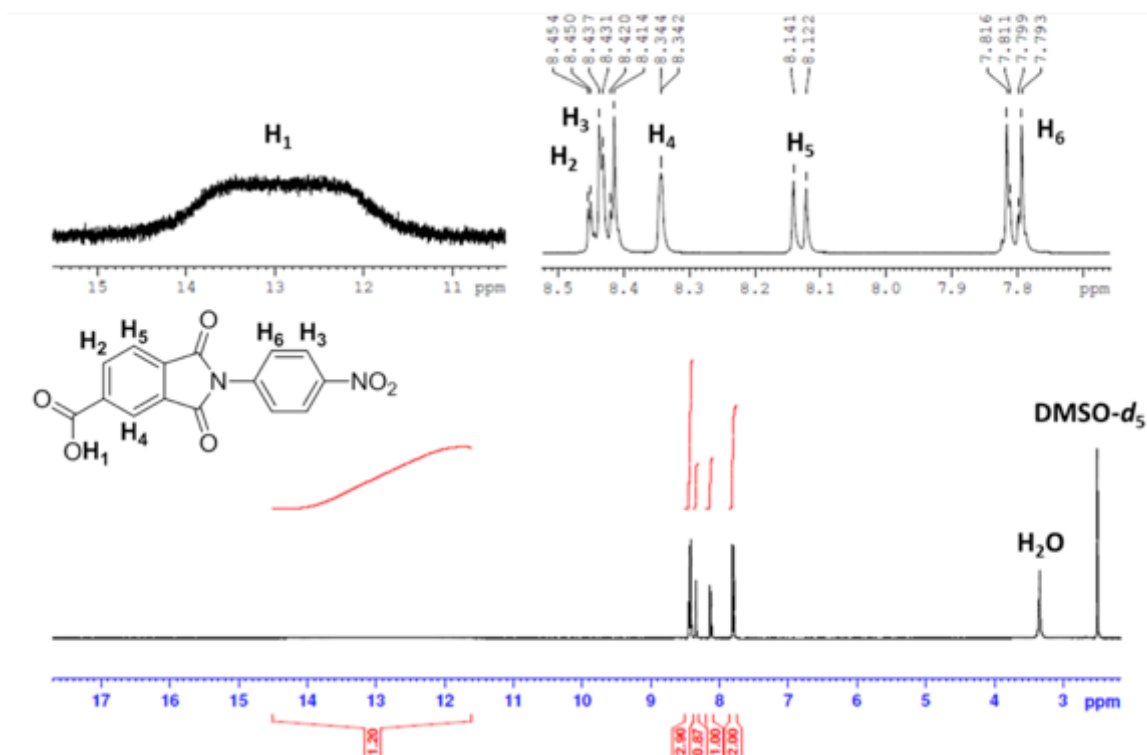
1) General information

All chemical reagents were used as received. 2-Bromoanthracene (ref S1) and [5,15-bis-(3,5-bis-*tert*-butylphenyl)-10,20-bisbromoporphinato]zinc(II) (ref S2) were synthesized following a literature procedure. Dichloromethane (DCM) and tetrahydrofuran (THF) were dried over activated alumina prior to use. Anhydrous *N,N*-dimethylformamide (DMF), acetic acid, nitrobenzene, pyridine, toluene, xylenes and anhydrous 2-methyltetrahydrofuran (MTHF) were supplied by Aldrich and used without further purification. Purge gas was high purity argon. Chromatography was performed on silica (200–400 mesh). All reported ^1H NMR spectra were collected using a 400 MHz (Bruker AVII 400) or a 500 MHz (Bruker AVII 500) spectrometer. Chemical shifts (in the ppm scale) were determined versus TMS using the residual solvent peak as the internal reference (CHCl_3 , $\delta = 7.26$ ppm). Deuterated chloroform was stored over potassium carbonate to avoid any acid trace. The UV/Vis absorption spectra were recorded in MTHF using a Perkin Elmer Lambda 20 UV-Vis Spectrometer. The absorption wavelengths are reported in nm with the extinction coefficient in $\text{M}^{-1} \text{cm}^{-1}$. Infra-red spectra were recorded in the solid state (neat) using a Bruker Tensor27 FT-IR spectrometer. Mass spectroscopy was performed either on ESI-TOF (Waters LCT Premier) or on MALDI-TOF (Waters MALDI Micro MX) spectrometer. Preparative scale size exclusion chromatography (SEC) was carried out using BioRad Bio-Beads S-X1 with toluene as eluent. ESR samples were prepared in 3.8 mm quartz tubes, sealed under vacuum and kept at 77 K in the dark.

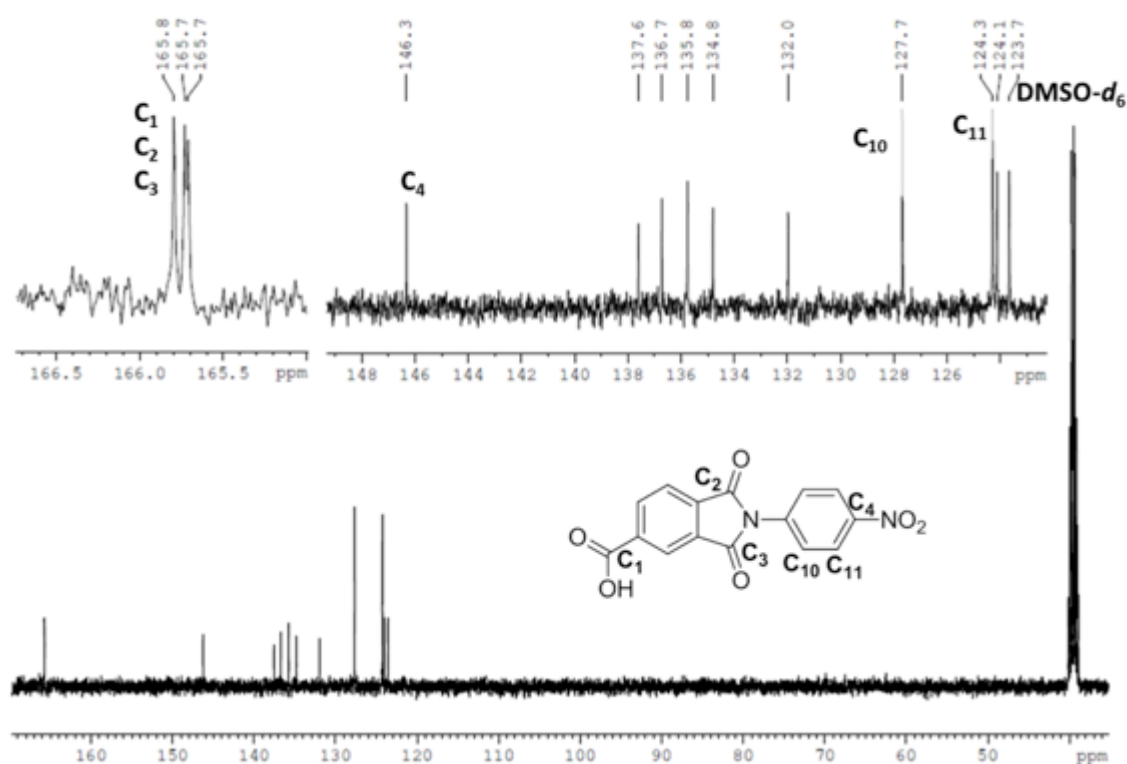
2) Characterization of new compounds

a. 2-(4-Nitrophenyl)isoindoline-1,3-dione-5-benzoic acid (**1**)

¹H NMR ; 400MHz ; DMSO-*d*₅+ H₂O



¹³C NMR ; 100MHz ; DMSO-*d*₆+ H₂O



Mass Spectrum SmartFormula Report

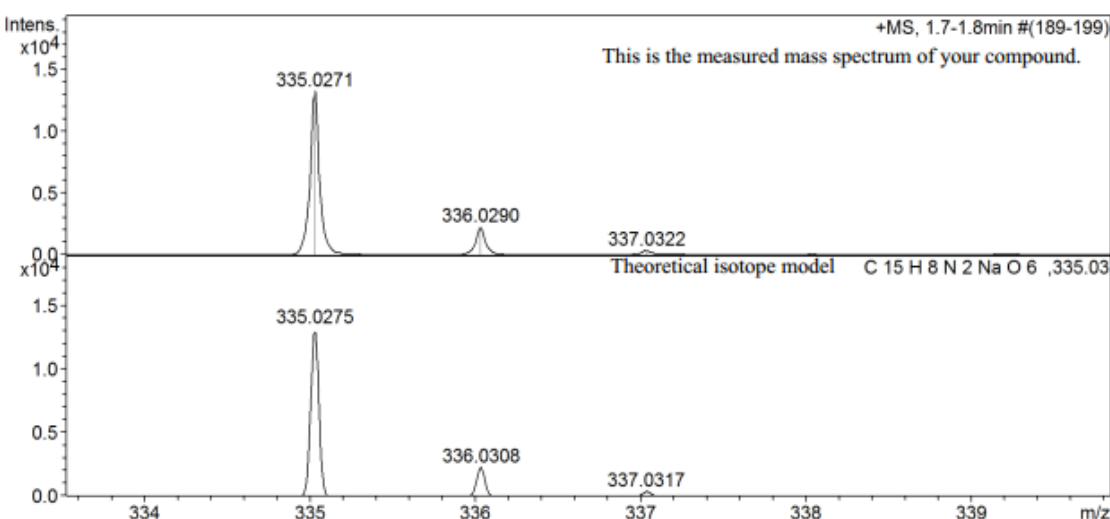
Analysis Info

Analysis Name \\Utof\\data\\Mar 14\\ESI45309_4_01_17597.d
Method 2.5min_cal_sample_pos_naf_05-08-13.m
Sample Name ESI45309
Comment

Acquisition Date 17/03/2014 08:09:07
Operator Mass Spec
Instrument / Ser# micrOTOF 92

Acquisition Parameter

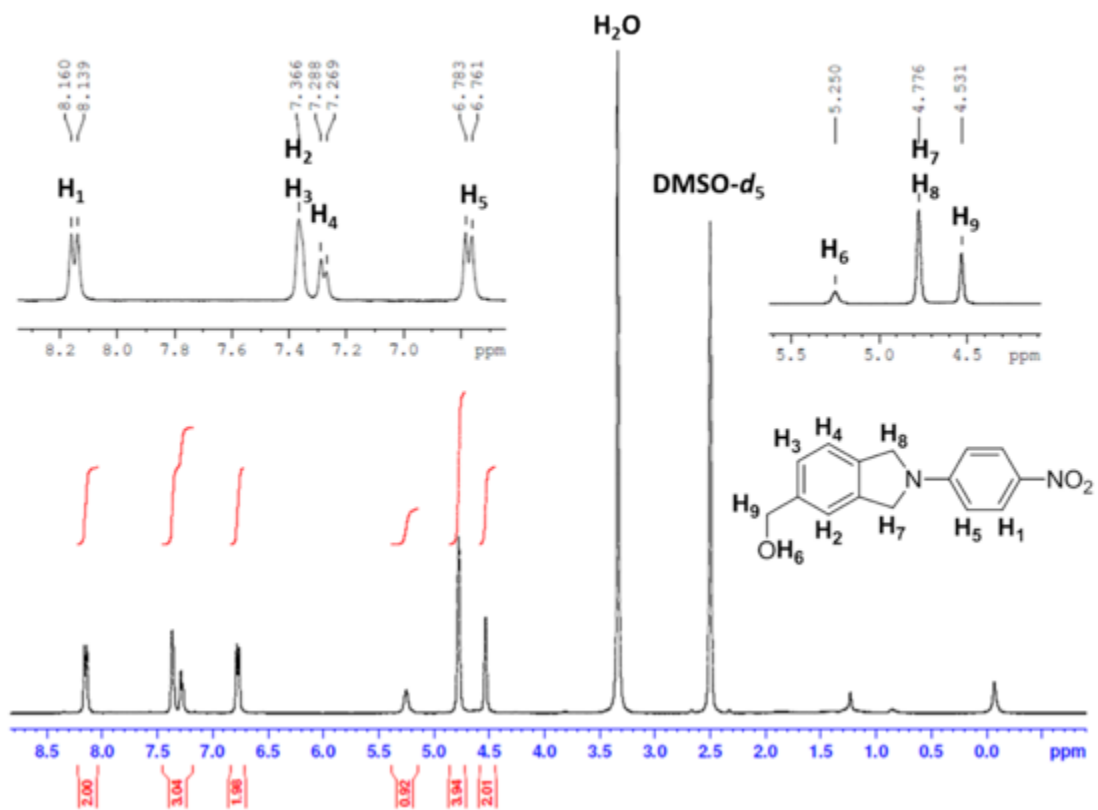
Source Type	ESI	Ion Polarity	Positive	Set Nebulizer	2.0 Bar
Focus	Not active			Set Dry Heater	180 °C
Scan Begin	100 m/z	Set Capillary	4500 V	Set Dry Gas	10.0 l/min
Scan End	1000 m/z	Set End Plate Offset	-500 V	Set Divert Valve	Source



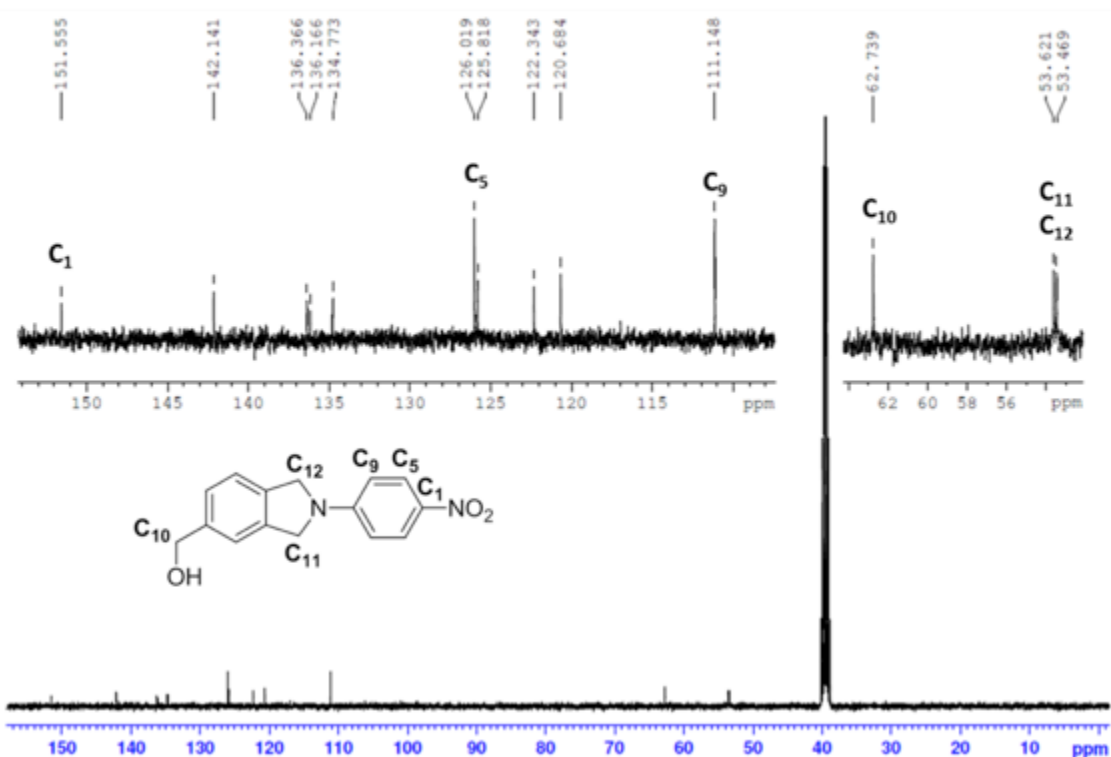
Meas. m/z	#	Formula	m/z	err [ppm]	Mean err [ppm]	rdb	e ⁻ Conf	mSigma
335.0271	1	C 15 H 8 N 2 Na O 6	335.0275	1.1	1.1	1.6	12.5 even	1.43

b. (2-(4-Nitrophenyl)isoindolin-5-yl)methanol (**2**)

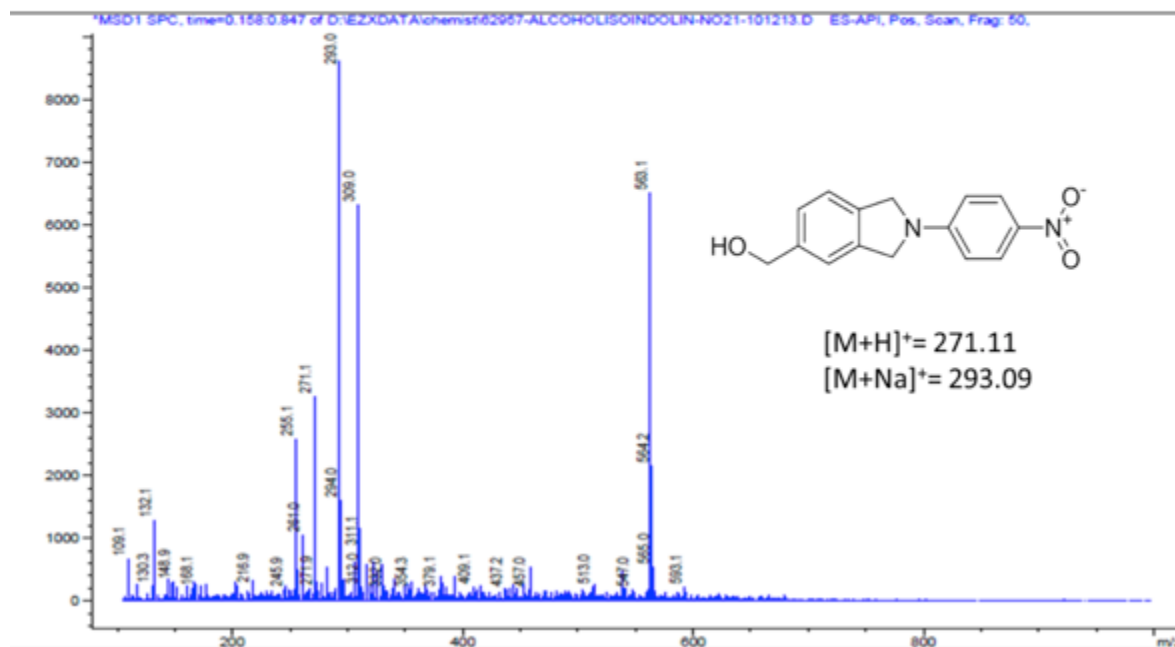
¹H NMR ; 400MHz ; DMSO-*d*₆+ H₂O



¹³C NMR ; 100MHz ; DMSO-*d*₆+ H₂O



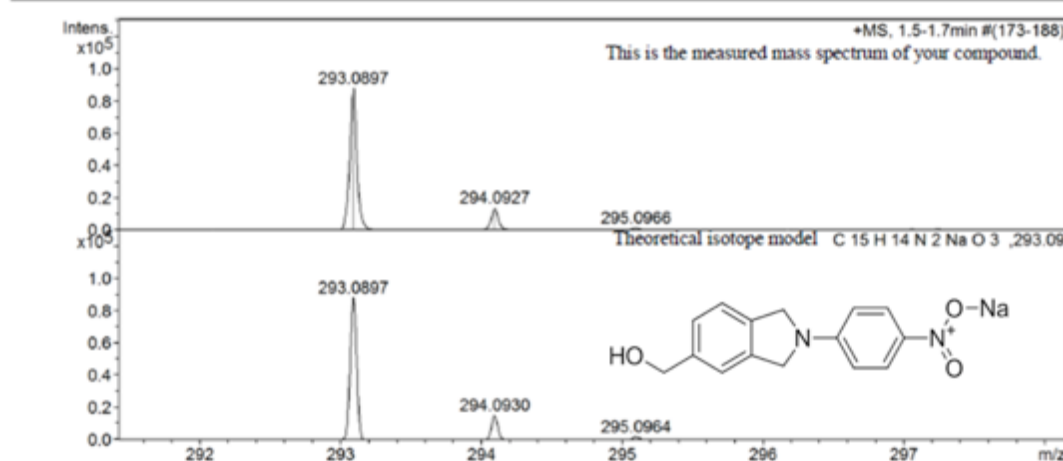
Data File: D:\EZXDATA\CHEMIST\62957-ALCOHOLISOINDOLIN-NO21-101213.D
User Name: Julien kelber
Sample Name: alcoholisoindolin-NO2
Location: P4-C-08
Sample Info: Easy-Access Method: '1_POS1000'
Method Info: Positive open access method
105-1000



ESI⁺ HRMS

Analysis Info		Acquisition Date 11/12/2013 09:05:07	
Analysis Name	\Utof\data\Dec 13\ESI43875_12_01_14935.d	Operator	Mass Spec
Method	2.5min_cal_sample_pos_naf_05-08-13.m	Instrument / Ser#	micrOTOF 92
Sample Name	ESI43875		
Comment			

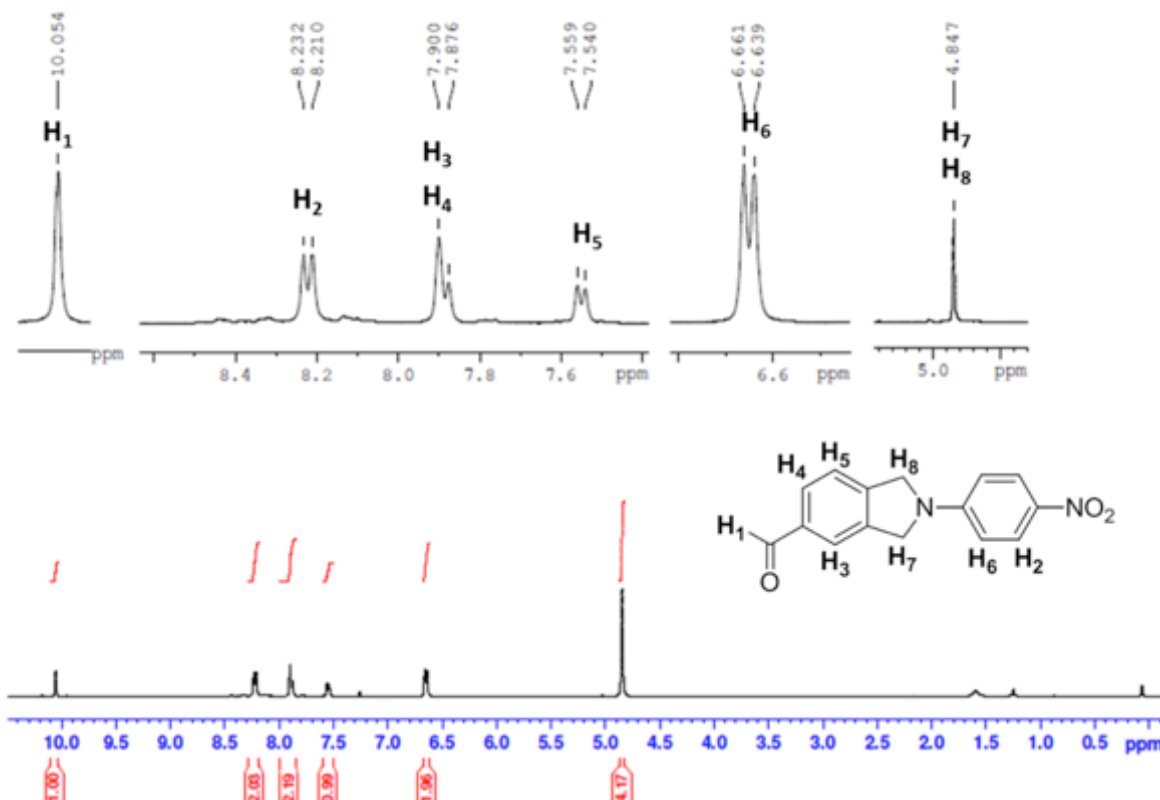
Acquisition Parameter					
Source Type	ESI	Ion Polarity	Positive	Set Nebulizer	2.0 Bar
Focus	Not active			Set Dry Heater	180 °C
Scan Begin	100 m/z	Set Capillary	4500 V	Set Dry Gas	10.0 l/min
Scan End	1000 m/z	Set End Plate Offset	-500 V	Set Divert Valve	Source



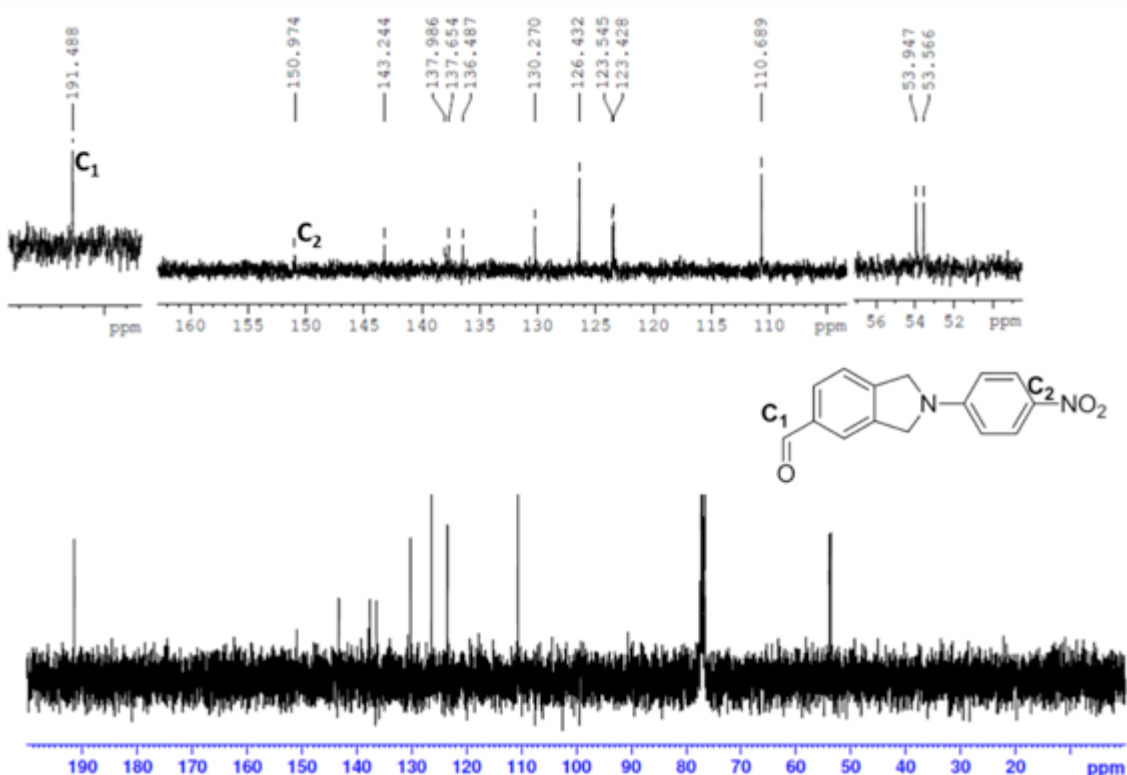
Meas. m/z	#	Formula	m/z	err [ppm]	Mean err [ppm]	rdb	e ⁻ Conf	mSigma
293.0897	1	C 15 H 14 N 2 Na O 3	293.0897	-0.1		0.1	9.5 even	6.97

c. (2-(4-Nitrophenyl)isoindoline-5-carbaldheyde (**3**)

¹H NMR ; 400MHz ; CDCl₃+ K₂CO₃



¹³C NMR ; 100MHz ; CDCl₃+ K₂CO₃



Mass Spectrum SmartFormula Report

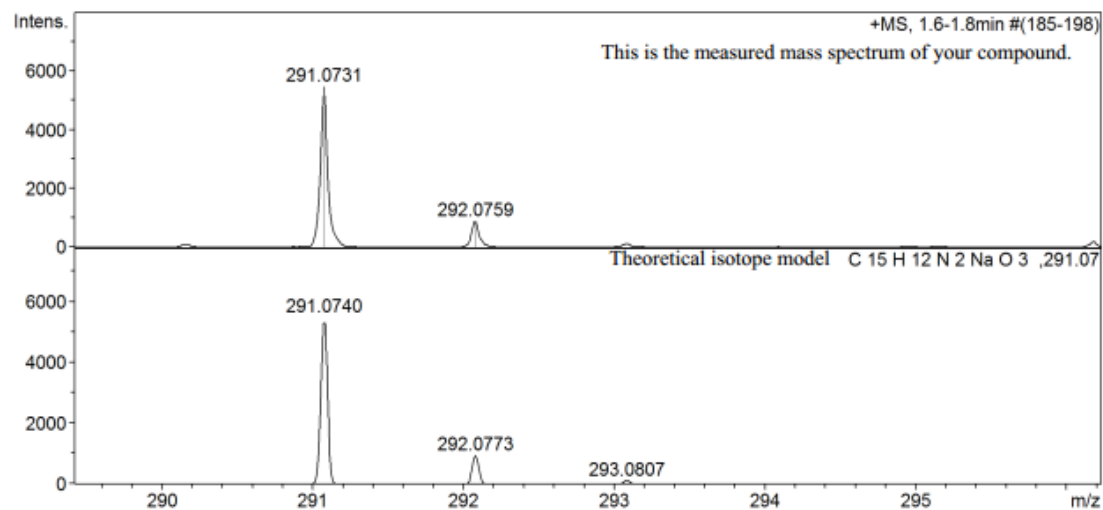
Analysis Info

Analysis Name \\Utof\\data\\Mar 14\\ESI45310_5_01_17598.d
Method 2.5min_cal_sample_pos_naf_05-08-13.m
Sample Name ESI45310
Comment

Acquisition Date 17/03/2014 08:12:59
Operator Mass Spec
Instrument / Ser# micrOTOF 92

Acquisition Parameter

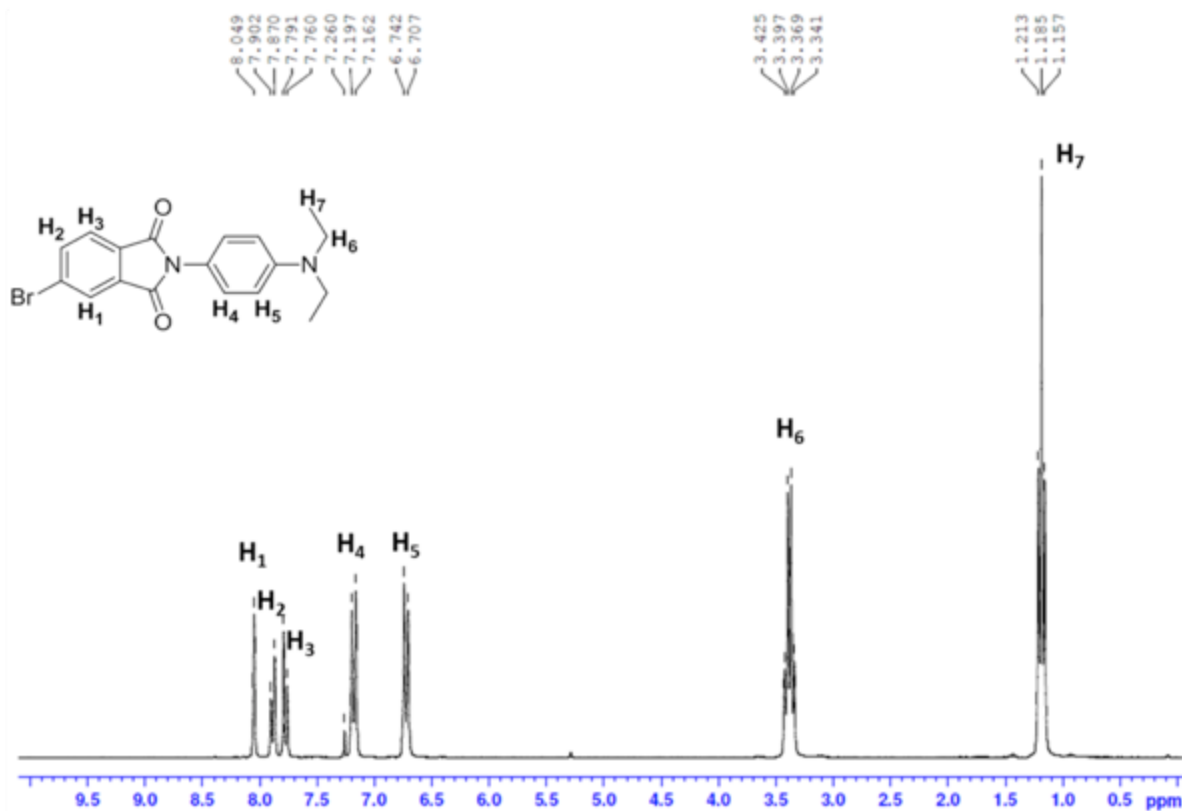
Source Type	ESI	Ion Polarity	Positive	Set Nebulizer	2.0 Bar
Focus	Not active			Set Dry Heater	180 °C
Scan Begin	100 m/z	Set Capillary	4500 V	Set Dry Gas	10.0 l/min
Scan End	1000 m/z	Set End Plate Offset	-500 V	Set Divert Valve	Source



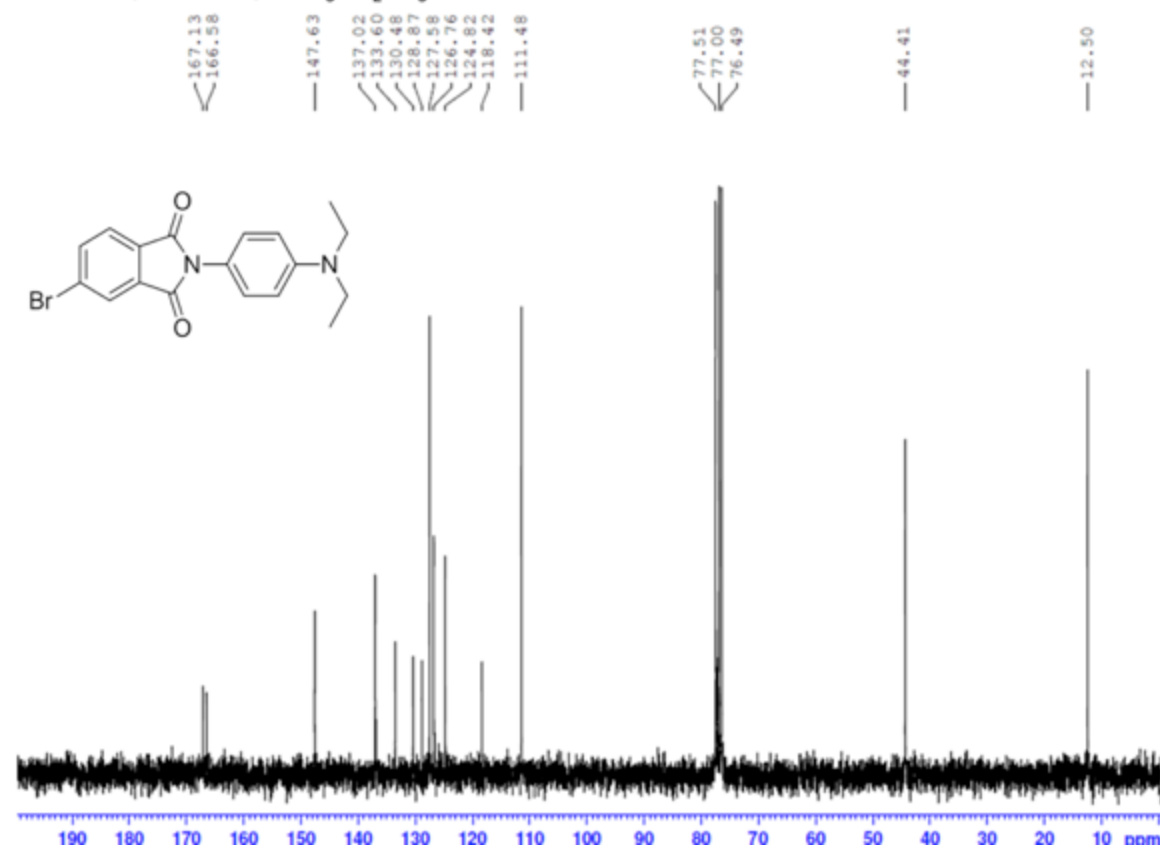
Meas. m/z	#	Formula	m/z	err [ppm]	Mean err [ppm]	rdb	e ⁻ Conf	mSigma
291.0731	1	C 15 H 12 N 2 Na O 3	291.0740	3.2	3.2	3.5	10.5 even	12.72

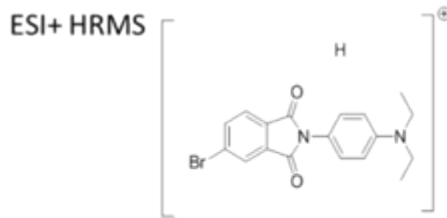
d. 5-Bromo-2-(4-(diethylamino)phenyl)isoindoline-1,3-dione (6)

¹H NMR ; 400MHz ; CDCl₃+ K₂CO₃

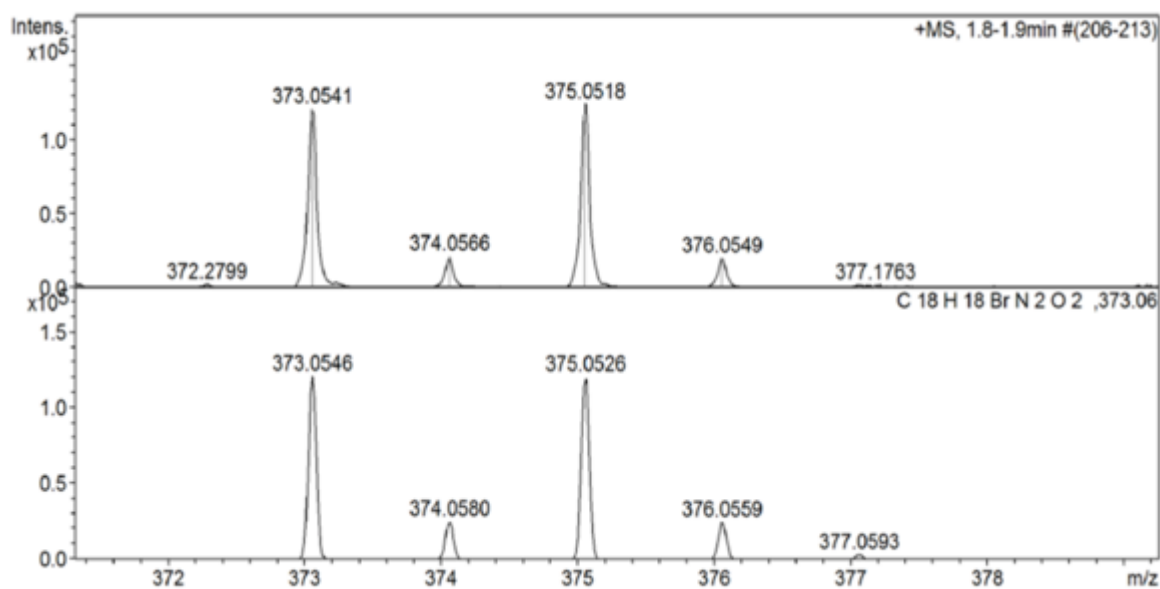


¹³C NMR ; 100MHz ; CDCl₃+ K₂CO₃

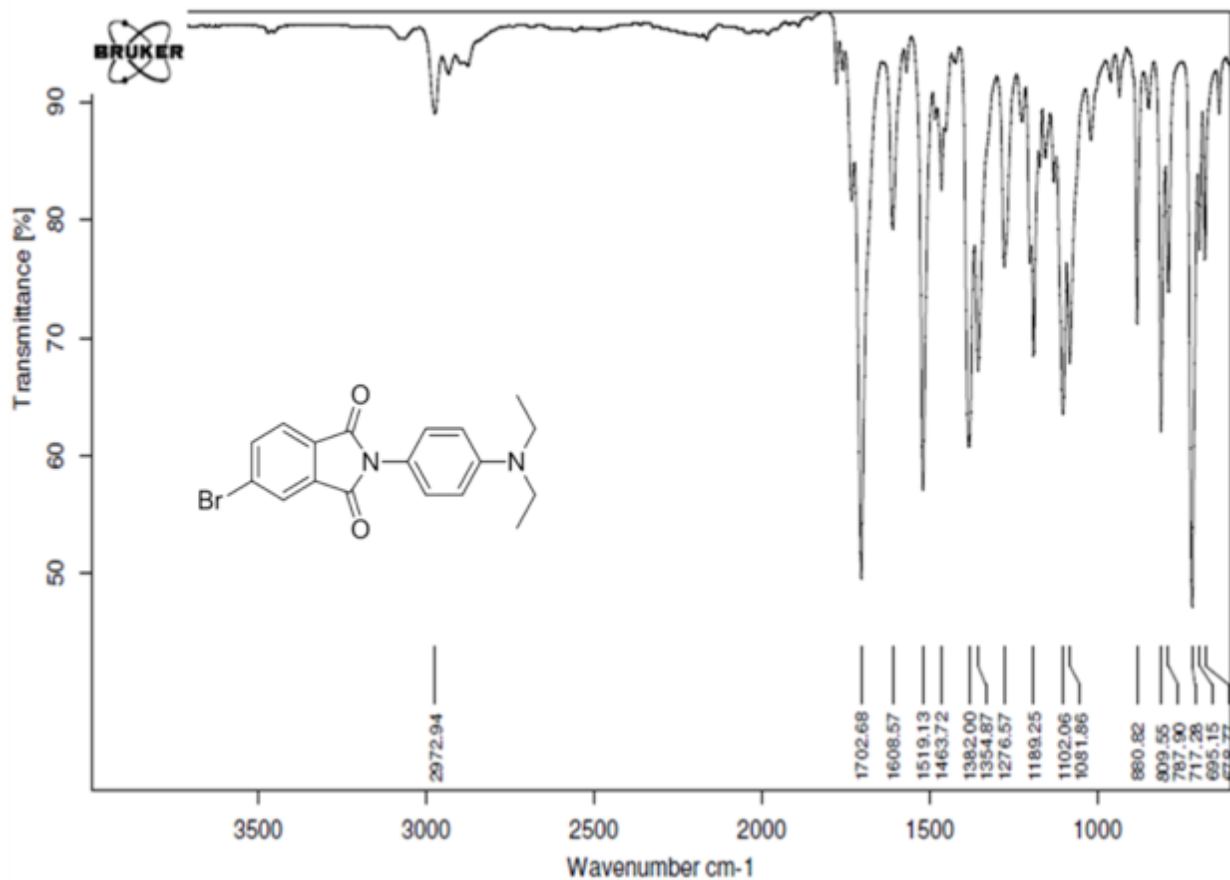




Mass Spectrum SmartFormula Report

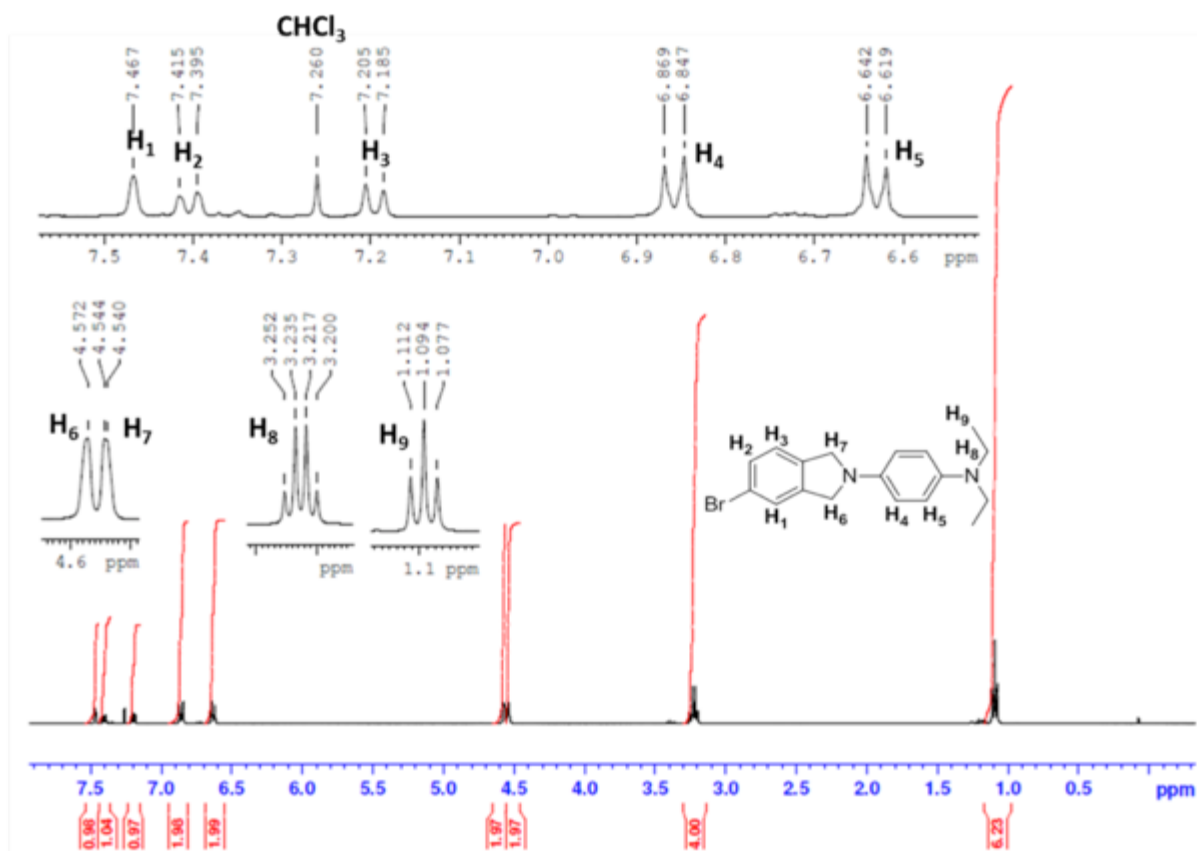


Infra-red vibrational spectroscopy

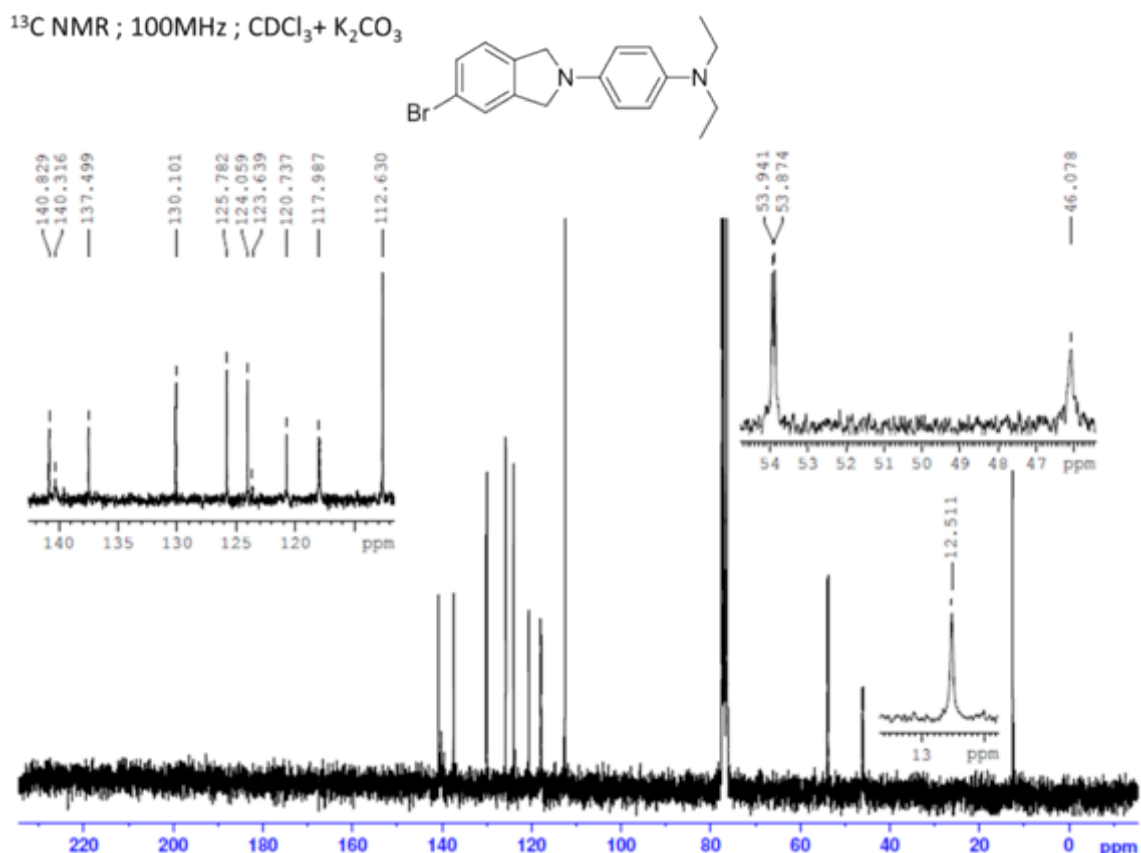


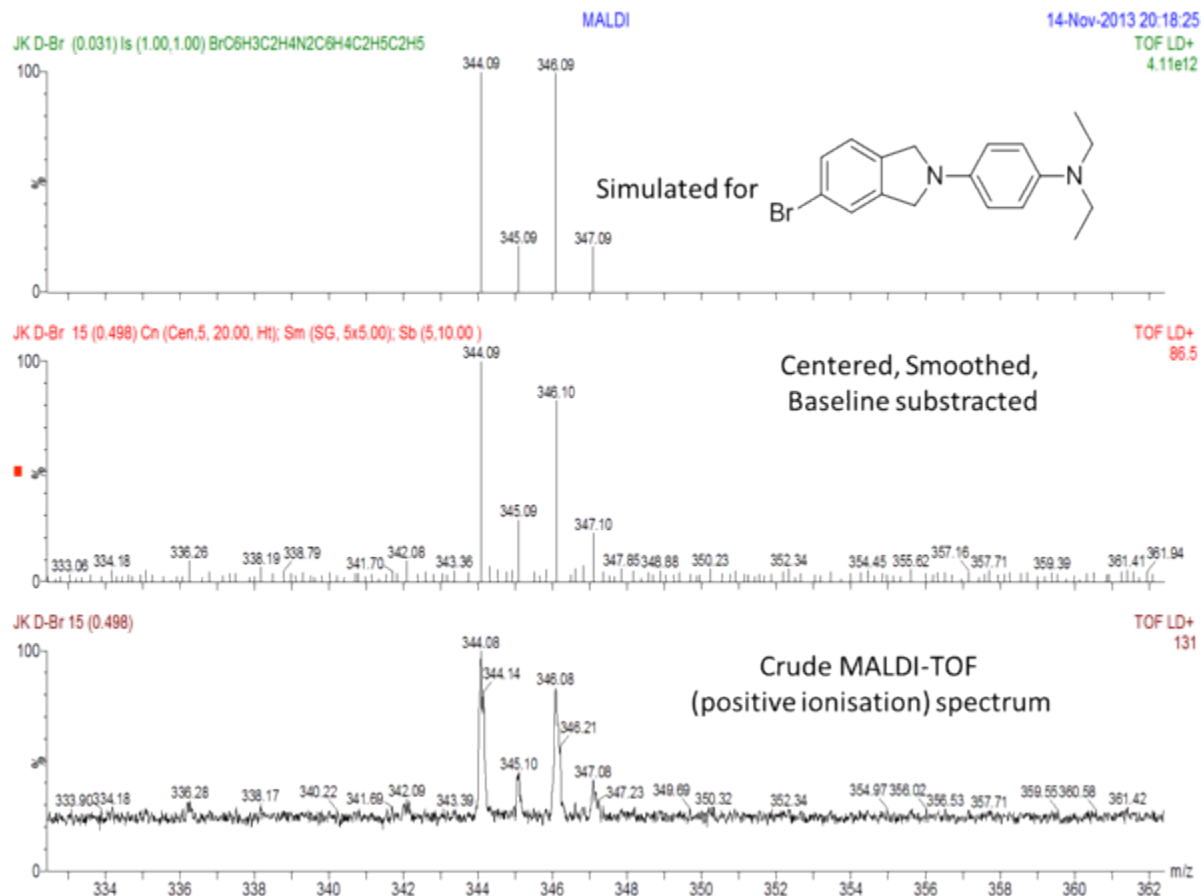
e. 5-Bromo-2-(4-(diethylamino)phenyl)-4H-isoindoline (7)

¹H NMR ; 400MHz ; CDCl₃+ K₂CO₃

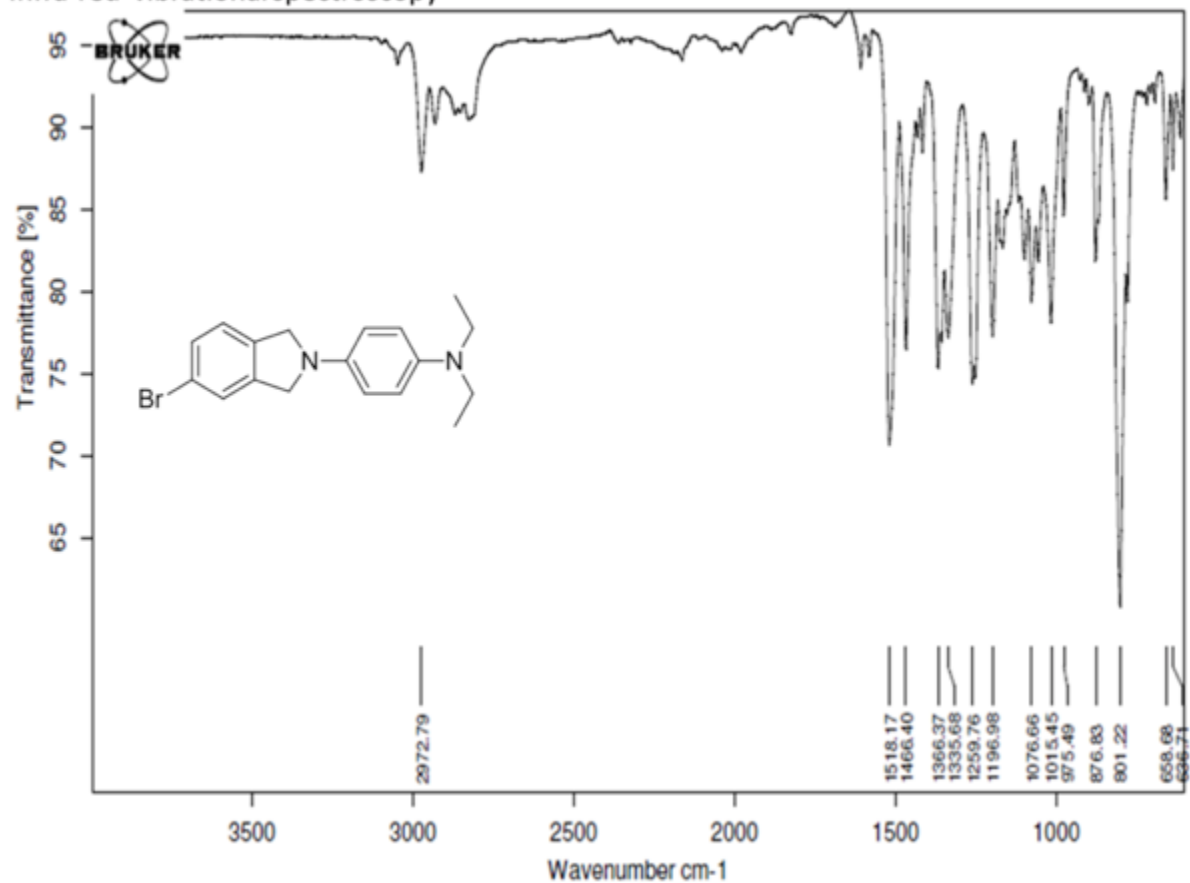


¹³C NMR ; 100MHz ; CDCl₃+ K₂CO₃



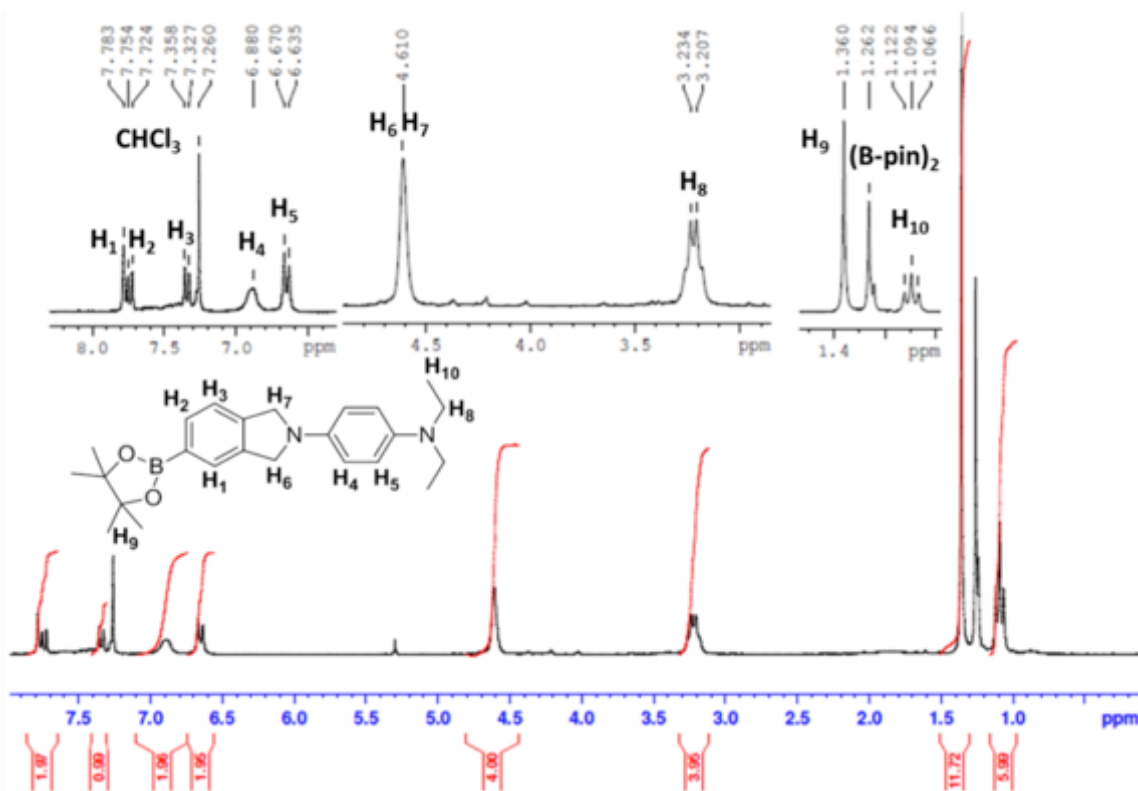


Infra-red vibrational spectroscopy

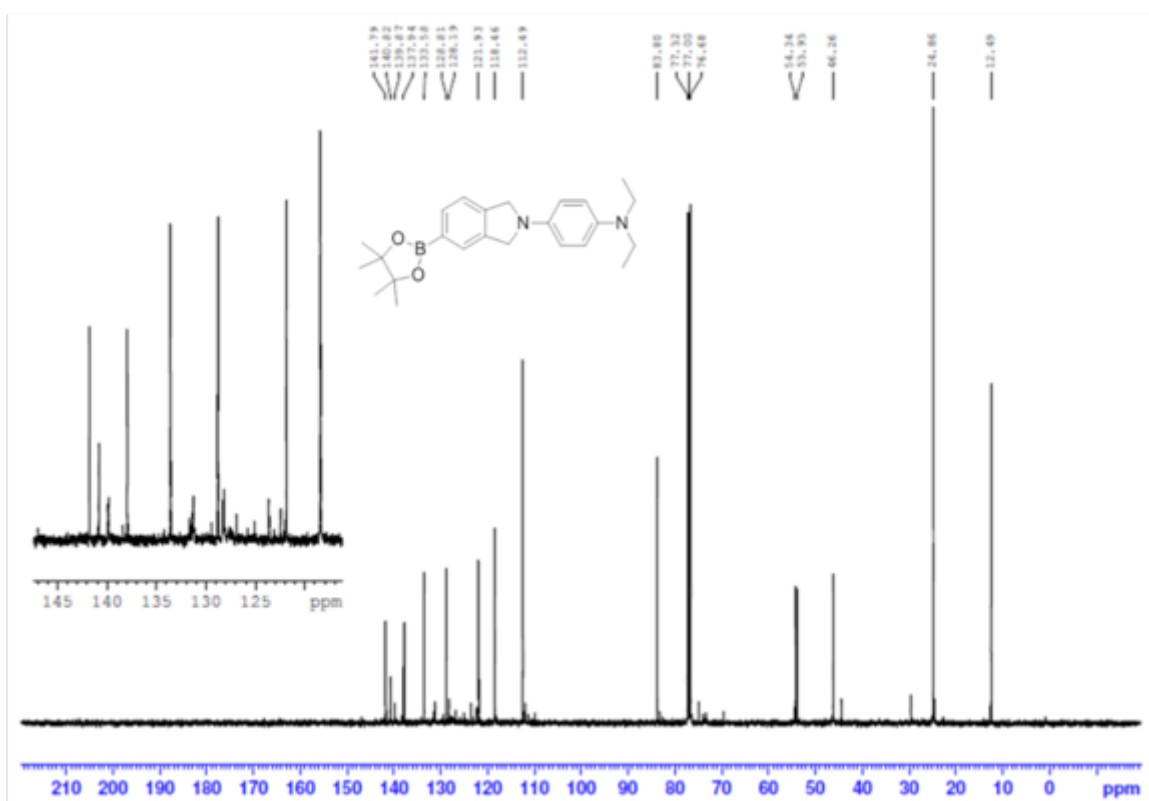


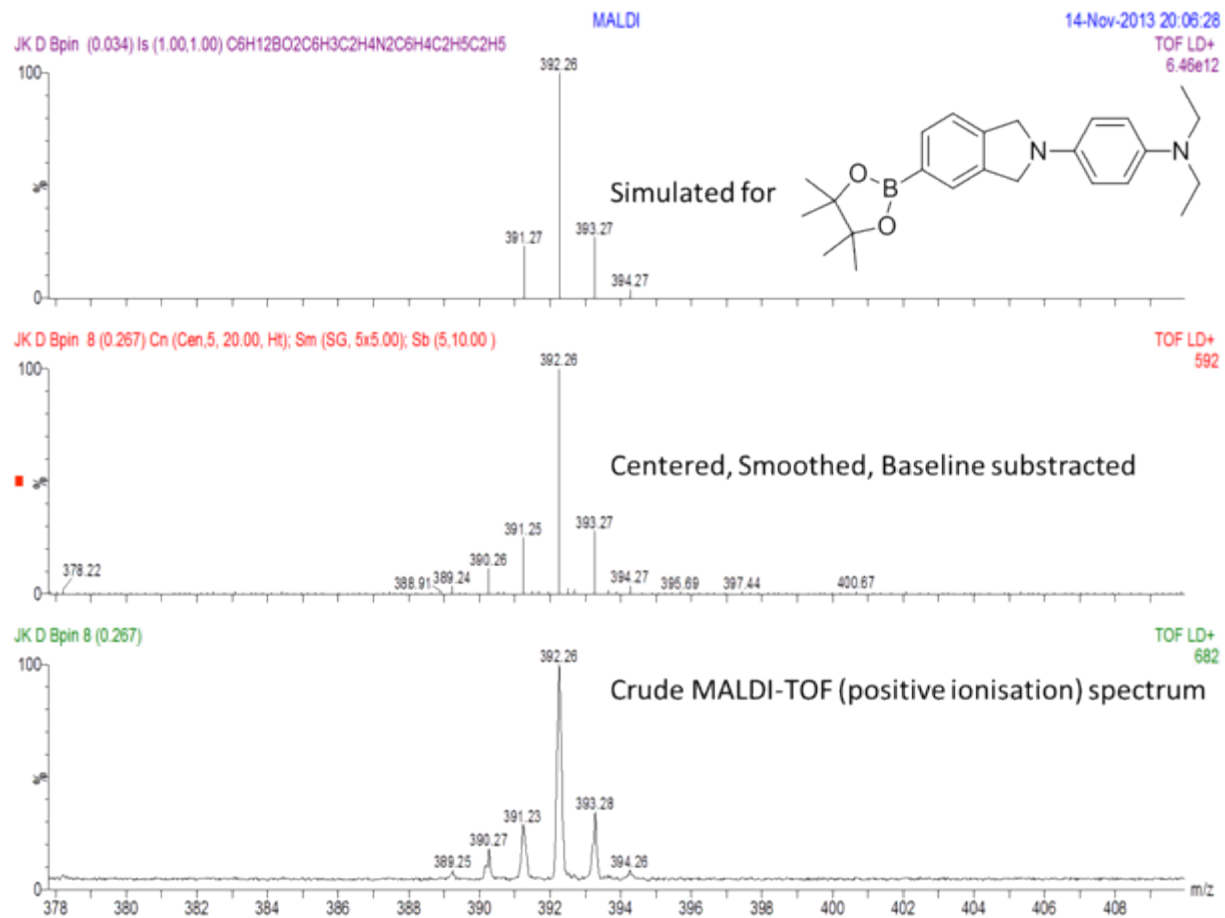
f. 5-(4,4,5,5-Tetramethyl-1,3,2-dioxaborolan)-2-(4-(diethylamino)phenyl)-4H-isoindoline (8)

^1H NMR ; 400MHz ; $\text{CDCl}_3 + \text{K}_2\text{CO}_3$

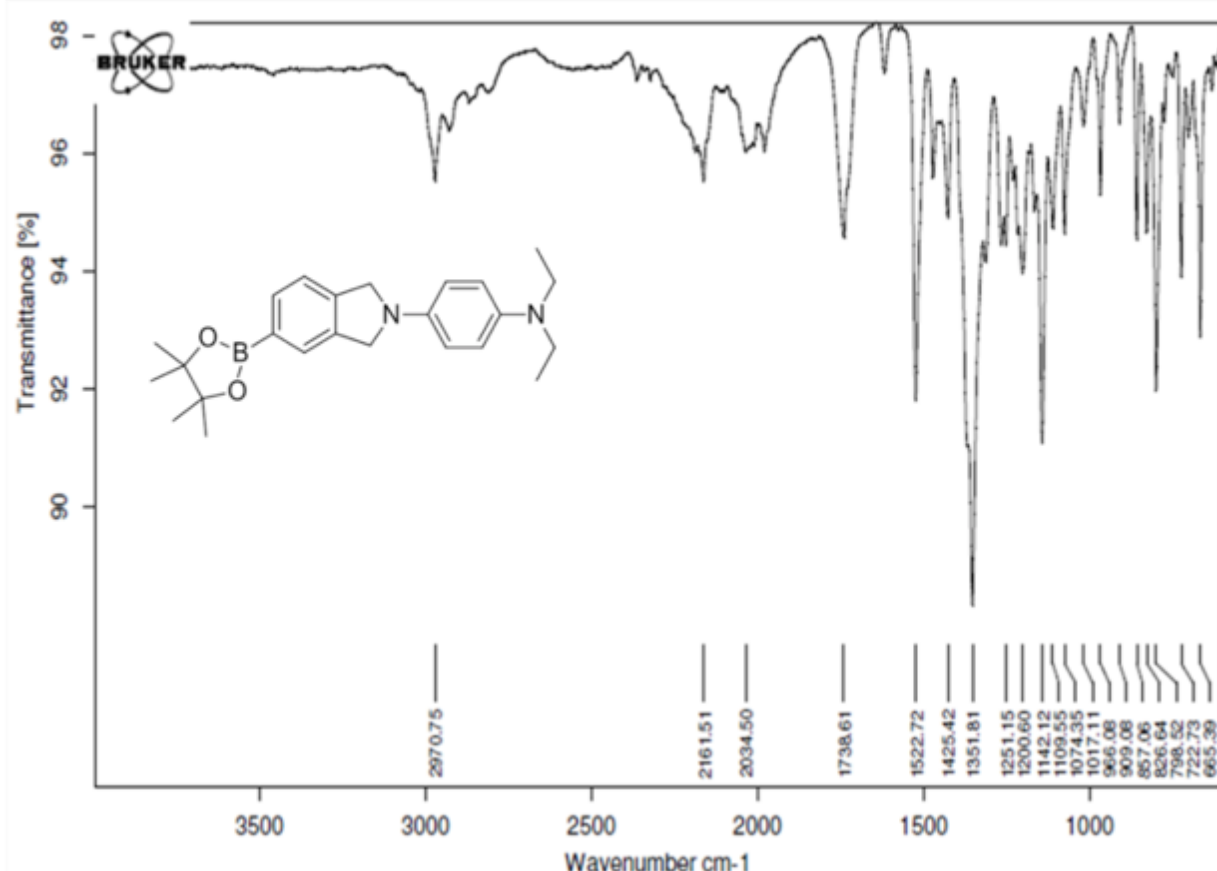


^{13}C NMR ; 100MHz ; $\text{CDCl}_3 + \text{K}_2\text{CO}_3$



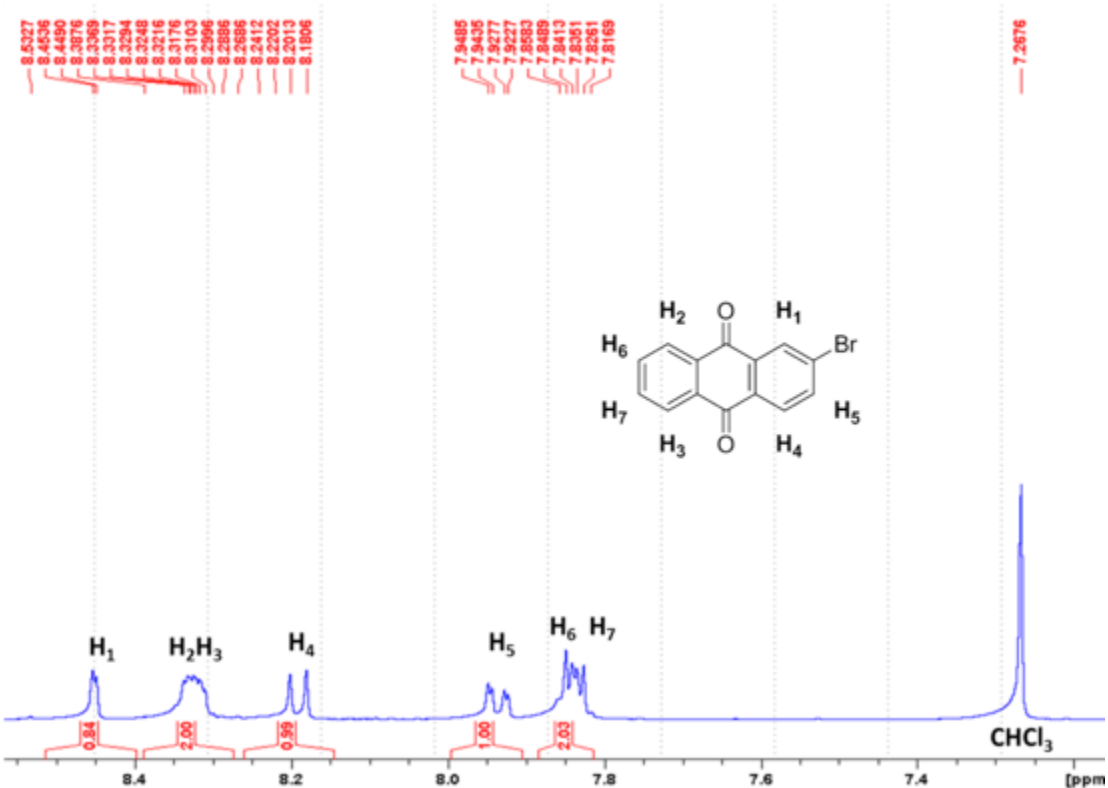


Infra-red vibrational spectroscopy



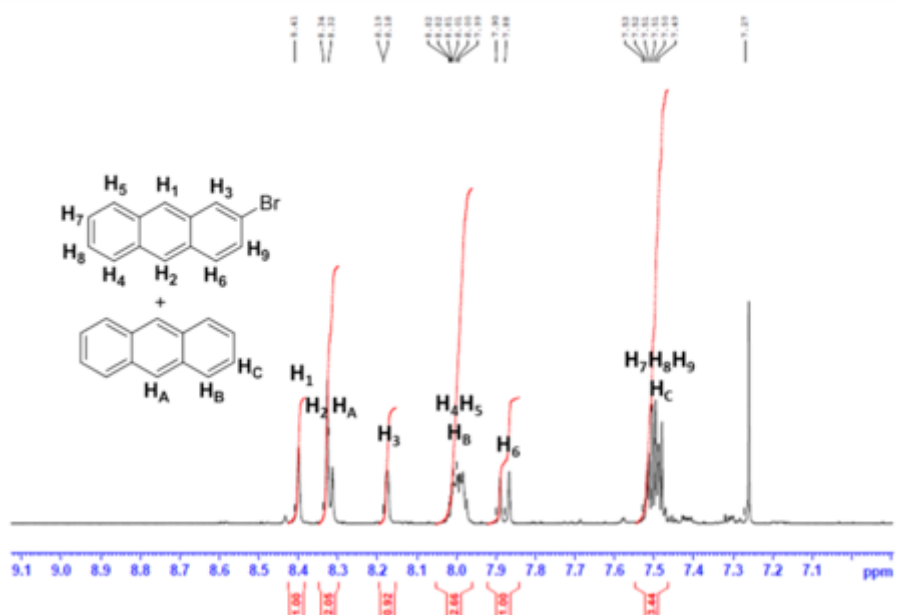
g. 2-Bromoanthraquinone

^1H NMR ; 400MHz ; $\text{CDCl}_3 + \text{K}_2\text{CO}_3$



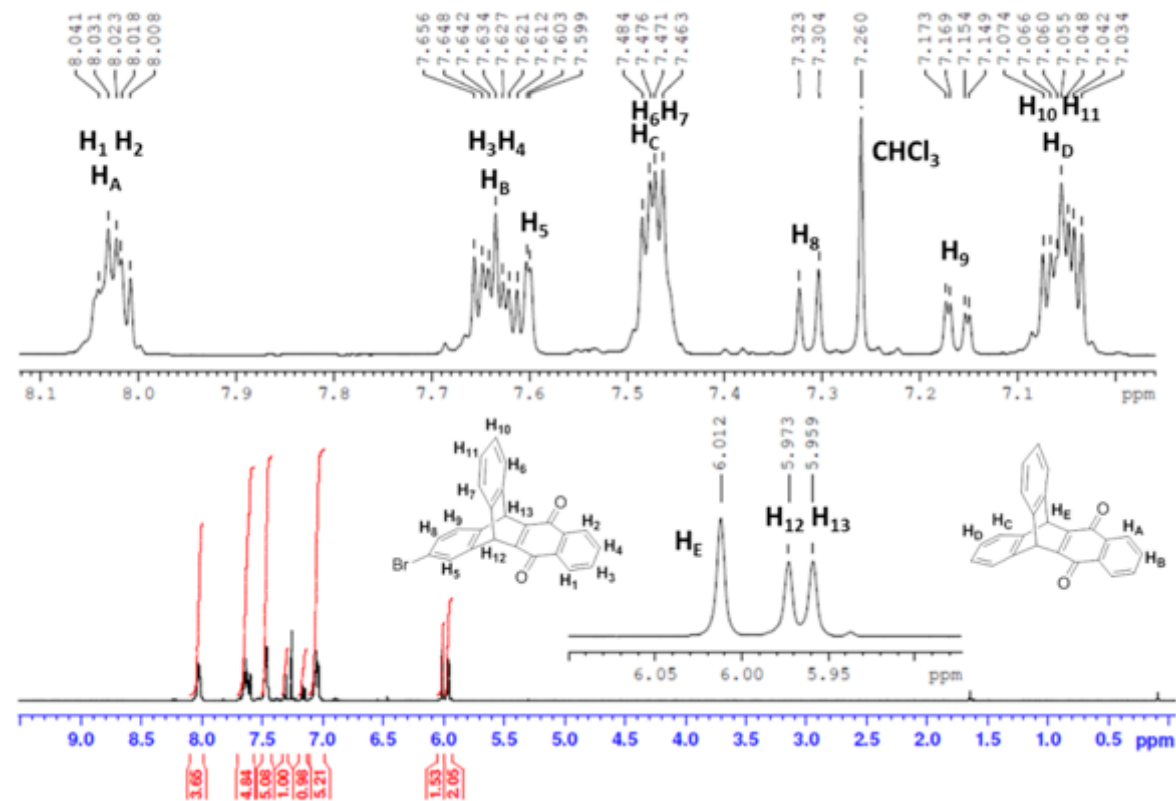
h. 2-Bromoanthracene (9) (mixture with anthracene)^{S1}

^1H NMR ; 400MHz ; $\text{CDCl}_3 + \text{K}_2\text{CO}_3$

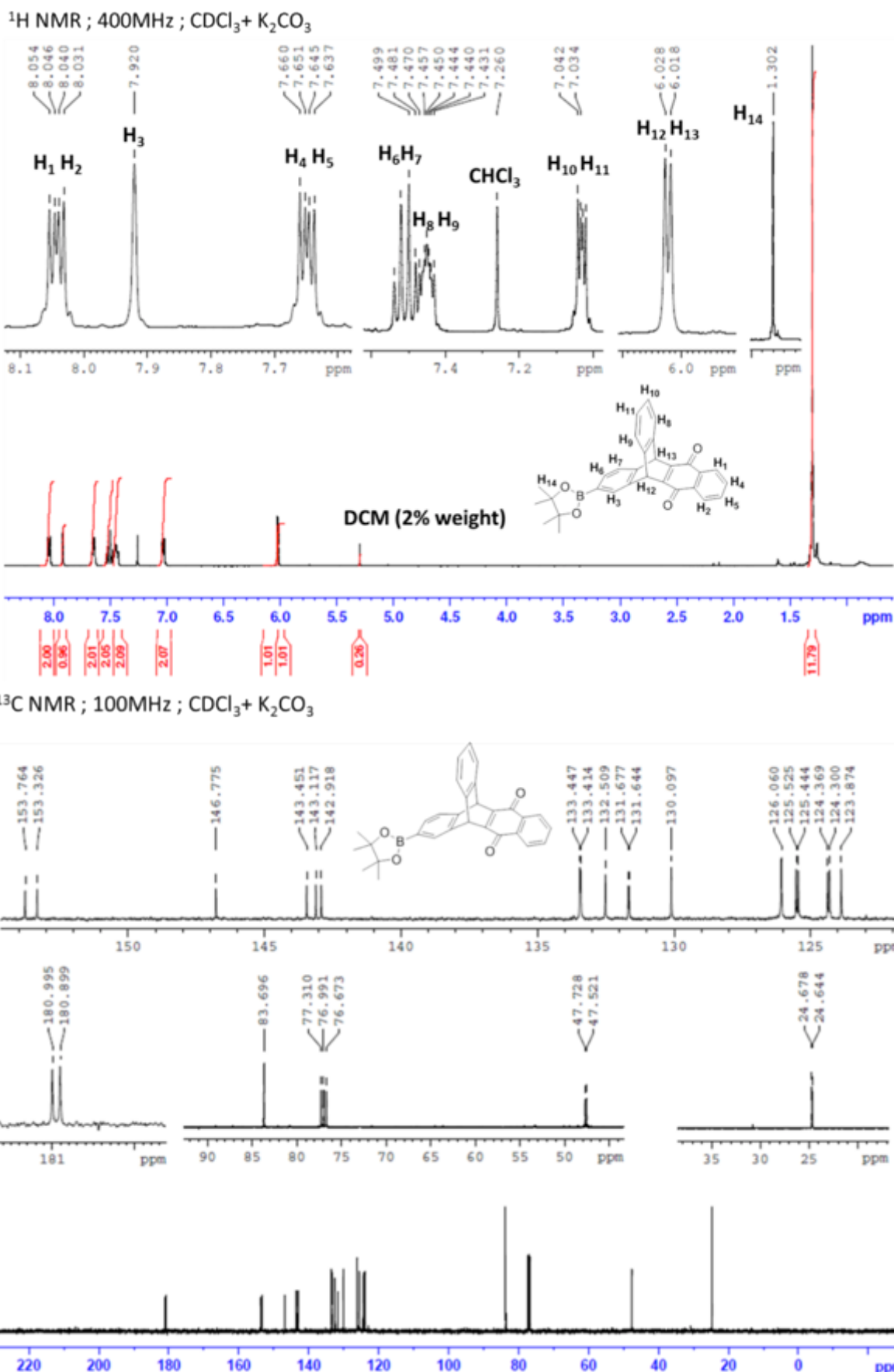


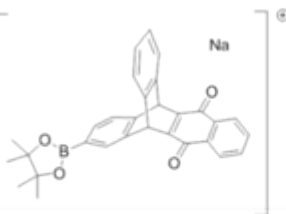
i. 2-Bromo-5,12-[1,2]benzenotetracene-6,11(5H,12H)-dione
 (mixture with 5,12-[1,2]benzenotetracene-6,11(5H,12H)-dione)

¹H NMR ; 400MHz ; CDCl₃+ K₂CO₃



j. 2-(4,4,5,5-Tetramethyl-1,3,2-dioxaborolan-2-yl)-5,12-[1,2]benzenotetracene-6,11(5H,12H)-dione (10)



ESI⁺ HRMS

Mass Spectrum SmartFormula Report

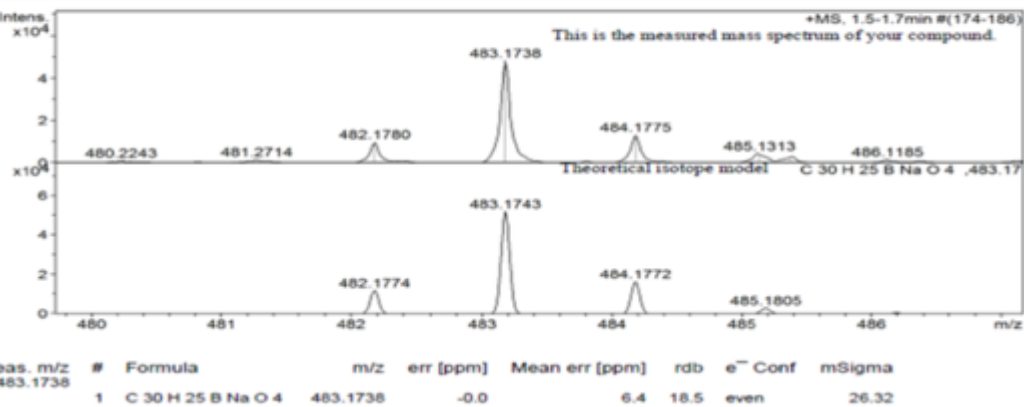
Analysis Info

Analysis Name \\Utof\\data\\Nov 13\\ESI43670_20_01_14587.d
 Method 2.5min_cal_sample_pos_naf_05-08-13.m
 Sample Name ESI43670
 Comment

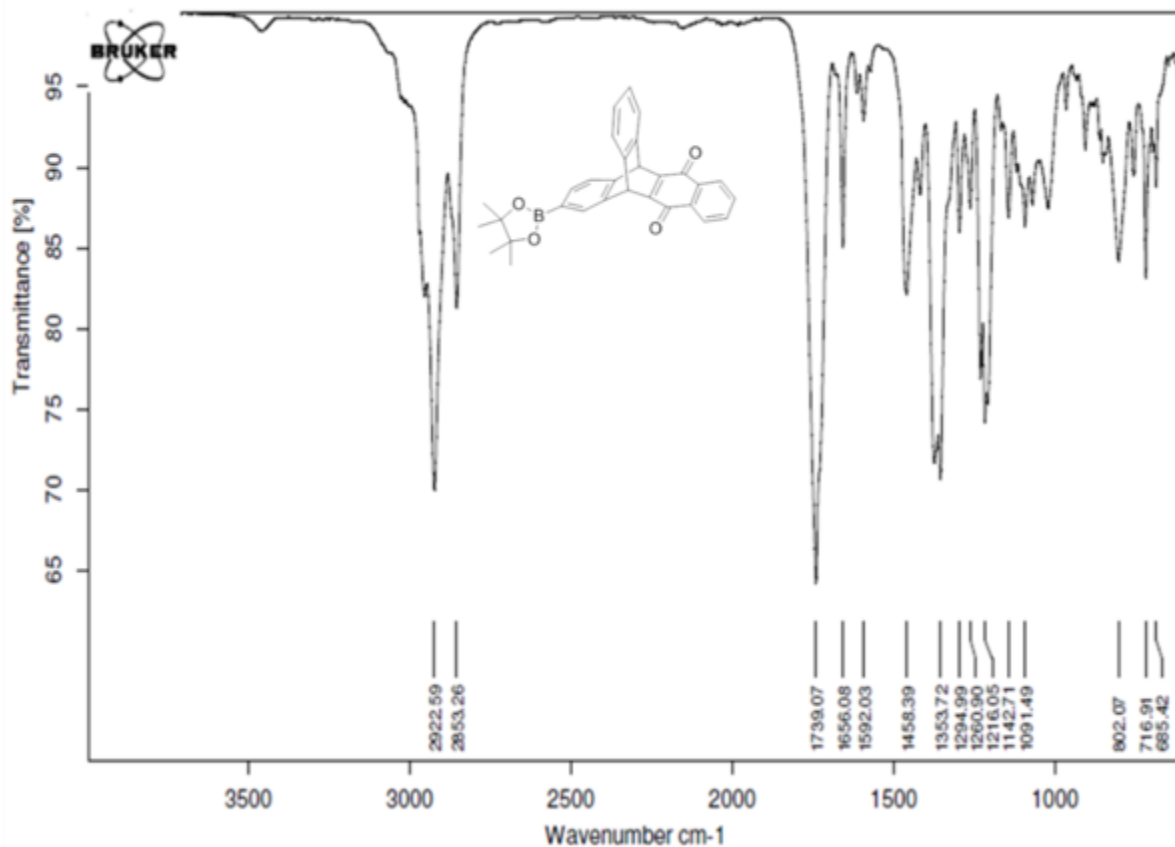
Acquisition Date 28/11/2013 09:26:46
 Operator Mass Spec
 Instrument / Ser# micrOTOF 92

Acquisition Parameter

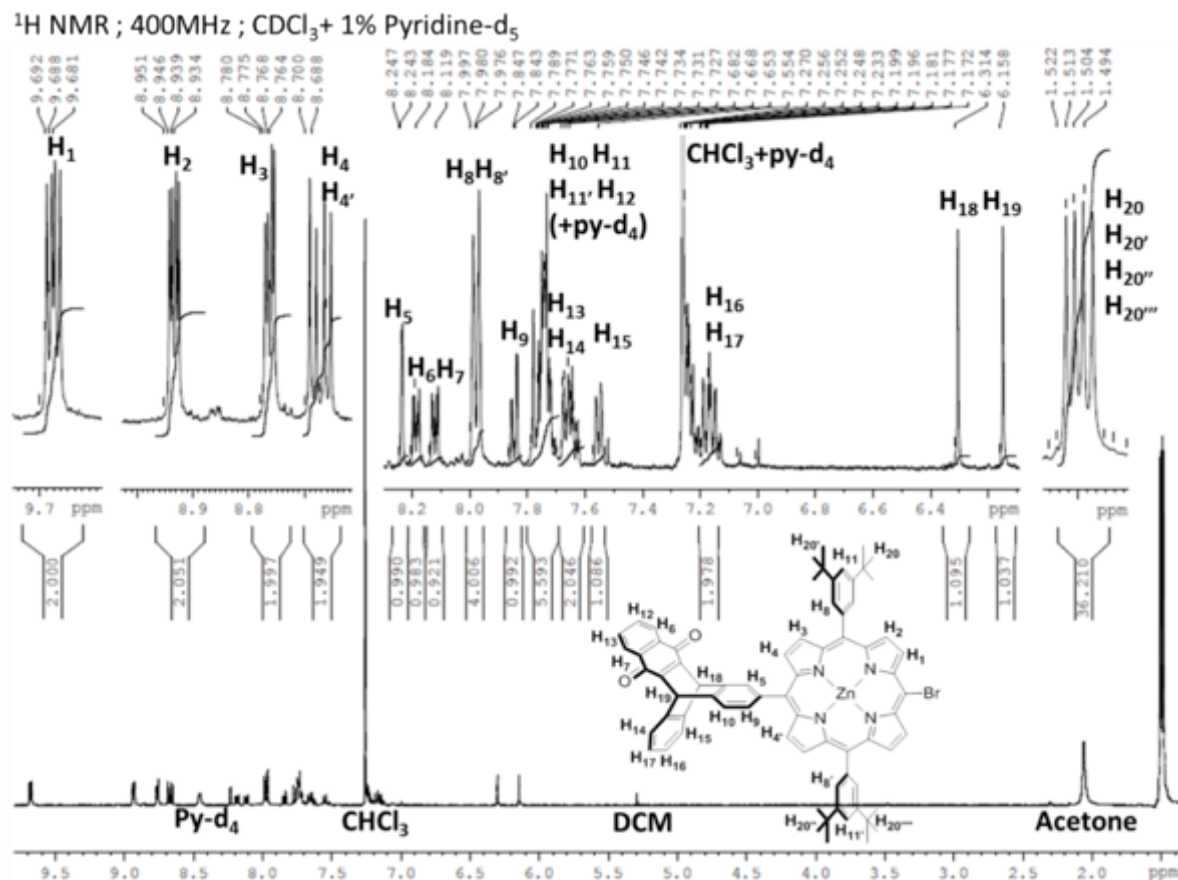
Source Type	ESI	Ion Polarity	Positive	Set Nebulizer	2.0 Bar
Focus	Not active			Set Dry Heater	180 °C
Scan Begin	100 m/z	Set Capillary	4500 V	Set Dry Gas	10.0 l/min
Scan End	1000 m/z	Set End Plate Offset	-500 V	Set Divert Valve	Source



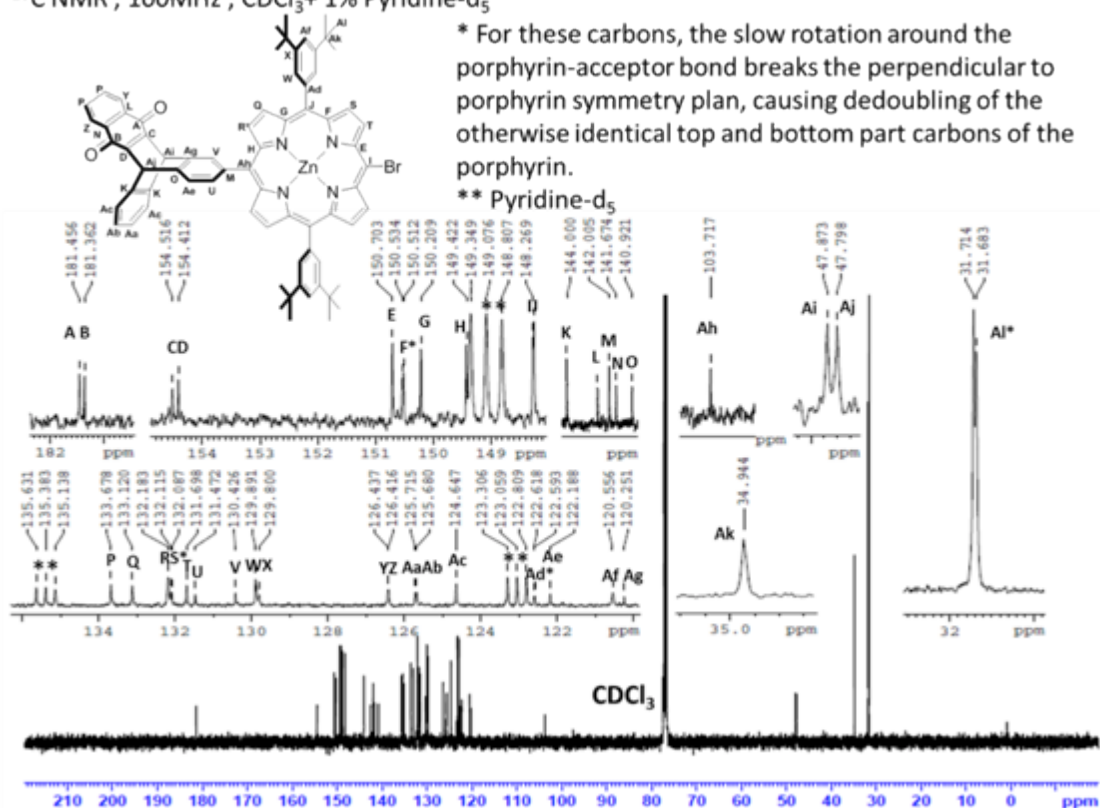
Infra-red vibrational spectroscopy

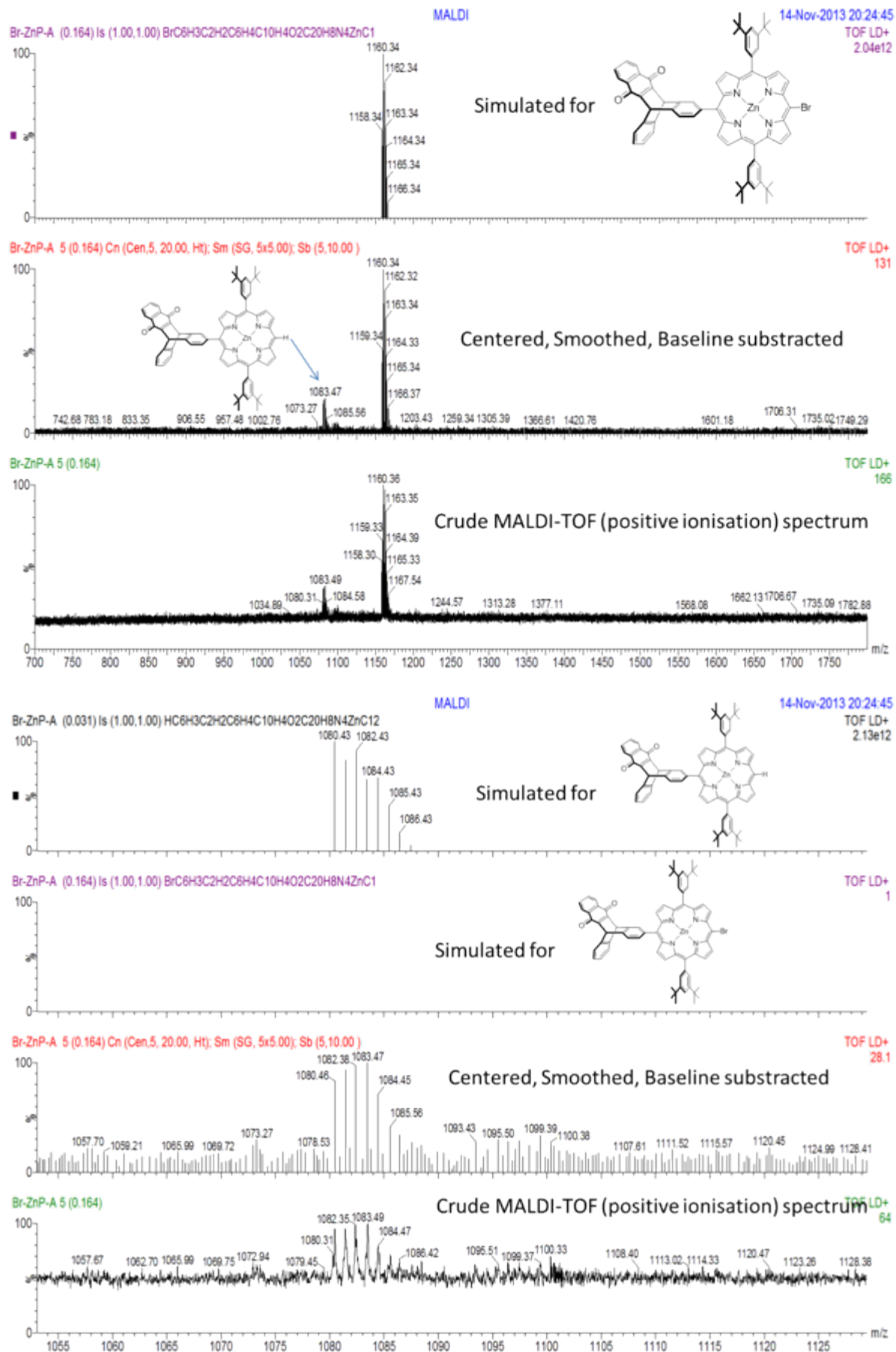


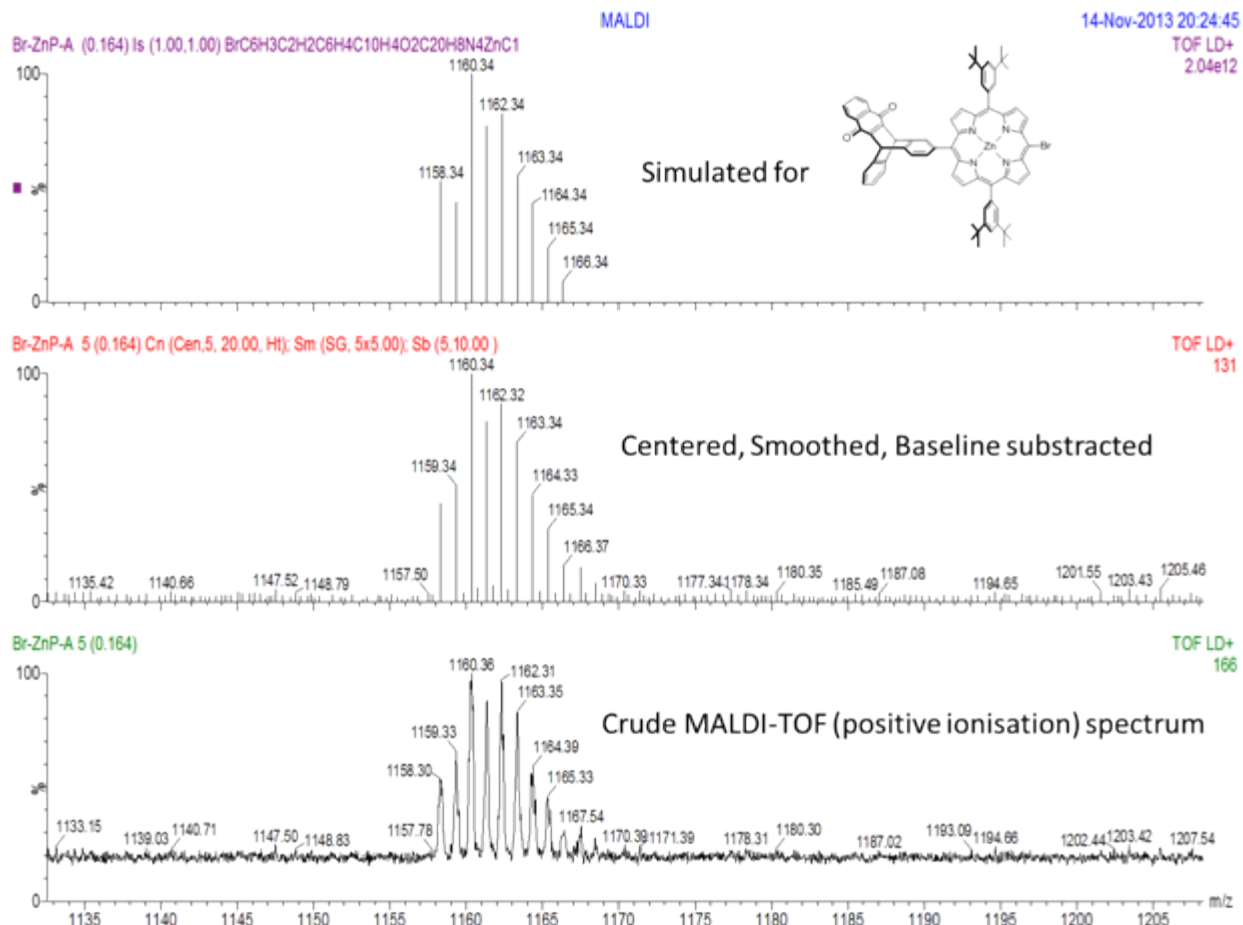
k. [5,15-Bis-(3,5-bis-*tert*-butylphenyl)-10-[5,12-[1,2]benzenotetracen-2-yl-6,11(5H,12H)-dione]-20-bromoporphinato]zinc(II) (12)



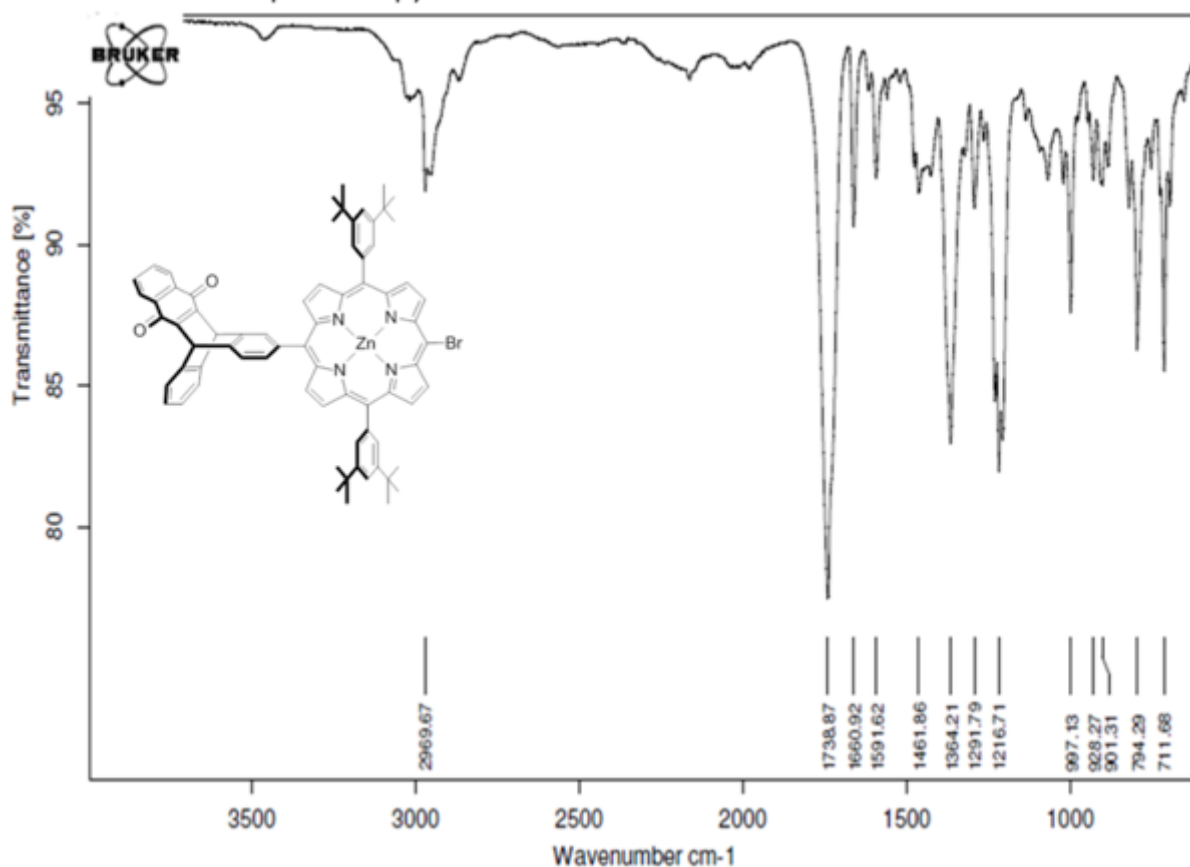
¹³C NMR ; 100MHz ; CDCl₃+ 1% Pyridine-d₅



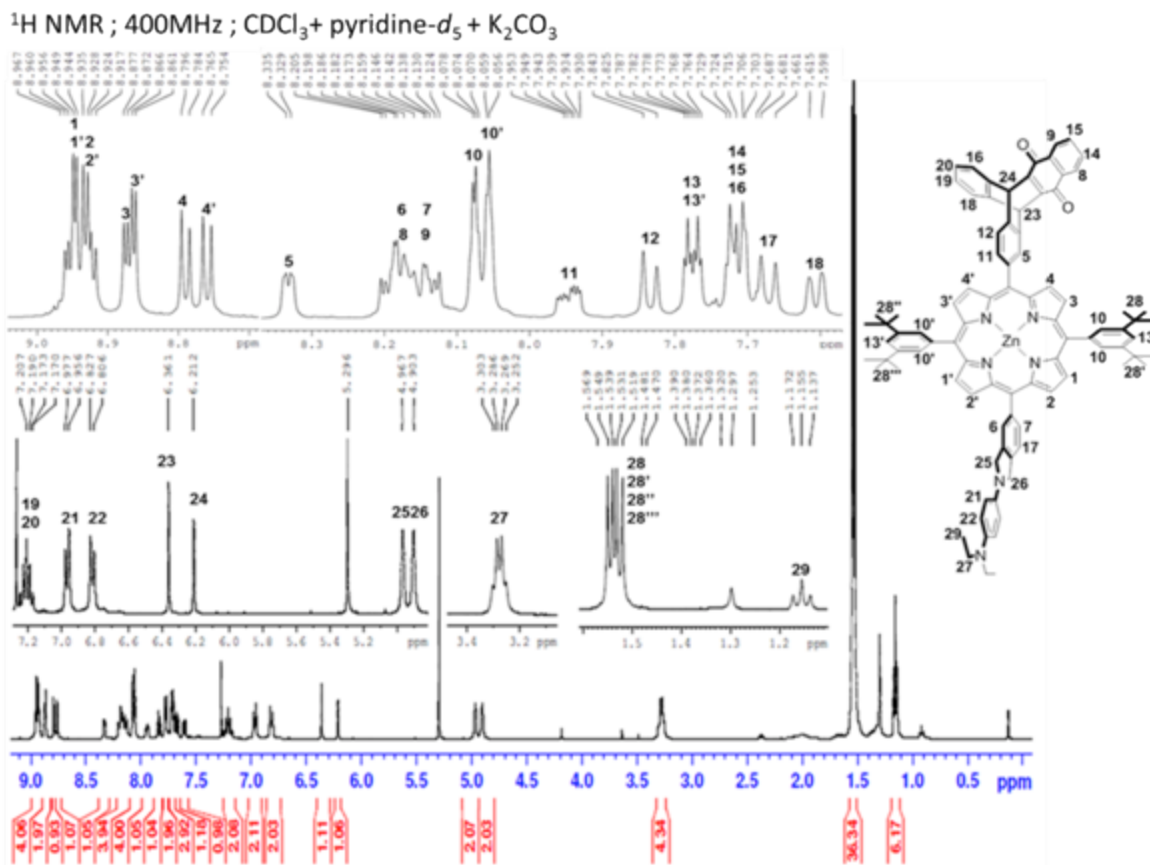




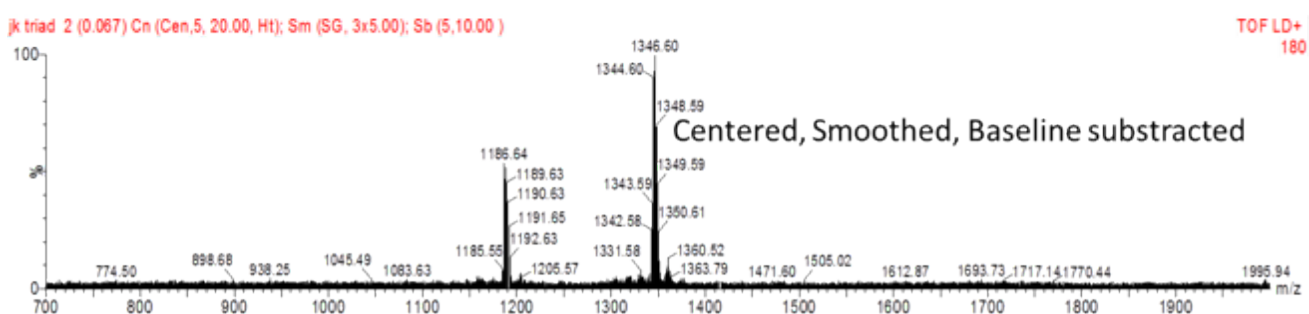
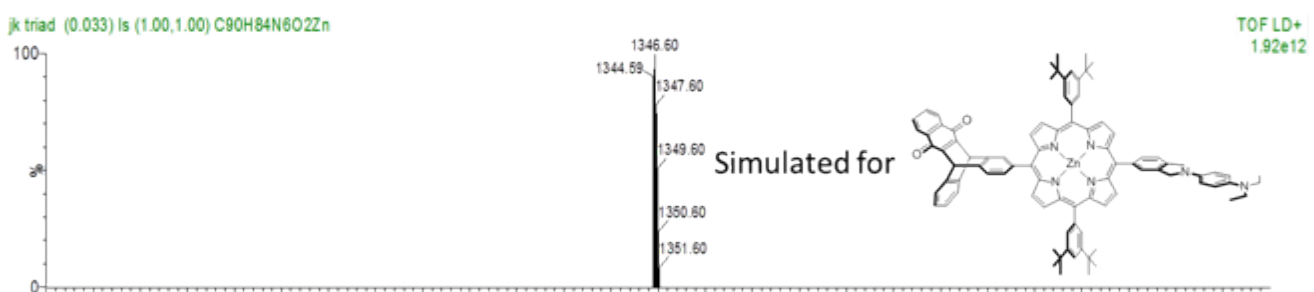
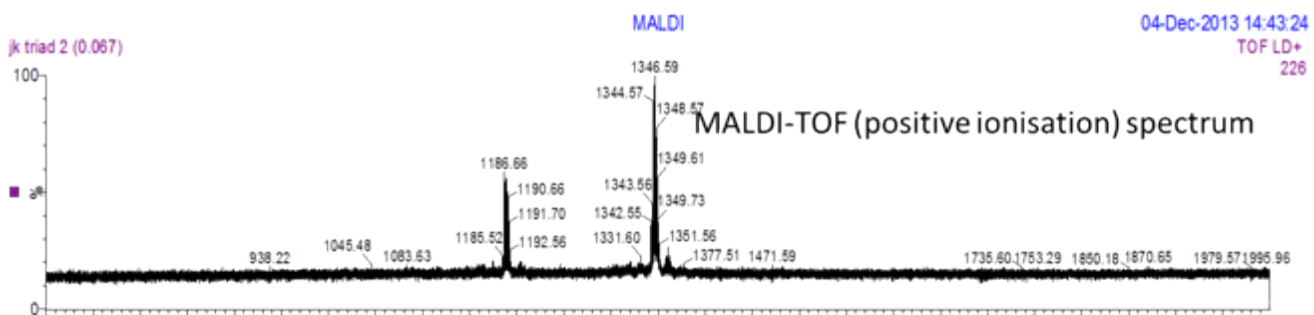
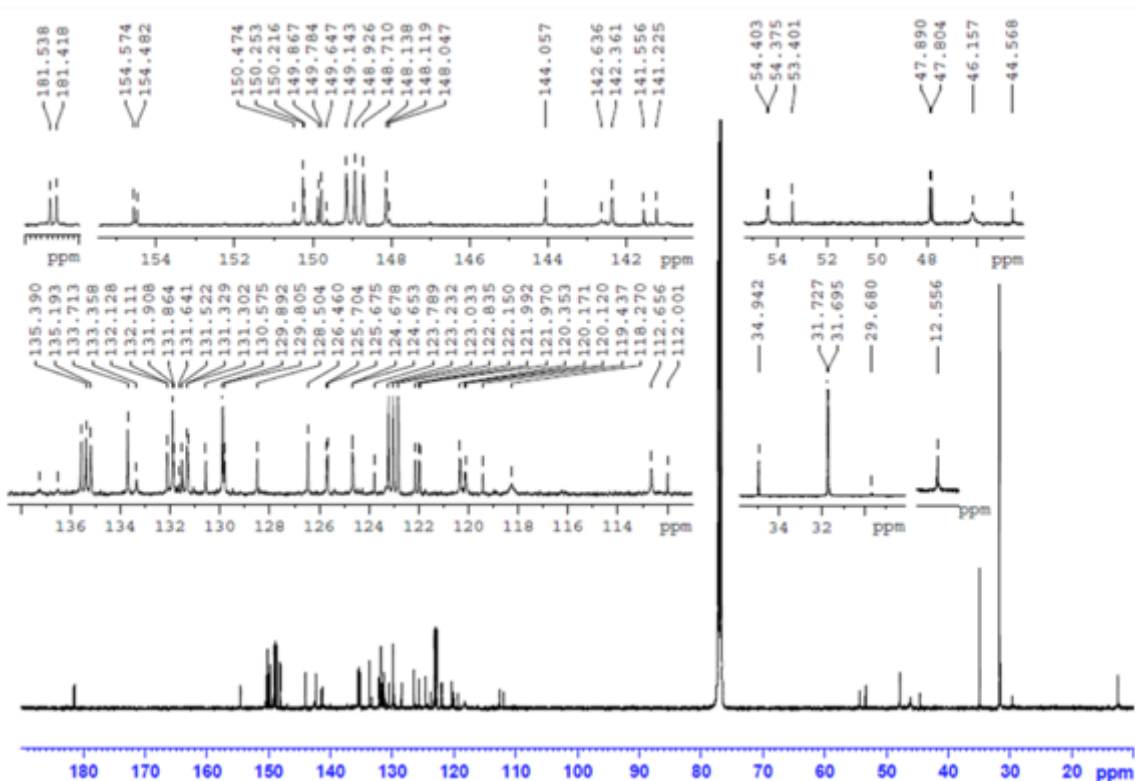
Infra-red vibrational spectroscopy

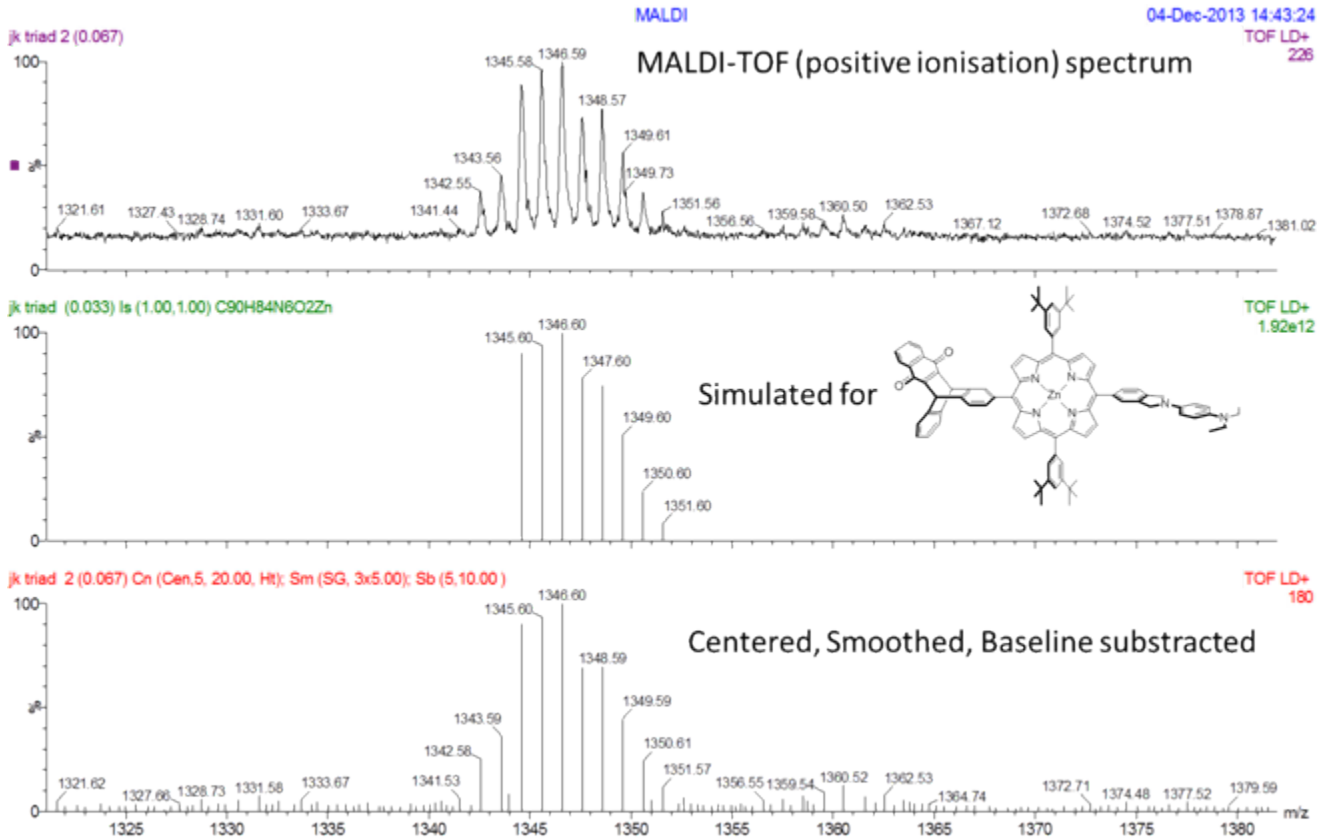


I. [5,15-Bis-(3,5-bis-*tert*-butylphenyl)-10-[5,12-[1,2]benzenotetracen-2-yl-6,11(5H,12H)-dione]-20-(4-(diethylamino)phenyl)-4*H*-isoindolin-2-yl]porphinatozinc(II) (TNQ-ZnP_{Ar}-TAPD)

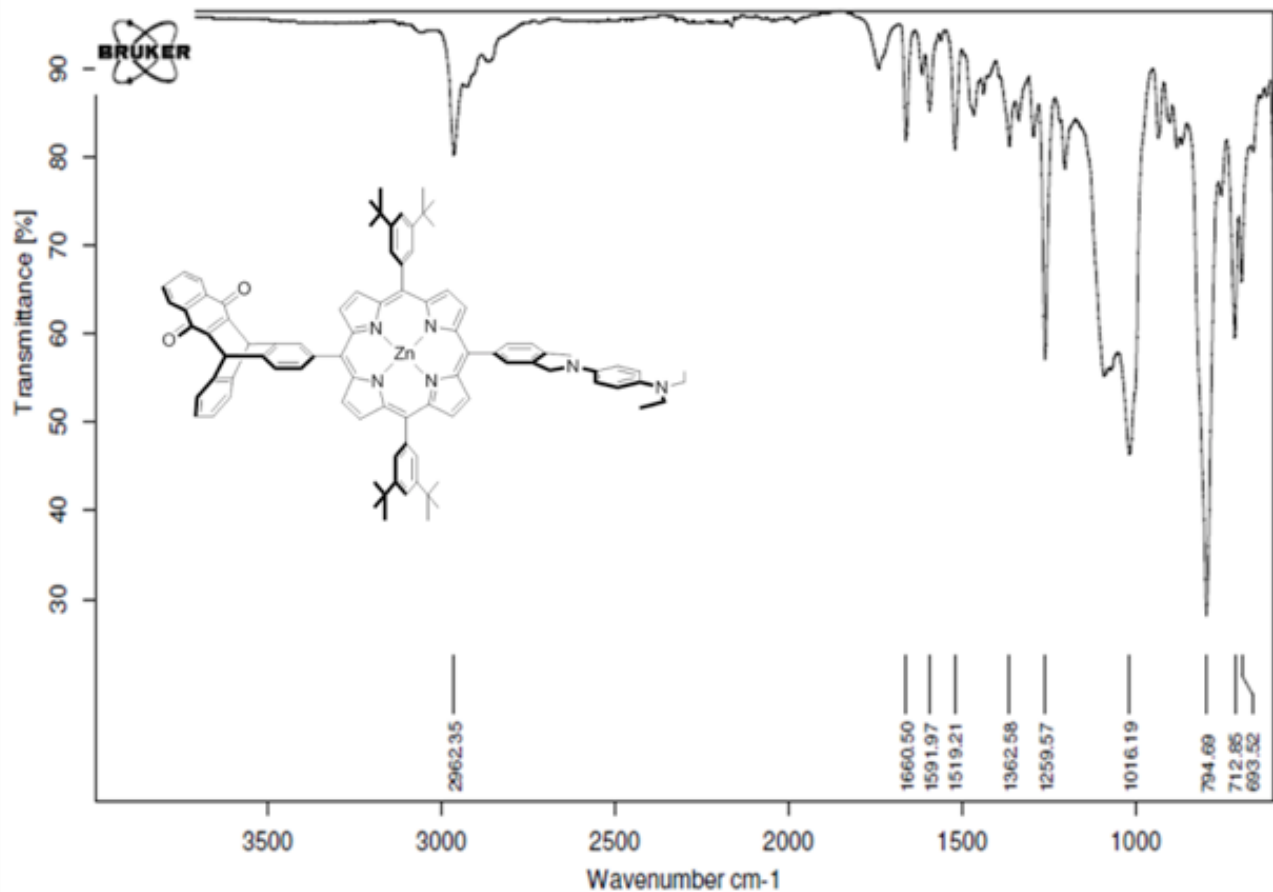


¹³C NMR ; 125MHz ; CDCl₃+ 1% Pyridine-d₅

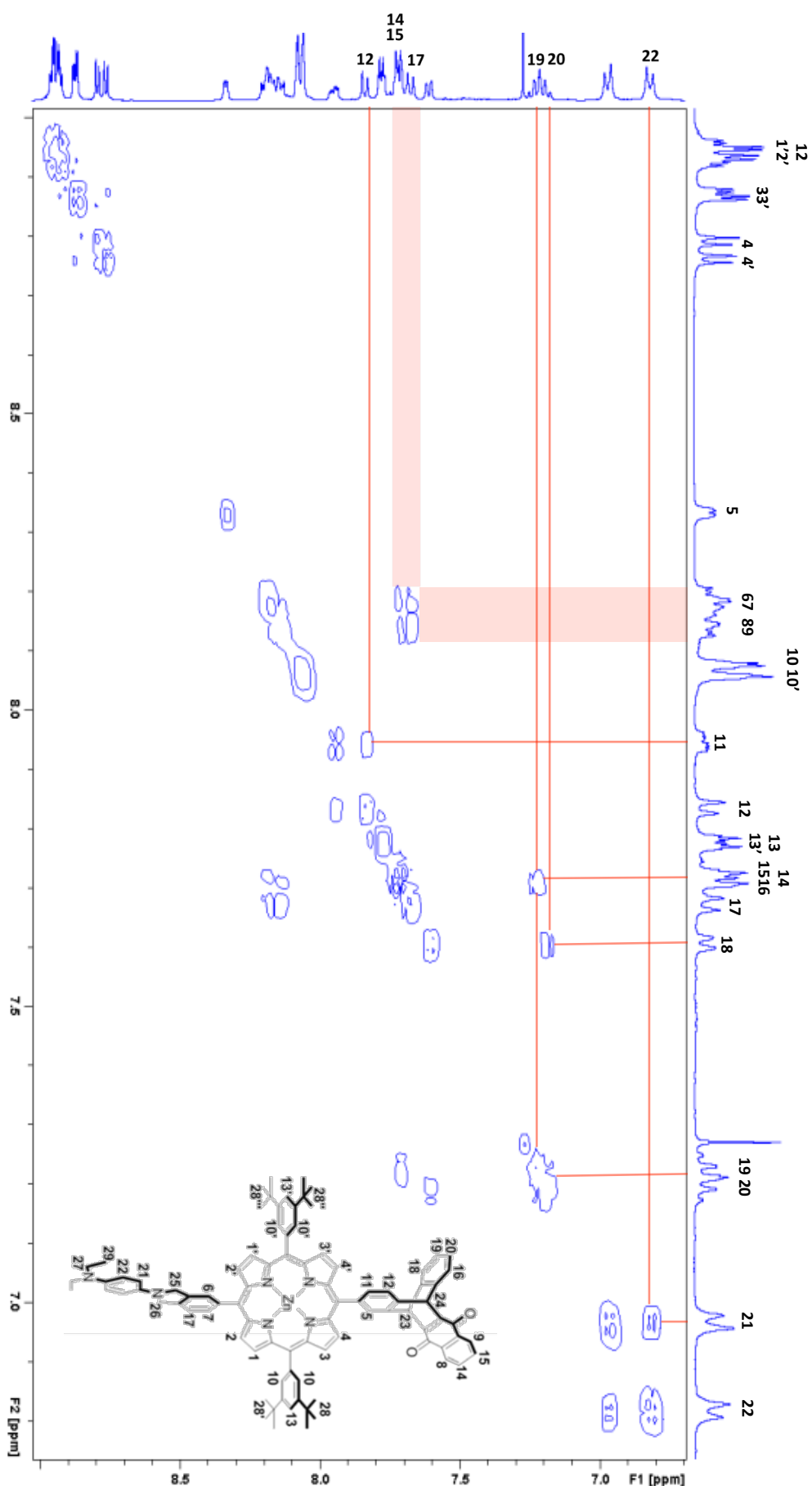




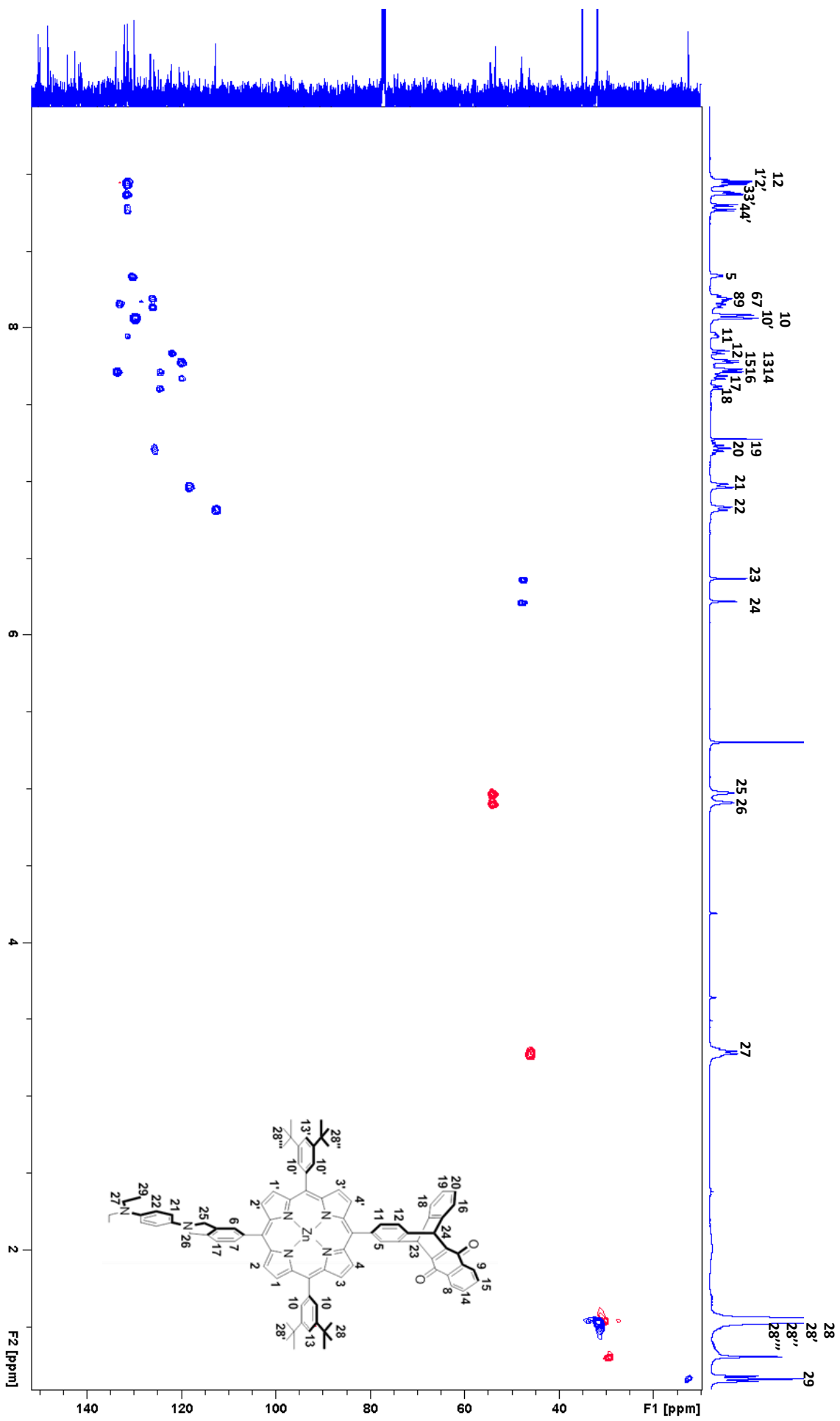
Infra-red vibrational spectroscopy



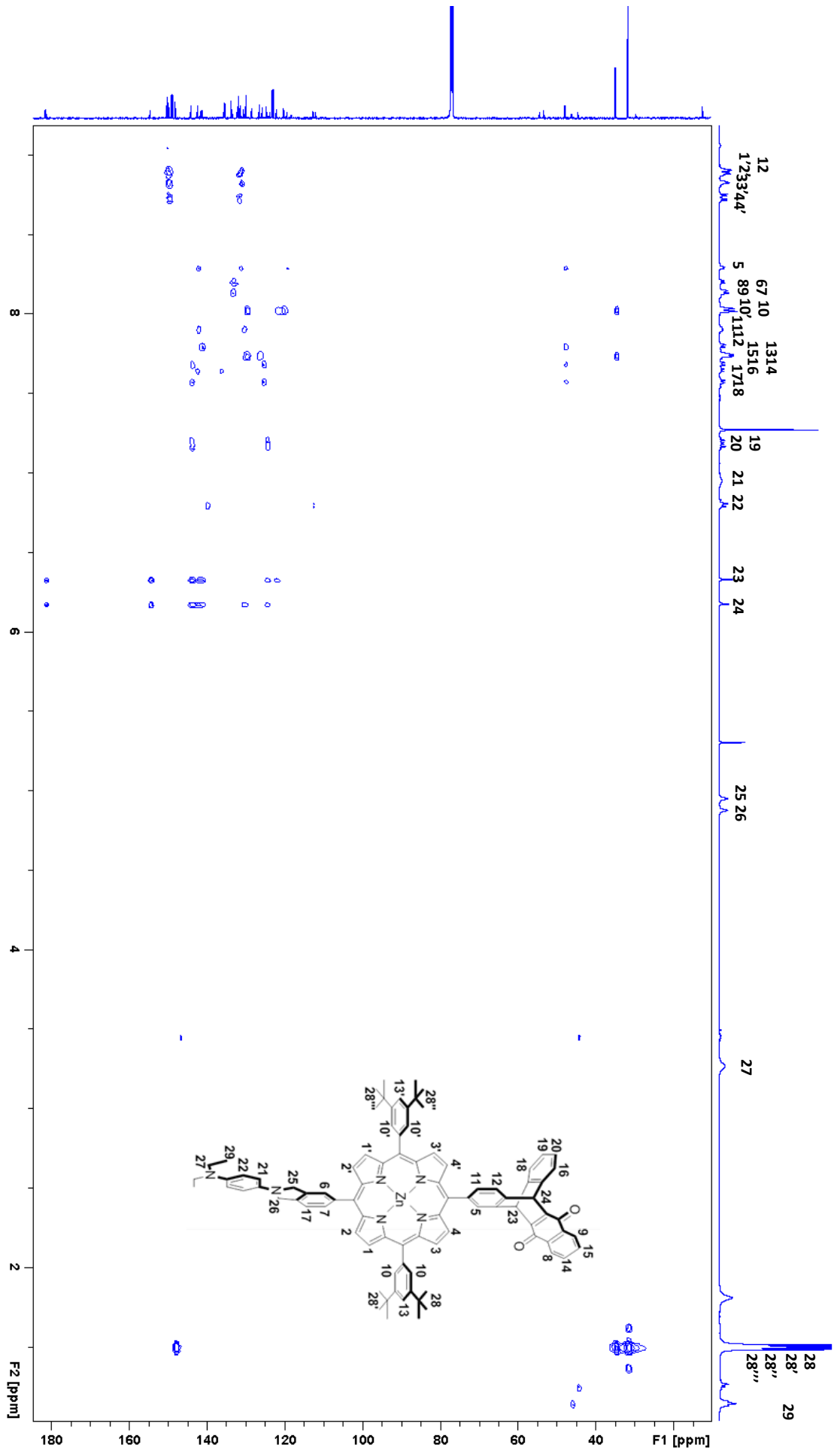
COSY (^1H - ^1H) 400 MHz, $\text{CDCl}_3 + 1\%$ Py-d₅



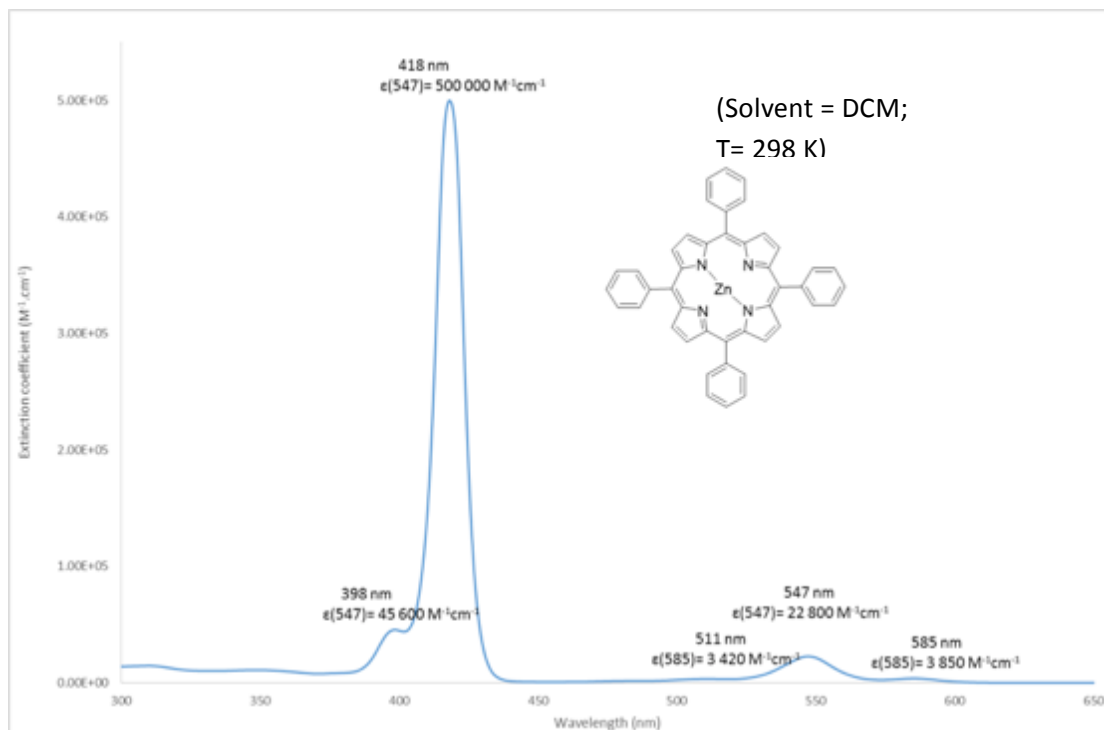
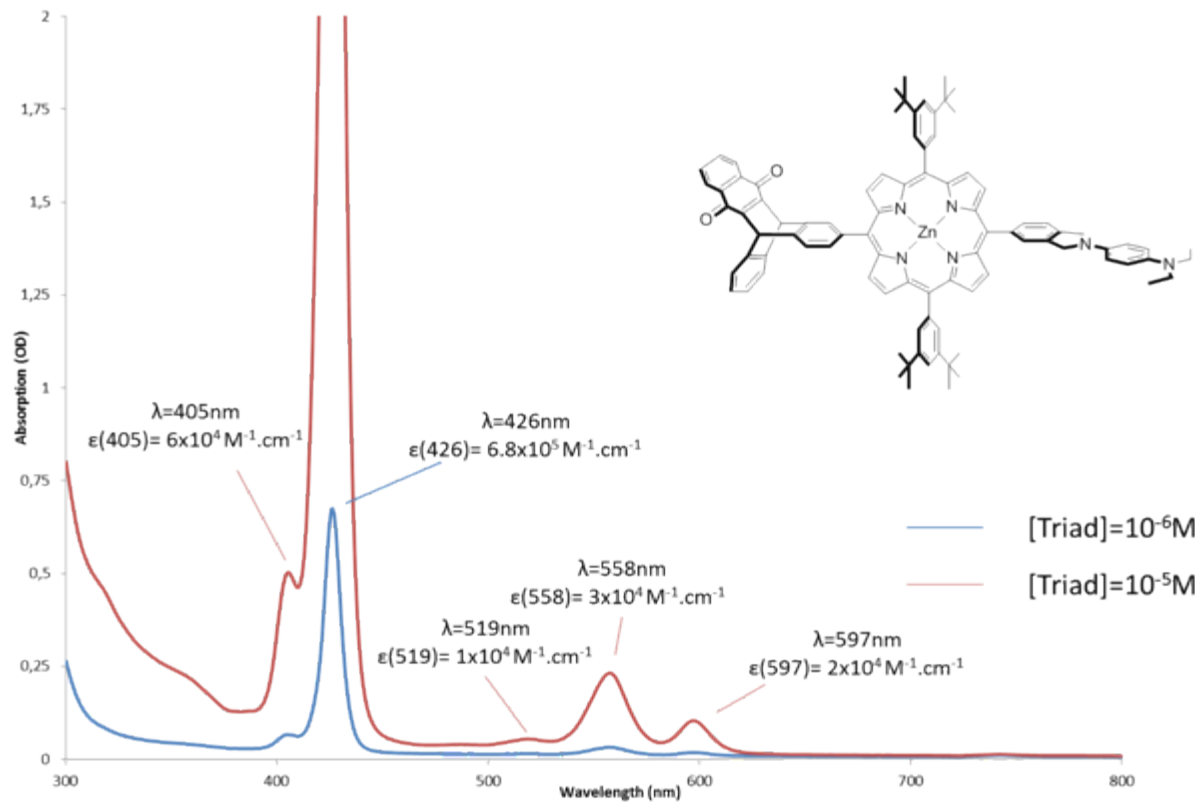
HSQC (^1H - ^{13}C) 400 MHz, $\text{CDCl}_3 + 1\%$ Py-d₅

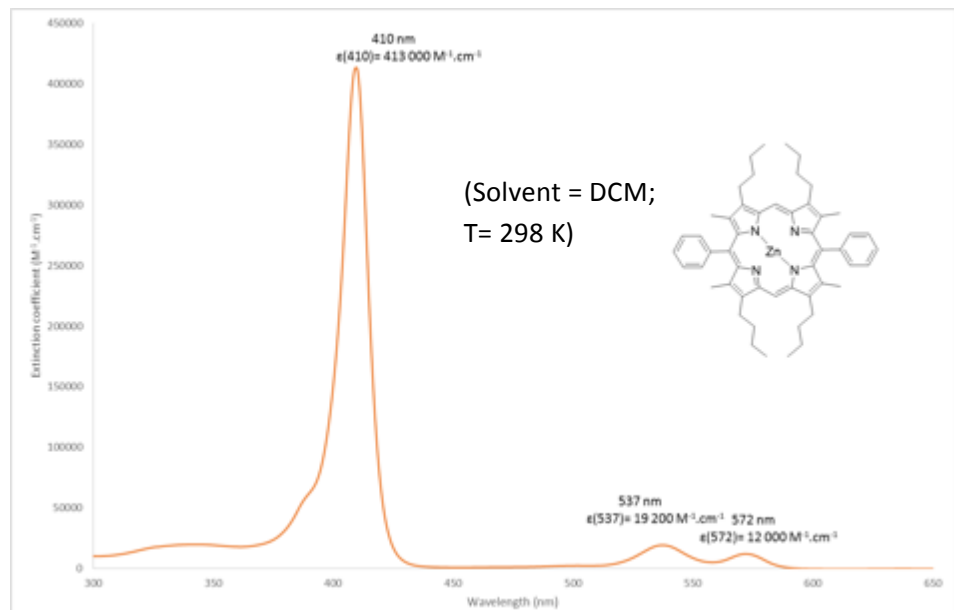


HMBC (^1H - ^{13}C) 400 MHz, $\text{CDCl}_3 + 1\%$ Py-d₅

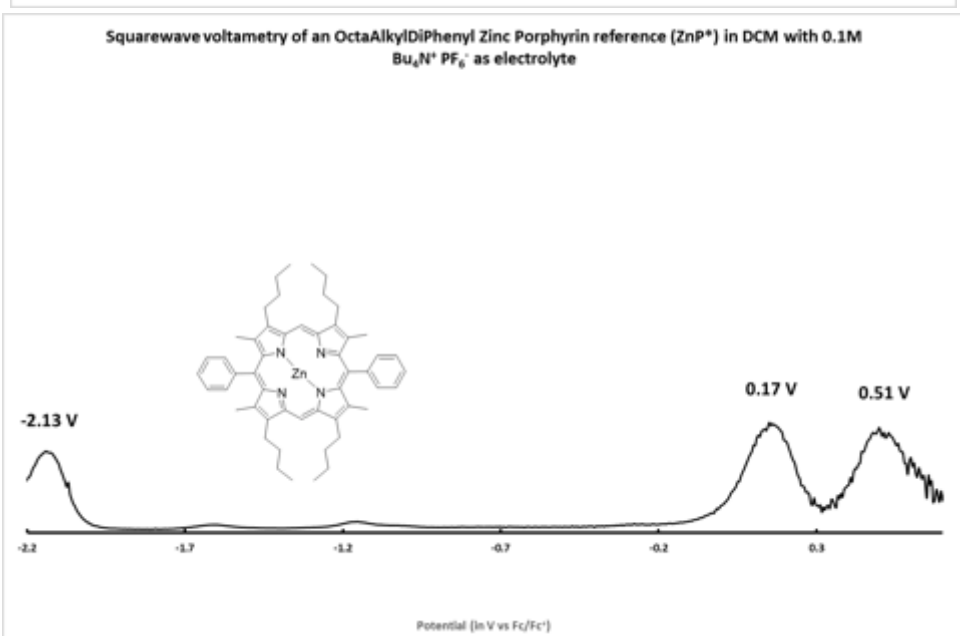


Steady-state absorption spectroscopy of the triad (298K, solvent MTHF)

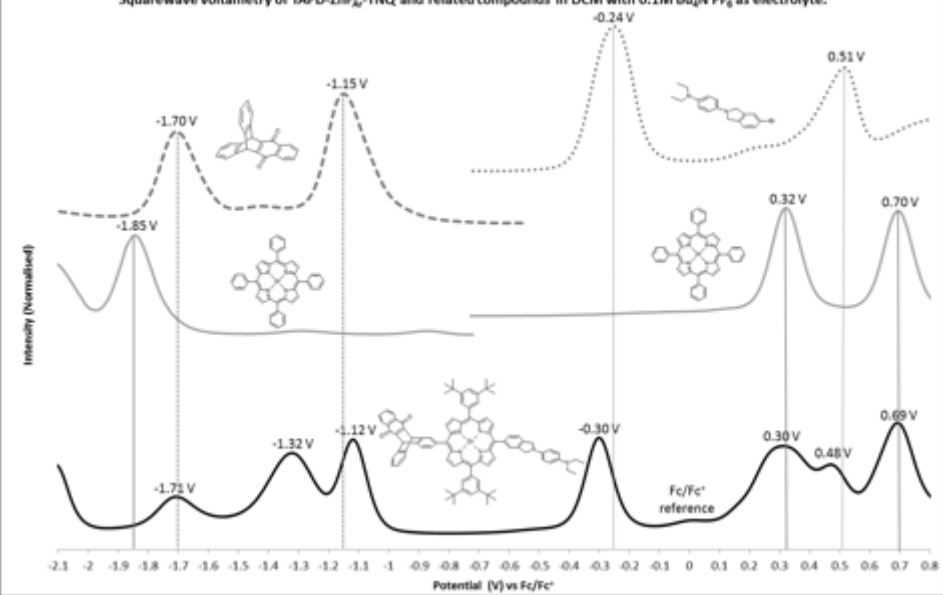




Squarewave voltammetry of an OctaAlkylDiPhenyl Zinc Porphyrin reference (ZnP^*) in DCM with 0.1M $\text{Bu}_4\text{N}^+ \text{PF}_6^-$ as electrolyte

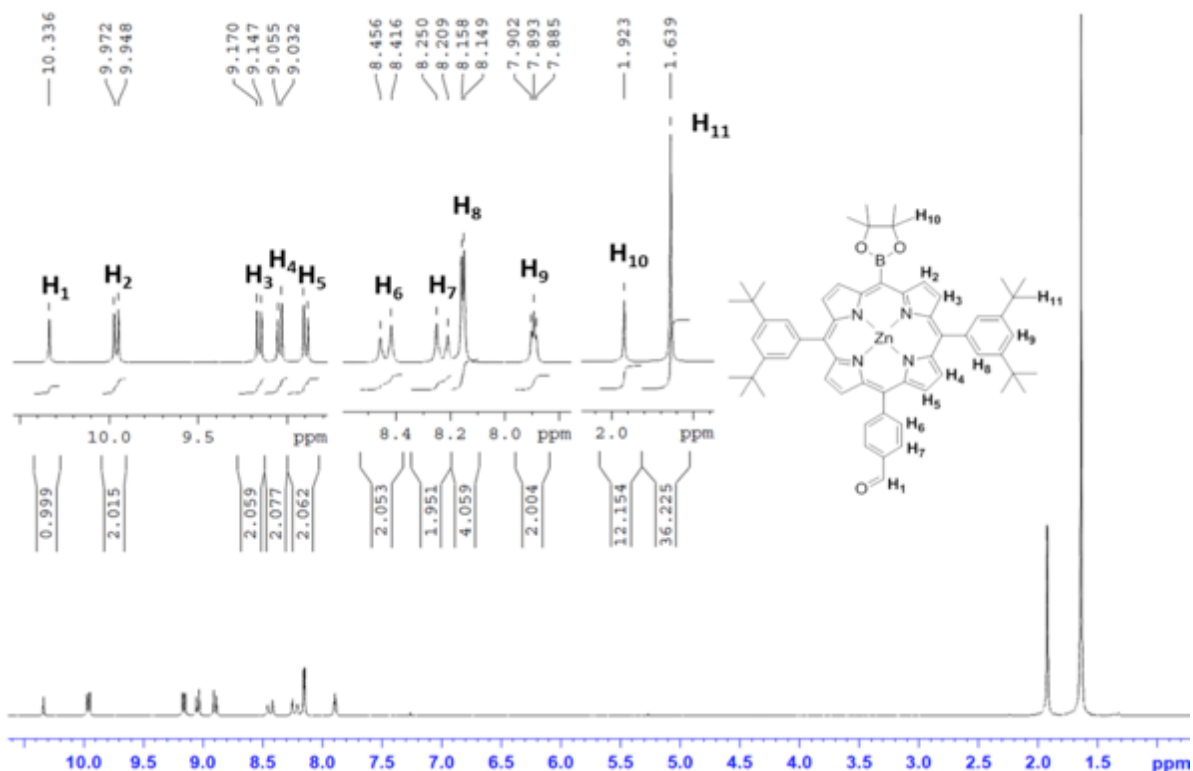


Squarewave voltammetry of TAPD-ZnP_{Ar}-TNQ and related compounds in DCM with 0.1M $\text{Bu}_4\text{N}^+ \text{PF}_6^-$ as electrolyte.

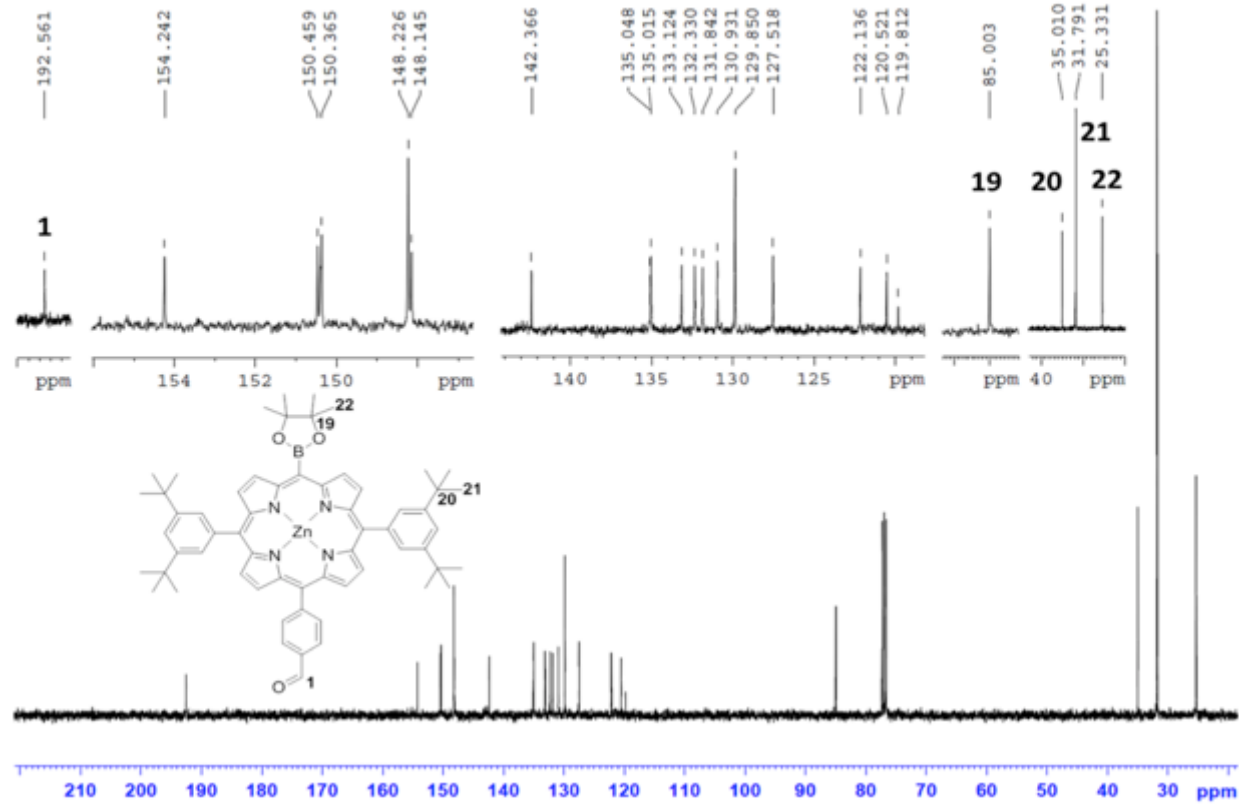


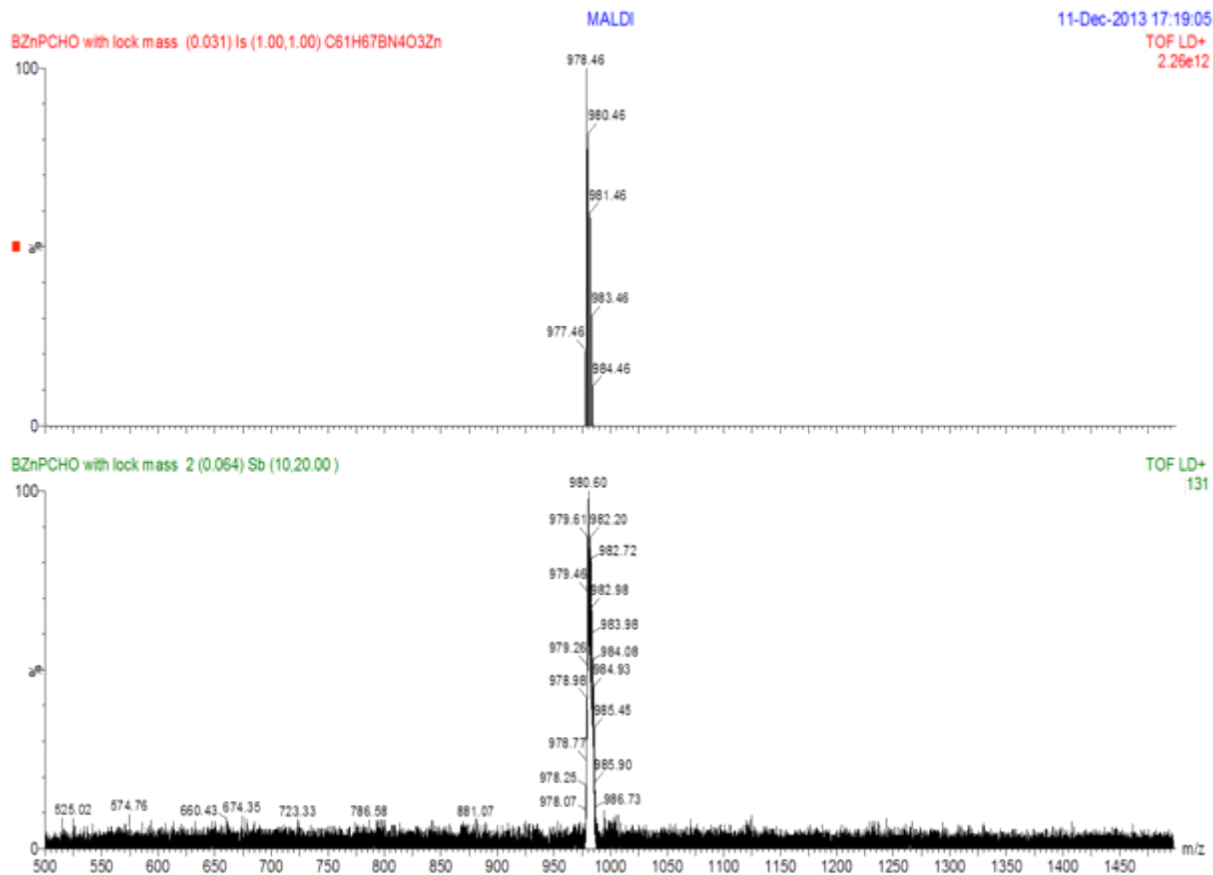
m. [5,15-Bis-(3,5-bis-*tert*-butyl-phenyl)-10-(4,4,5,5-tetramethyl-1,3,2-dioxaborolan-2-yl)-20-(4-benzaldehyde)-porphyrinato]zinc(II) (13)

¹H NMR ; 200MHz ; CDCl₃+ pyridine-*d*₅ + K₂CO₃



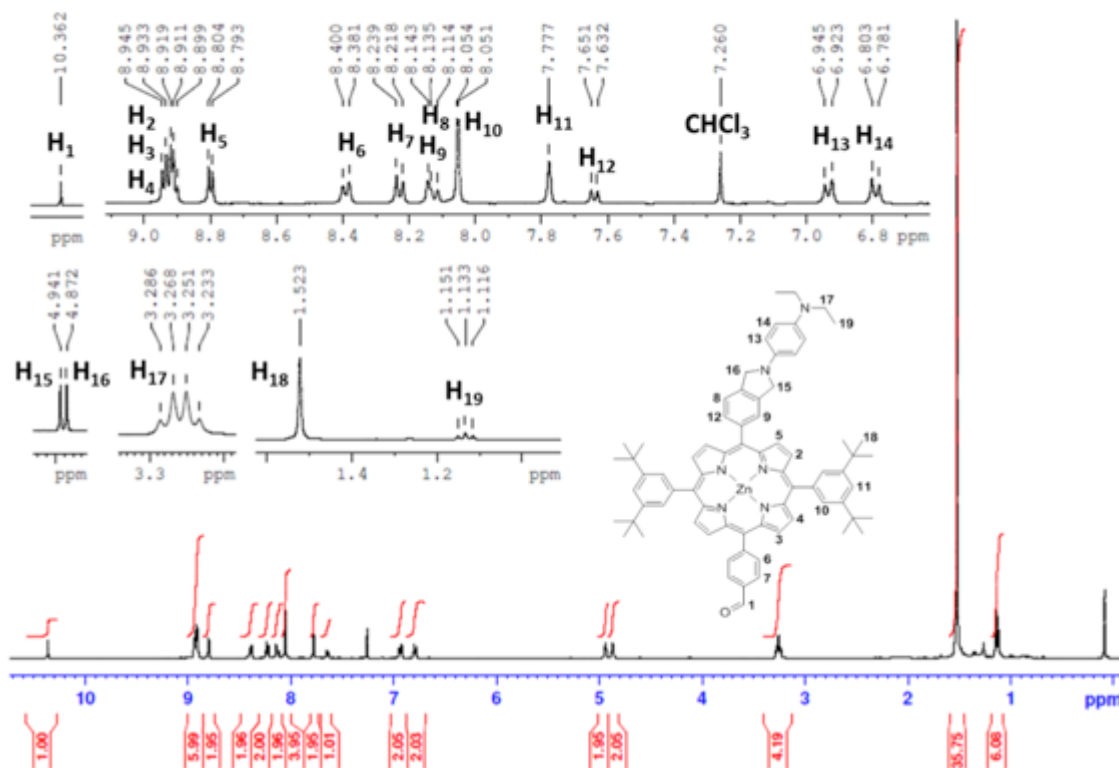
¹³C NMR ; 100MHz ; CDCl₃+ 1% Pyridine-*d*₅ + K₂CO₃



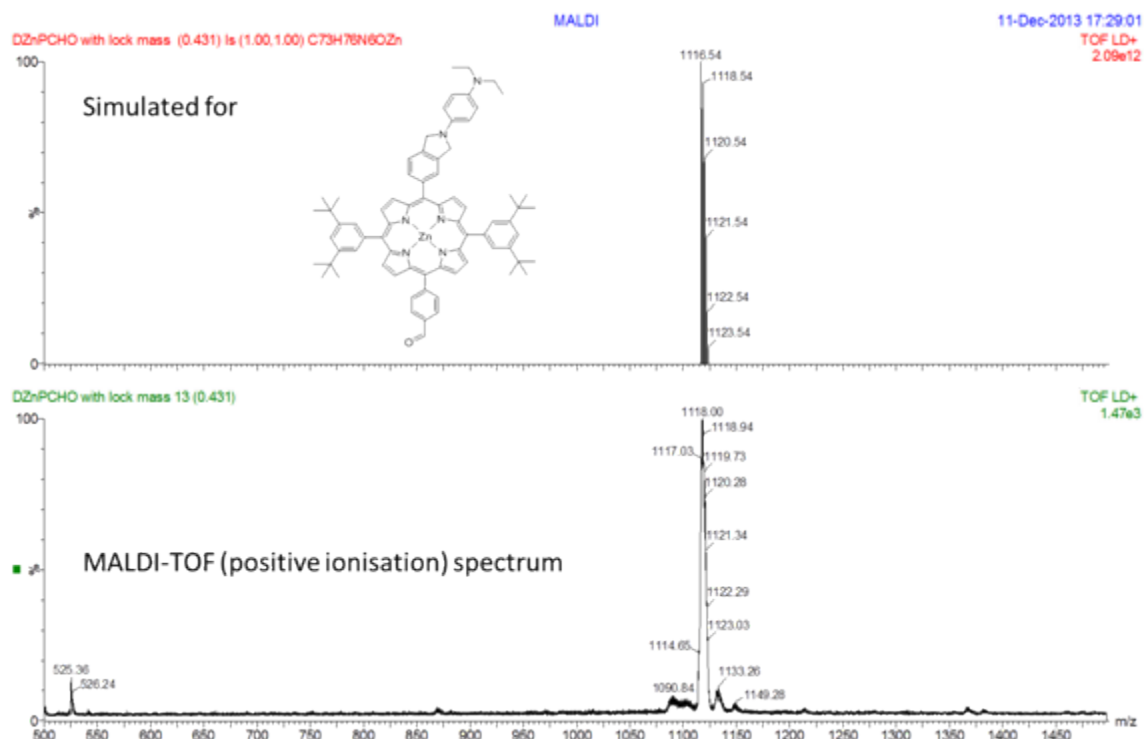
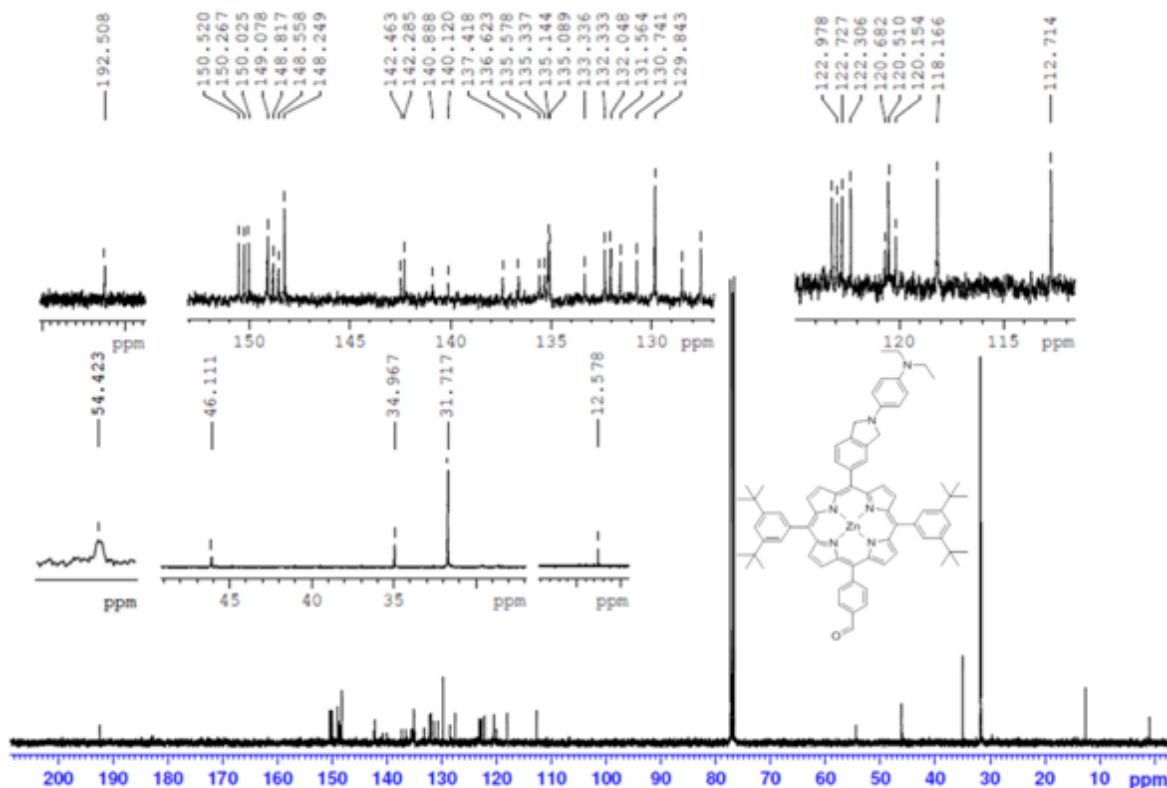


n. [5,15-Bis-(3,5-bis-*tert*-butylphenyl)-10-(4-carboxyphenyl)-20-(4-(diethylamino)phenyl)-4*H*-isoindolin-2-yl]porphinatozinc(II) (14):

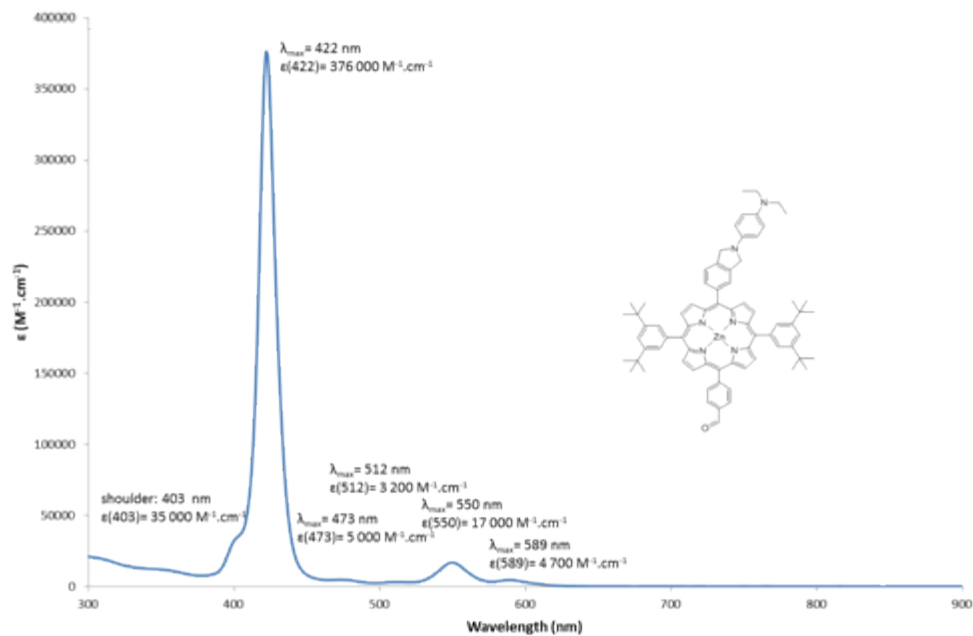
¹H NMR ; 400MHz ; CDCl₃+ 1% Pyridine-d₅



^{13}C NMR ; 100MHz ; $\text{CDCl}_3 + 1\%$ Pyridine-d₅ + K_2CO_3

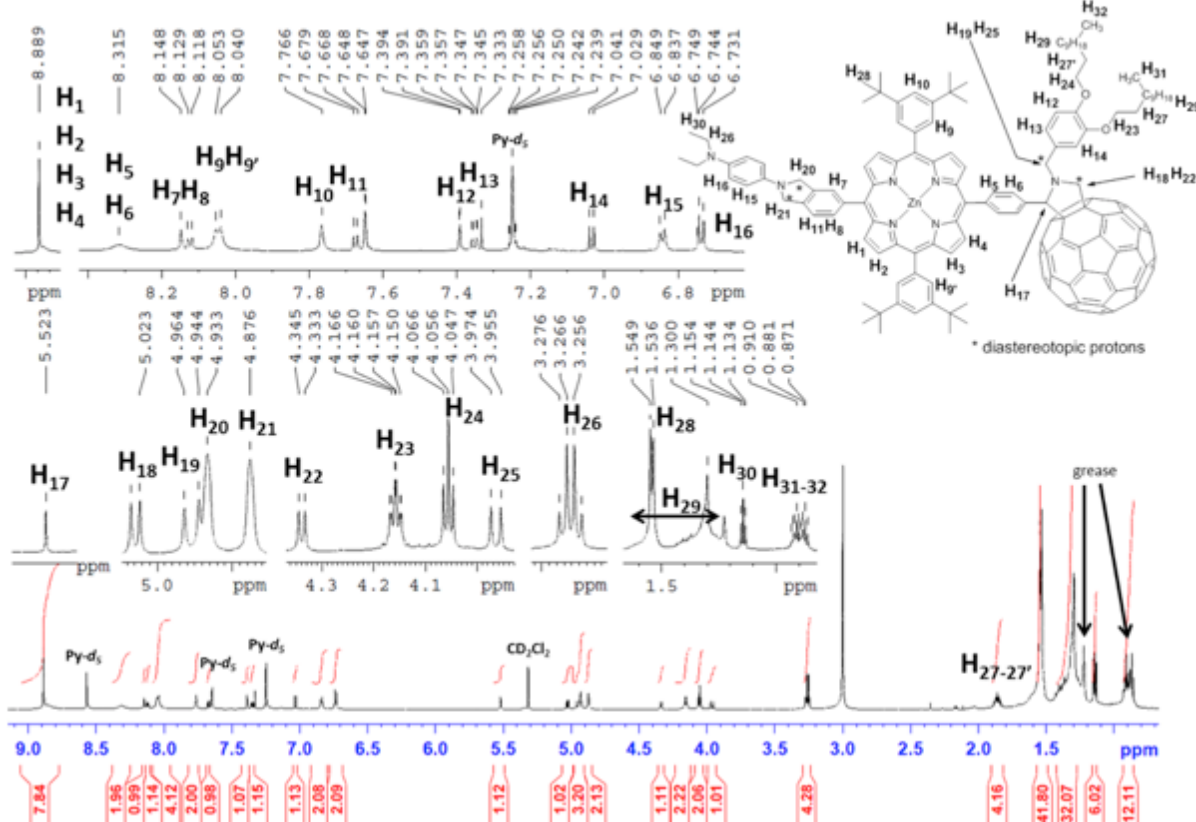


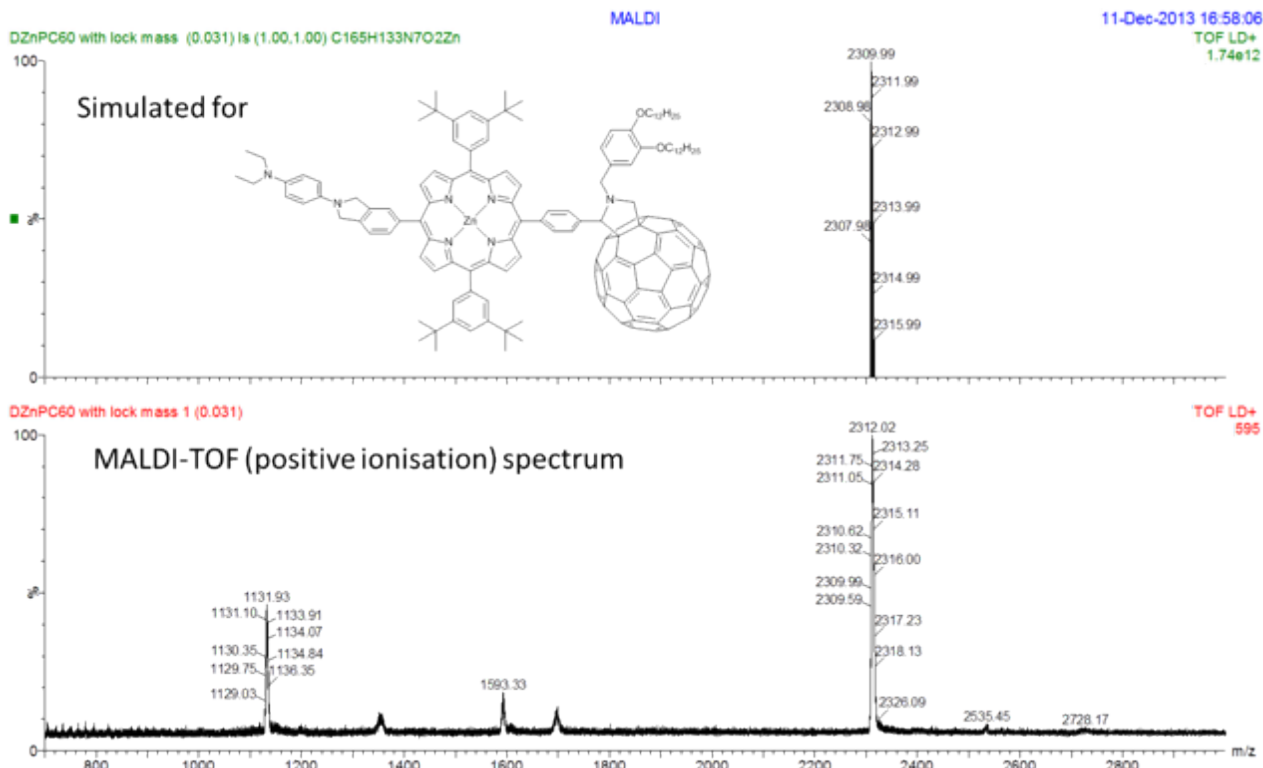
UV-visible absorption spectroscopy; 5 μ M in DCM; 298 K; 120 nm.min $^{-1}$



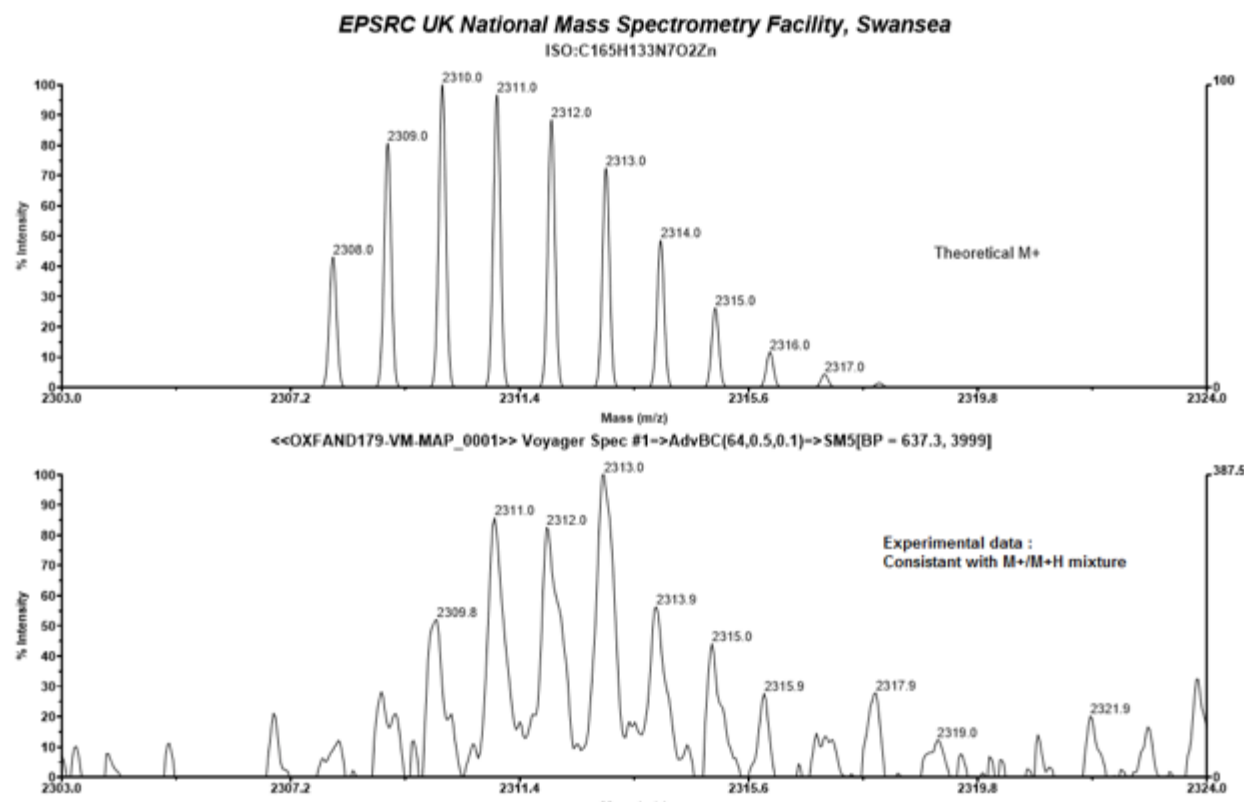
o. [5,15-Bis-(3,5-bis-tert-butylphenyl)-10-[4-(N-(3',4'-didodecoxybenzyl)-[60]fullero[c]tetrahydropyrrol-2-yl)phenyl]-20-(4-diethylamino)phenyl)-4H-isoindolin-2-yl]porphinatozinc(II) ($\text{C}_{60}\text{-ZnP}_{\text{Ar}}\text{-TAPD}$)

^1H NMR ; 700MHz ; CD_2Cl_2 : CS_2 : Pyridine-d₅ 48:50:2





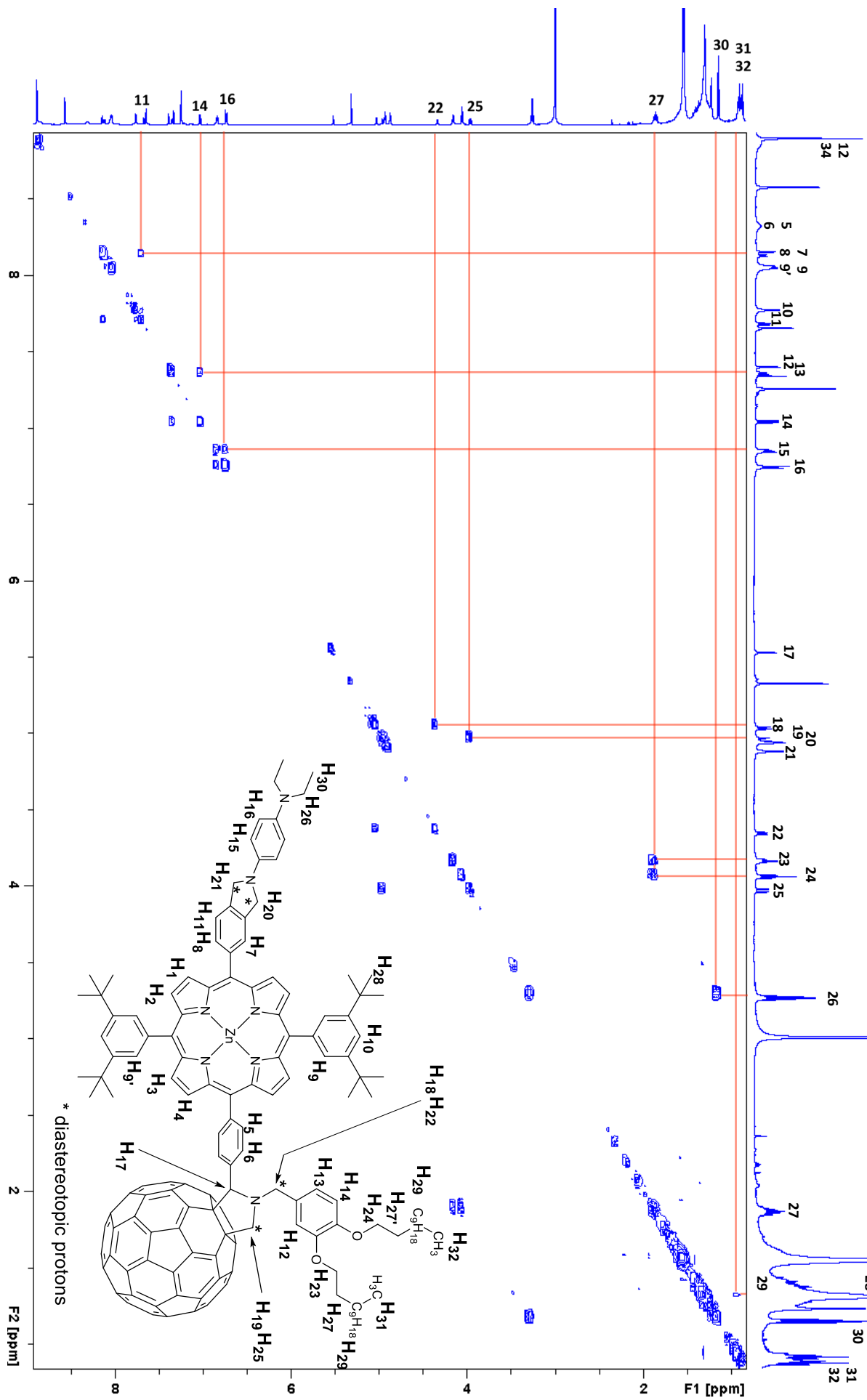
HMRS- MALDI TOF (Swansea National Mass-spectroscopy Facility):



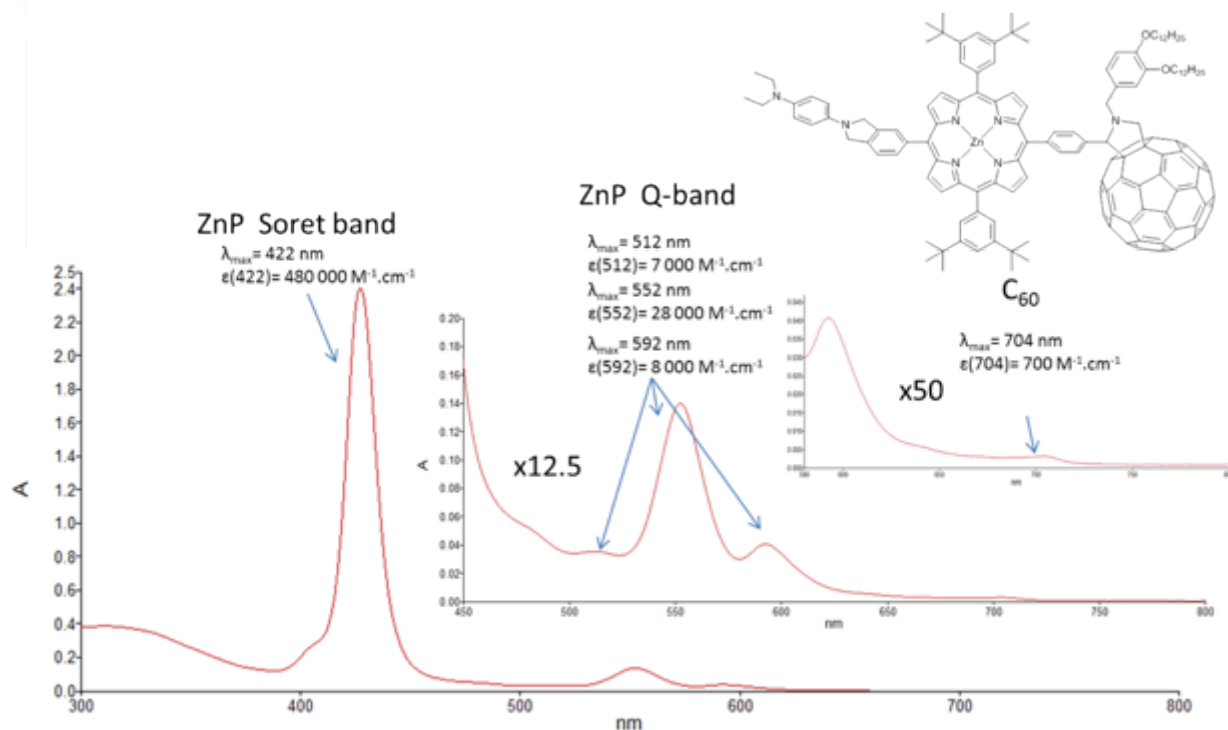
Acquired: 14:41:00, August 26, 2014
Keber DZnPC60 MV=2311?? DCM PosRef [1:49] (DCTB,DCM)
D:\2014\Aug\14\OXFAND179-VM-MAP_0001.dat

Printed: 14:54, August 26, 2014

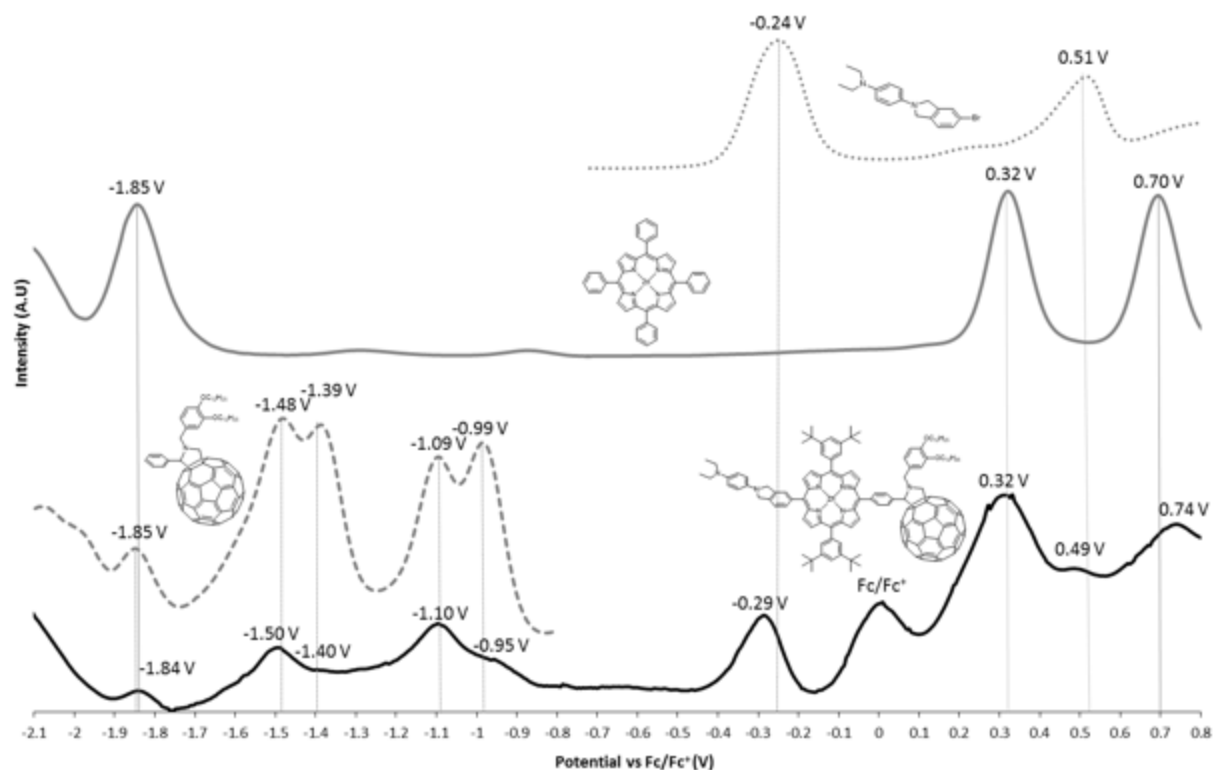
COSY (^1H - ^1H) 400 MHz, $\text{CDCl}_3 + 1\%$ Py-d₅



UV-visible absorption spectroscopy; 5 μ M in toluene ; 298 K; 120 nm.min⁻¹

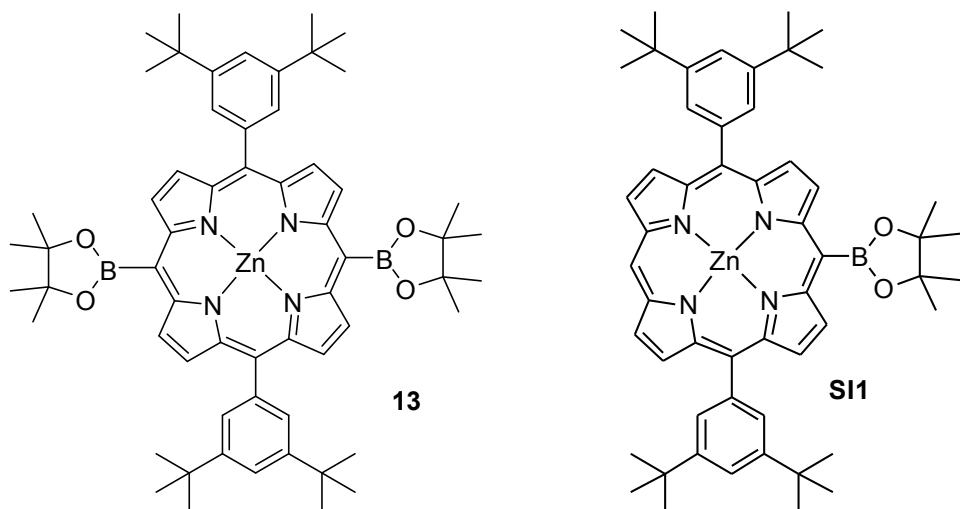


Squarewave voltammetry of TAPD-ZnP_{Ar}-C₆₀ and related compounds in DCM with 0.1M Bu₄N PF₆ as electrolyte.



3) Synthesis of reference and known compounds

- a. [5,15-Bis-(3,5-bis-*tert*-butylphenyl)-10,20-Bis-(4,4,5,5-tetramethyl-1,3,2-dioxaborolan-2-yl)porphinato]zinc(II) (**13**) + [5,15-Bis-(3,5-bis-*tert*-butylphenyl)-10-(4,4,5,5-tetramethyl-1,3,2-dioxaborolan-2-yl)porphinato]zinc(II) **S1**



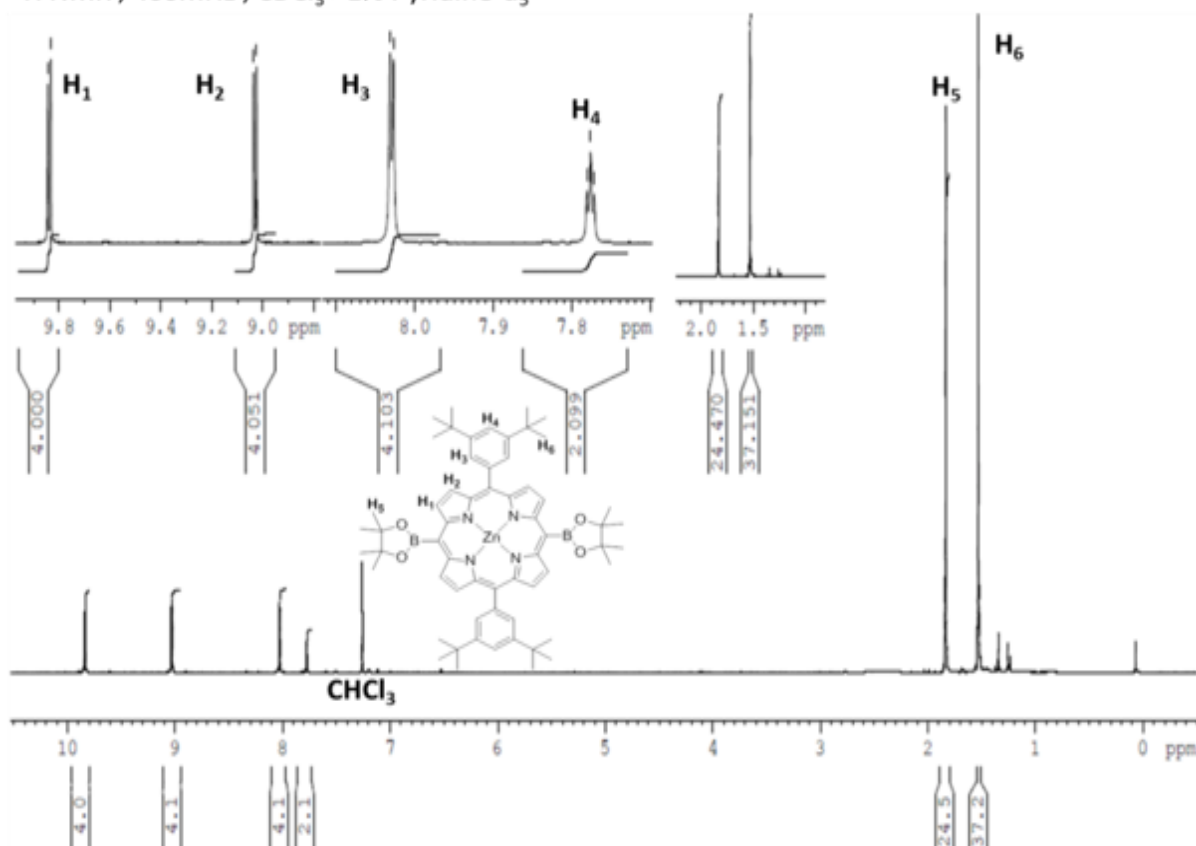
The procedure was adapted from a formerly reported method⁵³

A dry two-neck flask equipped with a condenser was charged with [5,15-bis-(3,5-bis-*tert*-butylphenyl)-10,20-dibromoporphinato]zinc(II)⁵² (400 mg; 440 µmol; 1 eq.) and *trans*-dichlorodi(triphenylphosphine)palladium(II) (62 mg; 88 µmol; 0.2 eq.). The mixture was purged 3 times with argon and dry toluene (40 mL), dry THF (40 mL) and distilled triethylamine (9 mL; 150 eq.) were added. The solution was purged 5 more times with argon and pinacolborane (2.30 mL; 15.8 mmol; 36 eq.) was added. The reaction mixture was stirred at 68 °C for one day. The excess of pinacolborane was neutralized by adding carefully water (20 mL, dropwise via syringe) at 0 °C. The organic phase was collected, washed three times with water (3 x 20 mL) and brine (20 mL), dried over MgSO₄ and filtered. The solvents were removed under reduced pressure and separation of **13** and **S1** was achieved by chromatography (SiO₂). The first fraction was collected while using dichloromethane 2:1 petroleum ether 40–60°C (**S1**; red powder; 76 mg; 21%) as eluent and the second fraction was collected while using dichloromethane/methanol 98/2 as eluent (**13**; pink powder; 326 mg; 74%).

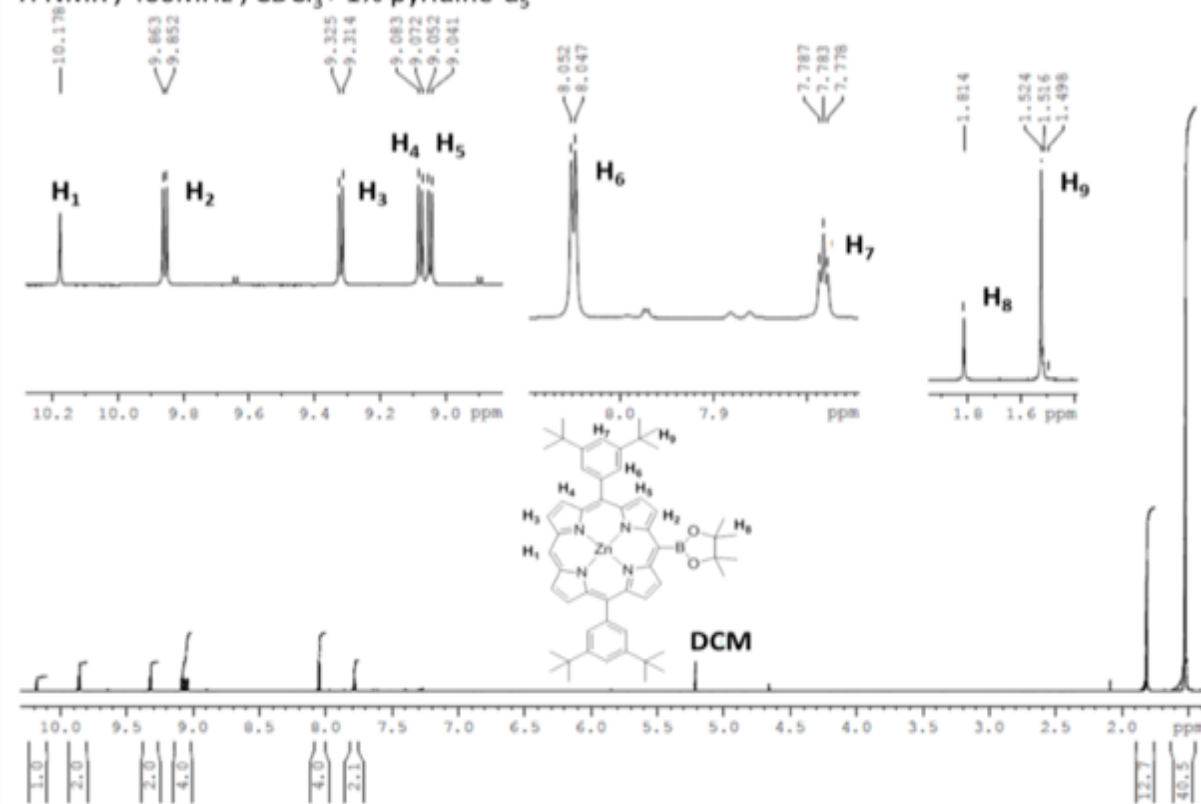
¹H NMR (400 MHz, CDCl₃ + 1 % Pyridine-d₅): δ = 9.84 (d, 4.6 Hz, 4H), 9.03 (d, 4.6 Hz, 4H), 8.03 (d, 1.8 Hz, 4H), 7.77 (t, 1.8 Hz, 2H), 1.83 (s, 12H), 1.53 (s, 36H) ppm.

¹³C NMR (100 MHz, CDCl₃ + 1 % Pyridine-d₅): δ = 152.9, 150.0, 147.9, 142.5, 132.3, 132.0, 129.7, 125.2, 121.4, 120.2, 84.8, 34.8, 31.6, 25.1 ppm.

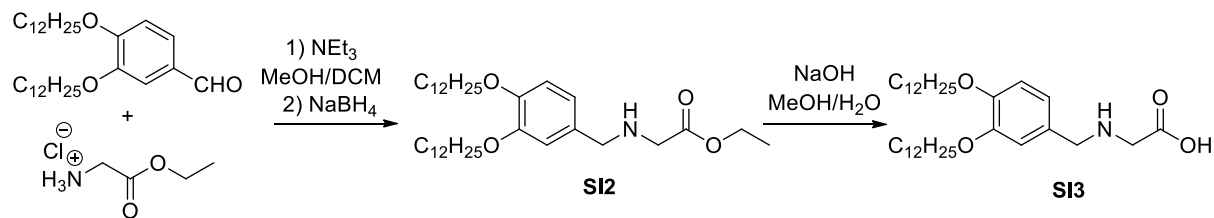
¹H NMR ; 400MHz ; CDCl₃+ 1% Pyridine-d₅



¹H NMR ; 400MHz ; CDCl₃+ 1% pyridine-d₅



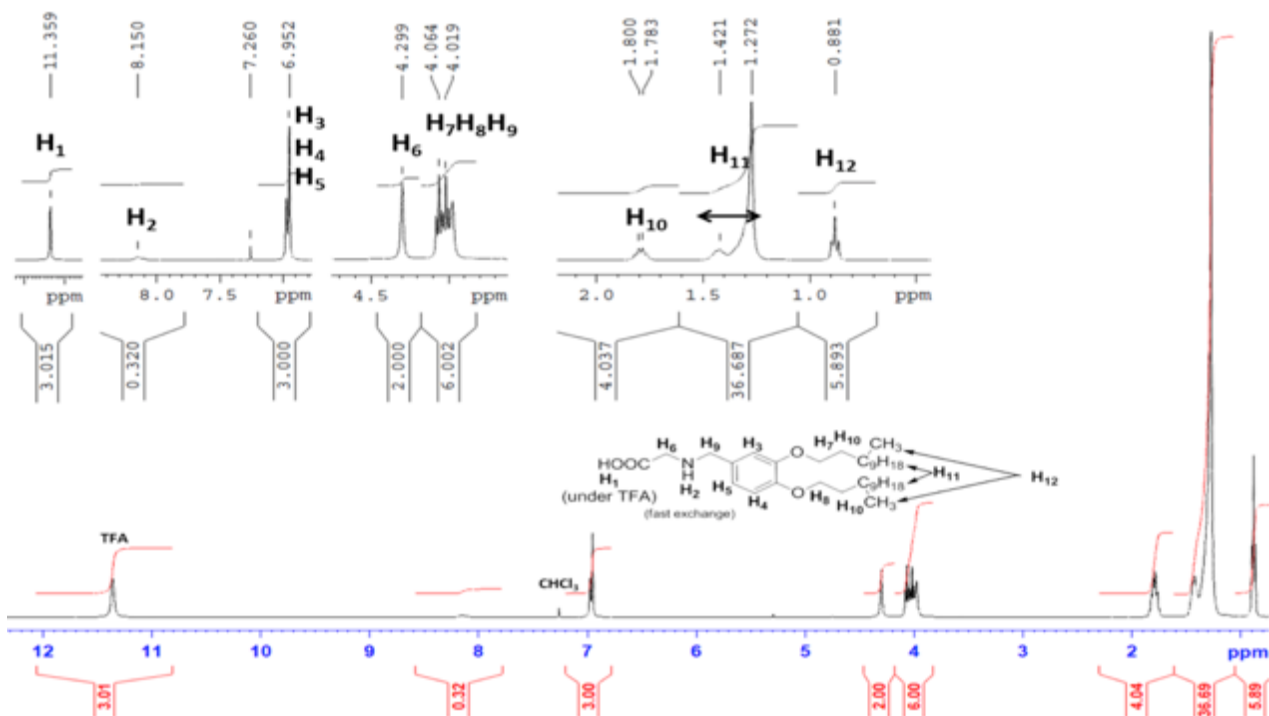
b. 2-((3,4-Bis(dodecyloxy)benzyl)amino)acetic acid (**S3**)



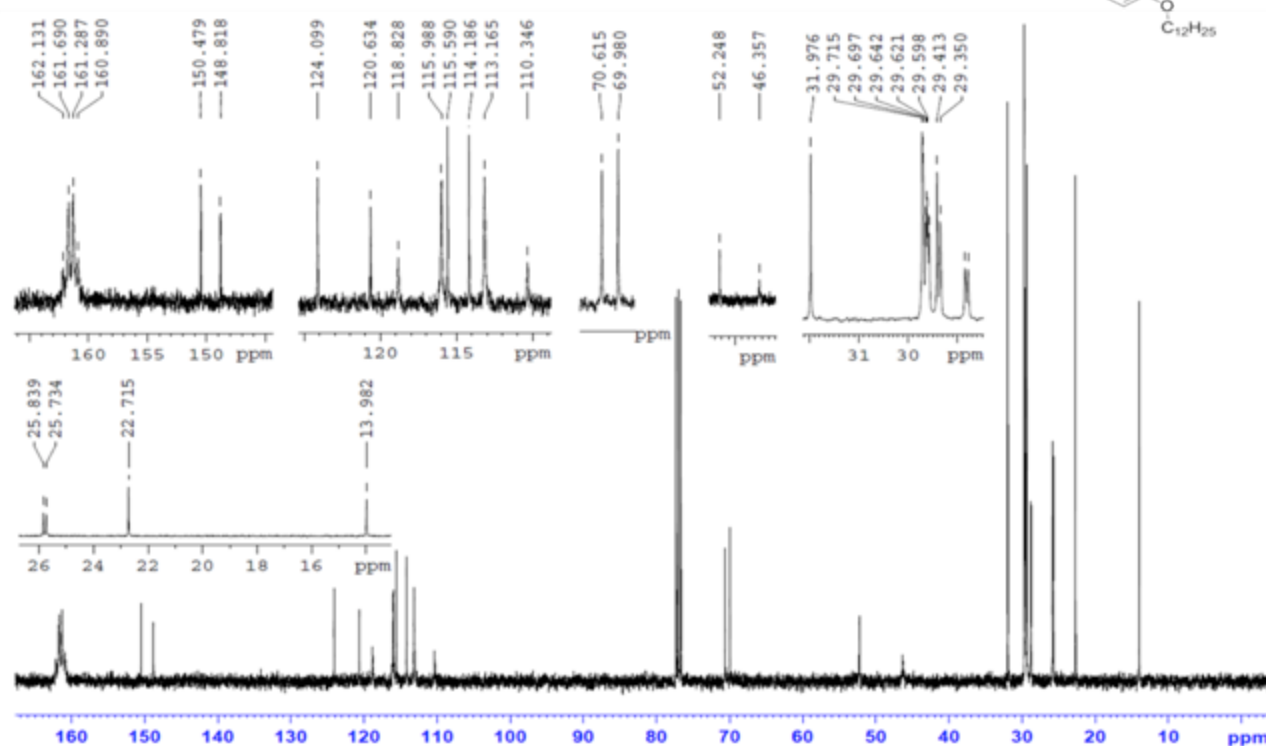
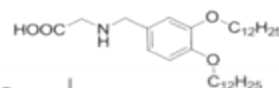
2-((3,4-Bis(dodecyloxy)benzyl)amino)acetic acid **S3** was synthesized in two steps: reductive amination of 3,4-didocylbenzaldehyde with glycine ethyl ester and sodium borohydride, followed by saponification of the ester with aqueous sodium hydroxide.

3,4-Didodecyloxybenzaldehyde (1.4 g; 10 mmol; 1.25 eq.) was dissolved in a methanol/dichloromethane (10/1 mixture; 20 mL). Triethylamine (1.4 mL; 10 mmol; 1.25 eq.) and glycine ethyl ester hydrochloride (4.2 g; 8 mmol; 1 eq.) were added. The mixture was stirred for 1 h at room temperature and sodium borohydride (0.72 g; 20 mmol; 2.5 eq.) was then added in portions at 0 °C. The solution was subsequently stirred overnight at room temperature. Water (10 mL) was added and the amino-ester **S12** was extracted with ethyl acetate (2 x 15 mL), washed with water (2 x 10 mL) and brine (1 x 10 mL), dried over MgSO_4 and filtrated. The solvent was evaporated, and **S2** was further purified by chromatography (SiO_2 ; *Eluent 1* = petroleum ether 40–60 °C /ethyl acetate 4/1 to remove the remaining starting material; *Eluent 2* = petroleum ether 40–60 °C /ethyl acetate 1/1 to get the desired product). This yielded **S2** as a pale yellow oil, which was then added mixture of aqueous concentrate sodium hydroxide (10 mL; 277 mmol) and methanol (5 mL). The suspension was then vigorously stirred 2 days at 70 °C and the solution was neutralized at 0 °C with concentrated aqueous hydrochloric acid (23.1 mL; 277 mmol). The precipitate was then filtered-off, washed several time with water until the pH of the mother-liquid reaches 7, and dried under vacuum over P_2O_5 to yield **S3** as a white powder (3.4 g; 6.3 mmol; 79%).

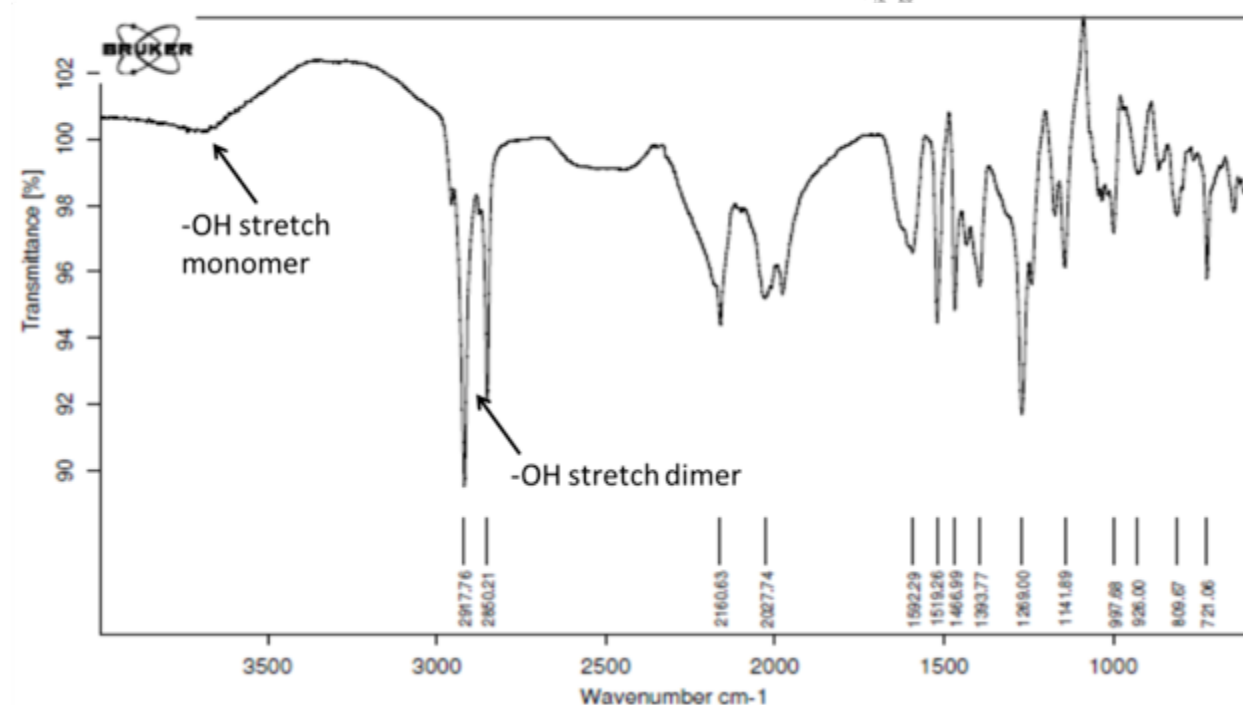
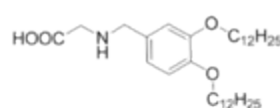
$^1\text{H NMR}$; 400MHz ; $\text{CDCl}_3 + \text{TFA}$



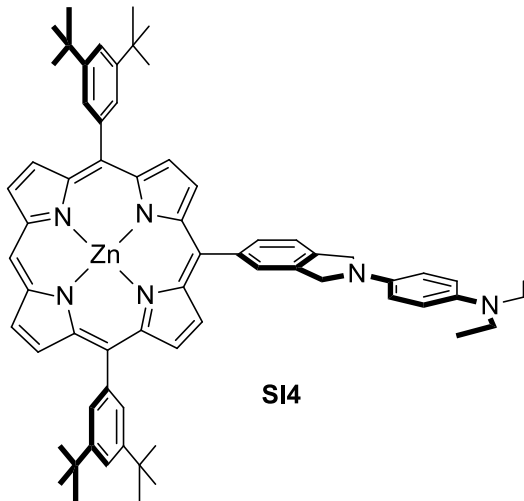
^{13}C NMR ; 100MHz ; $\text{CDCl}_3 + 1\%$ Pyridine-d₅



Infra-red vibrational spectroscopy (neat)

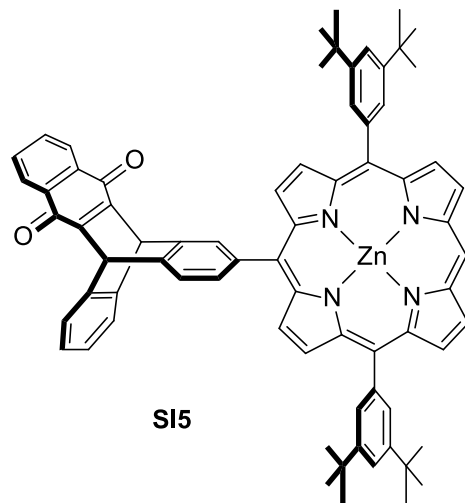


- c. [5,15-Bis-(3,5-bis-*tert*-butylphenyl)-10(4-(diethylamino)phenyl)-4*H*-isoindolin-2-yl]porphinato]zinc(II) (**SI4**) and [5,15-Bis-(3,5-bis-*tert*-butylphenyl)-10-(5,12-[1,2]benzenotetracen-2-yl-6,11(5*H*,12*H*)-dione]porphinato]zinc(II) (**S5**)



A dry two-neck flask equipped with a condenser was charged with **S1** (100 mg; 114 μ mol; 1 eq.), **7** (47 mg; 136 μ mol; 1.2 eq.), freshly recrystallized tetrakis(triphenylphosphine)palladium(0) (13 mg; 11.4 μ mol; 0.1 eq.) and cesium carbonate (111 mg; 342 μ mol; 3 eq.). The mixture was purged 3 times with argon and a mixture of toluene (10 mL) and pyridine (150 μ L) was added. The solution was purged 5 more times with argon and the reaction mixture was refluxed for 7 h. The solvent was evaporated and the product was purified by chromatography (SiO_2) using dichloromethane 98 : 2 methanol as eluent and further purified by size-exclusion column (eluent chloroform +1% pyridine) to yield after drying under vacuum **S4** as purple powder (95 mg; 93 μ mol; 82%).

$^1\text{H NMR}$ (400 MHz, $\text{CDCl}_3 + 1\%$ Pyridine- d_5): $\delta = 10.16$ (s, 1H), 9.36 (d, 4.5 Hz, 2H), 9.11 (d, 4.5 Hz, 2H), 9.02 (d, 4.5 Hz, 2H), 8.96 (d, 4.5 Hz, 2H), 8.17 (m, 2H), 8.12 (d, 1.8 Hz, 4H), 7.82 (t, 1.8 Hz, 2H), 7.65 (d, 8.3 Hz, 1H), 6.92 (m, 2H), 8.77 (m, 2H), 4.93 (s, 2H), 4.89 (s, 2H), 1.58 (s, 36H) ppm.

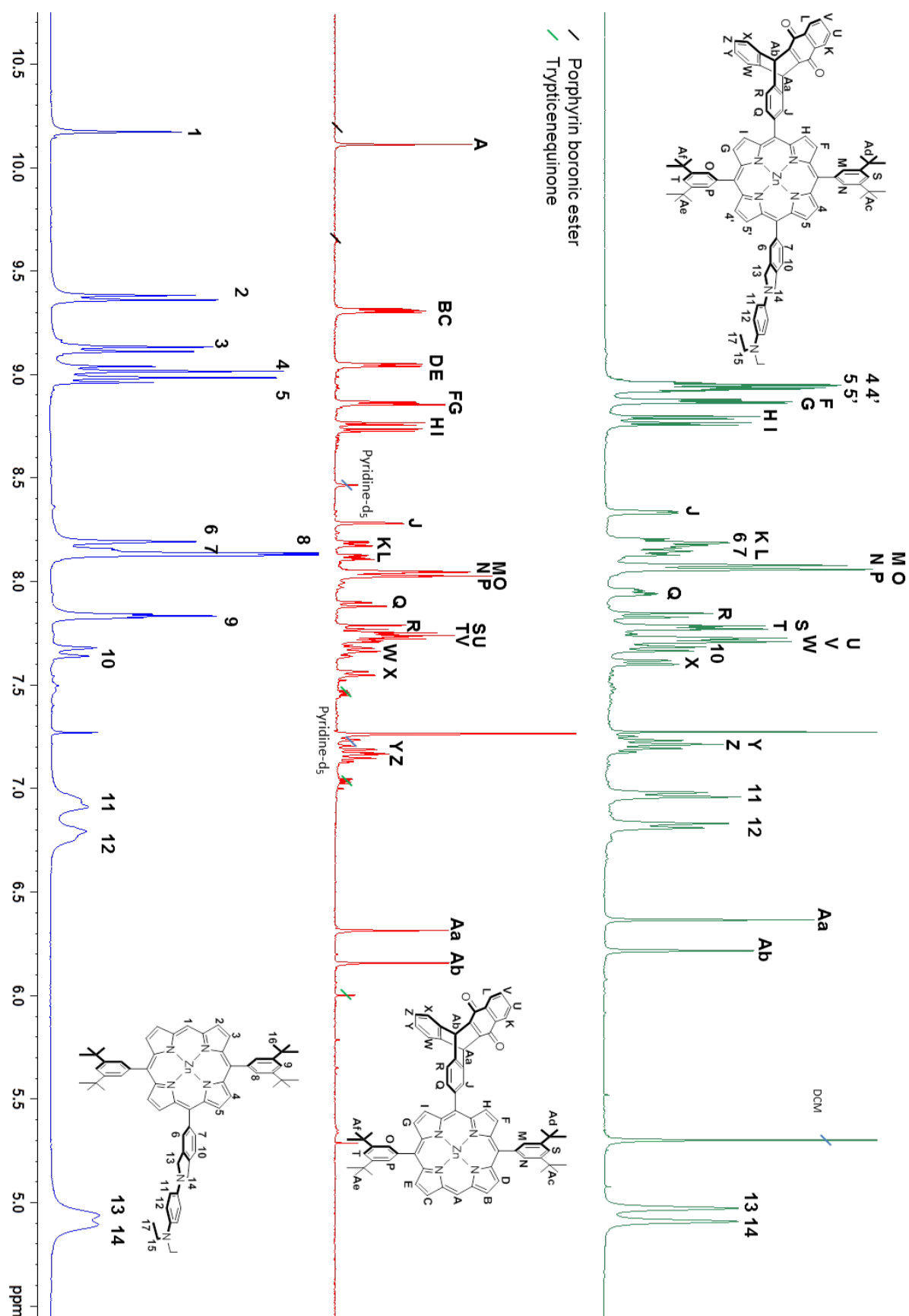


A dry two-neck flask equipped with a condenser was charged with **S1** (10.0 mg; 11.4 μ mol; 1 eq.), 7-bromo-triptyceneneaphtoquinone (intermediate in the synthesis of **10**, mixture with triptyceneneaphtoquinone, 6.1 mg; 13 μ mol; 1.2 eq.), freshly recrystallized tetrakis(triphenylphosphine)palladium(0) (1.2 mg; 1.1 μ mol; 0.1

eq.) and cesium carbonate (10.8 mg; 33.1 μ mol; 3.0 eq.). The mixture was purged 3 times with argon and a mixture of toluene (2 mL) and pyridine (30 μ L) was added. The solution was purged 5 more times with argon and the reaction mixture was refluxed for 2 days. The solvent was evaporated and the product was purified by chromatography (SiO_2) using dichloromethane 3 : 1 petrol ether 40–60°C as eluent to yield after drying under vacuum **S15** as purple powder (7.1 mg; 6.6 μ mol; 60%).

¹H NMR (400 MHz, $\text{CDCl}_3 + 1\% \text{Pyridine-}d_5$): $\delta = 10.11$ (s, 1H), 9.31 (d, 4.6 Hz, 1H), 9.30 (d, 4.6 Hz, 1H), 9.04 (d, 4.6 Hz, 1H), 8.86 (d, 4.6 Hz, 1H), 8.85 (d, 4.6 Hz, 1H), 8.76 (d, 4.6 Hz, 1H), 8.73 (d, 4.6 Hz, 1H), 8.28 (d, 1.6 Hz, 1H), 8.18 (m, 1H), 8.11 (m, 1H), 8.04 (m, 2H), 8.02 (m, 2H), 7.88 (dd, 7.2 Hz, 1.6 Hz, 1H), 7.77 (d, 7.2 Hz, 1H), 7.73 (m, 4H), 7.66 (m, 1H), 7.55 (dd, 7.2 Hz, 1.2 Hz, 1H), 7.16 (m, 2H), 6.31 (s, 1H), 6.15 (s, 1H), 1.52 (s, 9H), 1.51 (s, 9H), 1.50 (s, 9H), 1.49 (s, 9H) ppm.

4) Assignment of the TAPD-ZnP_{Ar}-TNQ triad ¹H NMR spectrum using reference compounds



5) Frontier orbital energies

B3LYP/6-31G*

	TNQ-ZnP-TAPD	TNQ-ZnPAr-TAPD	C ₆₀ -ZnPAr-TAPD
HOMO-2	-4.90	-5.08	-5.12
HOMO-1	-4.79	-4.92	-4.95
HOMO	-4.35	-4.25	-4.27
LUMO	-3.02	-3.07	-3.10; -2.99; -2.75*
LUMO+1	-1.82	-2.08	-2.10
LUMO+2	-1.80	-2.05	-2.09

* The LUMO of C₆₀ is triply degenerate, but the saturation at the pyrrolidine linking breaks the symmetry.

M062X /6-31G*

	TNQ-ZnP-TAPD	TNQ-ZnPAr-TAPD	C ₆₀ -ZnPAr-TAPD
HOMO-2	-5.91	-6.04	-6.08
HOMO-1	-5.71	-5.86	-5.89
HOMO	-5.66	-5.62	-5.85
LUMO	-2.12	-2.09	-2.61 / -2.47 / -2.21
LUMO+1	-1.34	-1.59	-1.64
LUMO+2	-1.33	-1.57	-1.62

CAM-B3LYP /6-31G*

	TNQ-ZnP-TAPD	TNQ-ZnPAr-TAPD	C ₆₀ -ZnPAr-TAPD
HOMO-2	-5.90	-5.98	-6.02
HOMO-1	-5.66	-5.89	-5.93
HOMO	-5.61	-5.59	-5.78
LUMO	-1.84	-1.81	-2.14 / -1.99 / -1.73
LUMO+1	-0.96	-1.20	-1.24
LUMO+2	-0.96	-1.18	-1.22

ω -B97xD/6-31G*

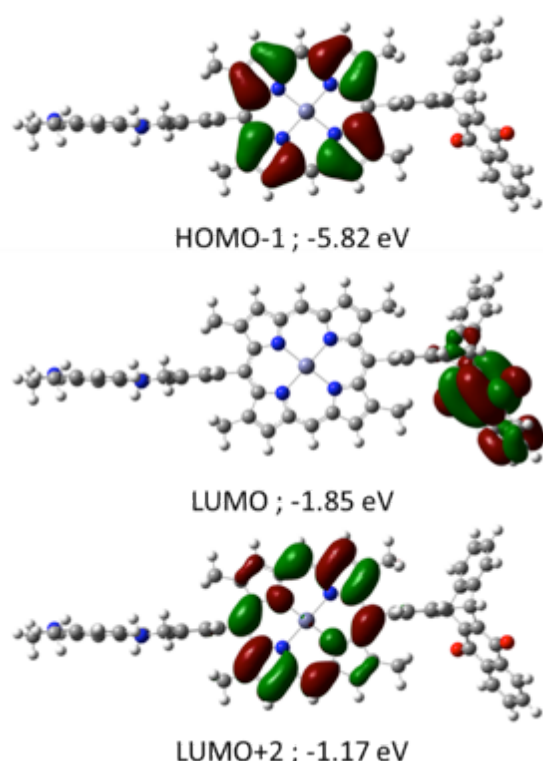
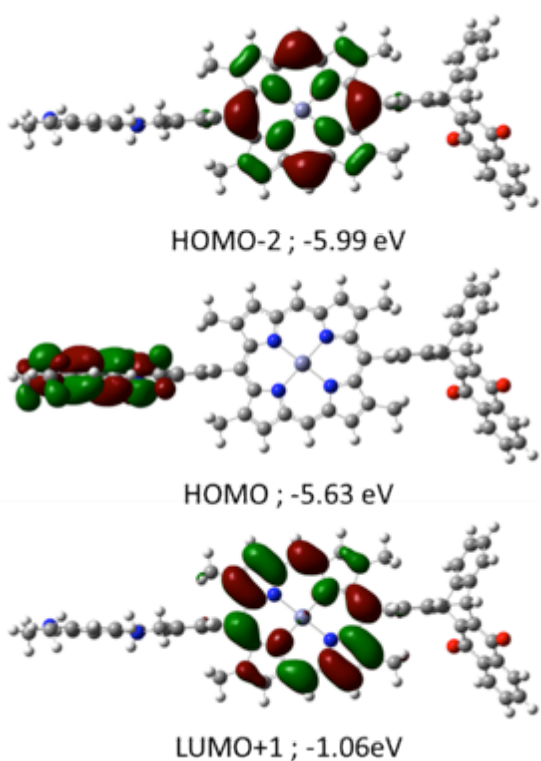
	TNQ-ZnP-TAPD	TNQ-ZnPAr-TAPD	C ₆₀ -ZnPAr-TAPD
HOMO-2	-4.90	-6.51	-6.55
HOMO-1	-4.79	-6.38	-6.42
HOMO	-4.35	-6.17	-6.41
LUMO	-3.02	-1.27	-1.71 / -1.55 / -1.29
LUMO+1	-1.82	-0.74	-0.78
LUMO+2	-1.80	-0.71	-0.75

HF/6-31G*

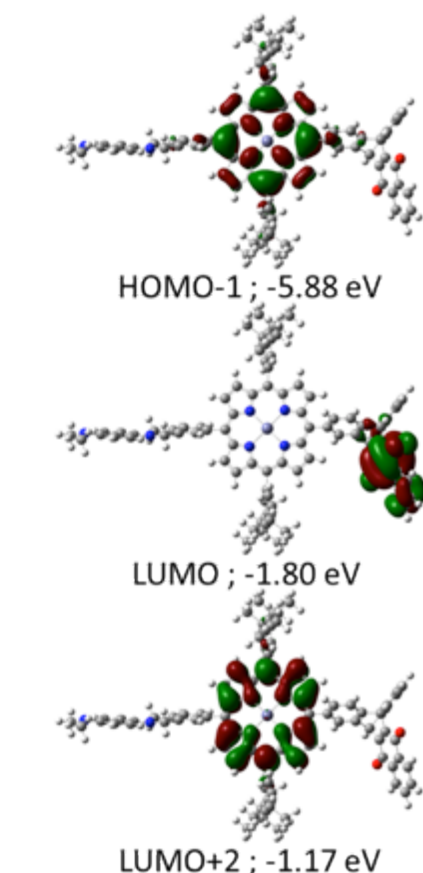
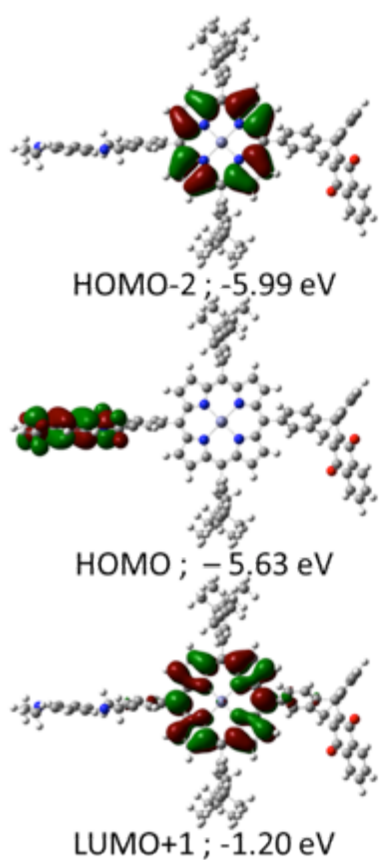
	TNQ-ZnP-TAPD	TNQ-ZnPAr-TAPD	C ₆₀ -ZnPAr-TAPD
HOMO-2	-6.43	-6.48	-6.51
HOMO-1	-5.64	-5.93	-5.95
HOMO	-6.69	-7.32	-7.29
LUMO	0.75	0.83	-0.18 / -0.05 / 0.33
LUMO+1	1.04	0.76	0.74
LUMO+2	1.10	0.77	0.80

6) Frontier orbitals distribution

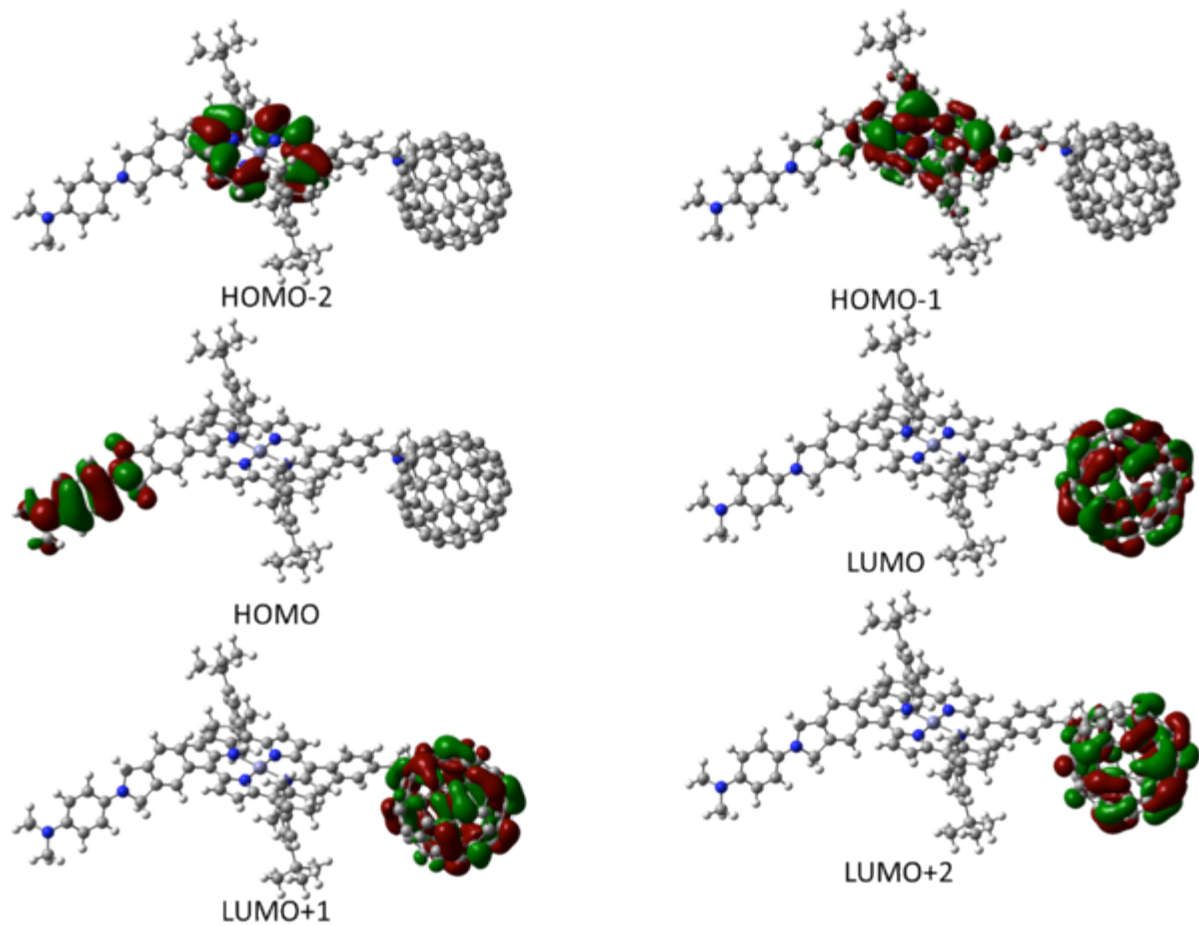
a. Triad TNQ-ZnP-TAPD



b. Triad TNQ-ZnP_{Ar}-TAPD



c. Triad C₆₀-ZnP_{Ar}-TAPD



7) Ionization energy and electron affinity of moieties

Ionization potential (IP) and electron affinity (EA) (eV)						
6-31G*, PCM in butyronitrile	CAM-B3LYP		M062X		B3LYP	
	IP	EA	IP	EA	IP	EA
TADP	4.24		4.42		4.15	
ZnP _{Ar}	4.98	-2.48	5.16	-2.43	4.95	-2.75
ZnP	4.72	-2.31	5.03	-2.22	4.81	-2.47
TNQ		-3.37		-3.48		-3.40
C ₆₀		-3.03		-3.31		-3.20
6-31G*, PCM in acetonitrile	CAM-B3LYP		M062X		B3LYP	
	IP	EA	IP	EA	IP	EA
TADP	4.22		4.40		4.13	
ZnP _{Ar}	4.96		5.21		4.94	-2.67
ZnP	4.71		5.01		4.79	-2.45
TNQ		-3.40		-3.51		-3.42
C ₆₀		-3.05		-3.33		-3.22
6-31G*, PCM in tetrahydrofuran	CAM-B3LYP		M062X		B3LYP	
	IP	EA	IP	EA	IP	EA
TADP	4.37		4.55		4.28	
ZnP _{Ar}	5.09		5.33		5.06	
TNQ		-3.17		-3.28		-3.20
C ₆₀		-2.91		-3.19		-3.08
6-31G*, Gas Phase	CAM-B3LYP		M062X		B3LYP	
	IP	EA	IP	EA	IP	EA
TADP	5.68		5.83		5.58	
ZnP _{Ar}	6.15		6.32		6.03	
ZnP			6.47			
TNQ		-1.60		-1.68		-1.65
C ₆₀		-1.81		-2.09		-1.99
6-311G**, PCM in butyronitrile	CAM-B3LYP		M062X		B3LYP	
	IP	EA	IP	EA	IP	EA
TADP	4.49		4.63		4.41	
TNQ		-3.84		-3.88		-3.86
6-311G**, PCM in acetonitrile	CAM-B3LYP		M062X		B3LYP	
	IP	EA	IP	EA	IP	EA
TADP	4.48		4.61		4.39	
TNQ		-3.87		-3.91		-3.89

8) Inner-sphere reorganization energies

We report inner-sphere reorganization energies at several levels of theory and solvent combinations for the moieties. These were computed as $\lambda_S = E_S^R - E_S^P$, where R and P represent reaction and product, and S represents the potential energy surface: either the charged ($-1e$ or $+1e$, for anion and cation respectively), or the neutral surfaces (N).

		Reorganization Energy (eV)								
		CAM-B3LYP				B3LYP		M062X		
6-31G*	PCM in Gas Phase	-1 e	N	+1 e	-1 e	N	+1 e	-1 e	N	+1 e
TADP		0.35	0.23		0.27	0.18		0.42	0.24	
TNQ			0.26	0.25		0.21	0.20		0.26	0.26
		CAM-B3LYP				B3LYP		M062X		
6-31G*	PCM in THF	-1 e	N	+1 e	-1 e	N	+1 e	-1 e	N	+1 e
TADP		0.37	0.22		0.29	0.17		0.44	0.24	
ZnP _{Ar}		0.05	0.05		0.04	0.04		0.07	0.13	
TNQ			0.26			0.21	0.21		0.27	0.26
C ₆₀					0.07	0.07		0.09	0.09	
		CAM-B3LYP				B3LYP		M062X		
6-31G*	PCM in butyronitrile	-1 e	N	+1 e	-1 e	N	+1 e	-1 e	N	+1 e
ZnP _{Ar}		0.06	0.05							
C ₆₀			0.09	0.09		0.07	0.07		0.09	0.09
		CAM-B3LYP				B3LYP		M062X		
6-31G*, PCM in acetonitrile		-1 e	N	+1 e	-1 e	N	+1 e	-1 e	N	+1 e
TADP		0.37	0.22		0.29	0.17		0.44	0.23	
ZnP _{Ar}		0.05	0.05		0.04	0.05		0.07	0.13	
ZnP		0.06	0.06		0.19	0.05		0.08	0.13	
TNQ			0.26	0.25		0.21	0.21		0.27	0.26
C ₆₀					0.07	0.07		0.09	0.09	

		CAM-B3LYP				B3LYP		M062X		
6-311G**	PCM in THF	-1 e	N	+1 e	-1 e	N	+1 e	-1 e	N	+1 e
TADP		0.39	0.23		0.31	0.18		0.46	0.24	
TNQ			0.28	0.28		0.23	0.23		0.29	0.28
C ₆₀						0.07				
		CAM-B3LYP				B3LYP		M062X		
6-311G**	PCM in acetonitrile	-1 e	N	+1 e	-1 e	N	+1 e	-1 e	N	+1 e
TADP		0.40	0.27		0.31	0.18		0.47	0.24	
TNQ			0.28	0.28		0.23	0.23		0.29	0.28
C ₆₀					0.07	0.07		0.08	0.09	

9) Predicted Recombination Rates

We report here the recombination rates from the long-lived radical pair state to the ground state, and the parameters used for that prediction:

- ΔG corresponds to the electronic energy difference between the ground state and the charge transfer state in solution (butyronitrile) at their respective equilibrium geometries. It corresponds to the energy difference between the bottoms of the parabola in the Marcus approximation.
- λ_{out} corresponds to the outer-sphere reorganization energy in upon electron transfer in solution. In frozen solvent, it is added to ΔG , to obtain the effective ΔG in frozen solvent, to capture the fact that only the electronic degrees of freedom of the solvent can respond to the charge transfer.
- $\lambda_{\text{in}}^{\text{vib}}$ corresponds to the inner-sphere reorganization calculated as ($\lambda_j = \sum_i S_{ij} \omega_{ij}$). We report different values depending of the energy surface on which the vibrational modes were calculated (the neutral or the charge-transfer species) and also depending on whether whole triads were used, or only the displacements and vibrational motions of isolated donor and acceptor units.
- Exclusively for reference, since it does not play any role in the calculation of the lifetimes, we report $\lambda_{\text{in}}^{\text{diff}}$. This magnitude corresponds to the energy differences between potential energy surfaces at either the reactant or product equilibrium geometry. They are reported above and included here for comparison with the values calculated from vibronic displacements.

Predicted recombination lifetimes for the TNQ-ZnP_{Ar}-TAPD triad

			ΔE (eV)	λ_{out} (eV)	$\lambda_{\text{in}}^{\text{vib}}$ (eV)	$\lambda_{\text{in}}^{\text{diff}}$ (eV)	Lifetime (ms)
CAMB3LYP	Neutral	Parts	0.79	1.38	0.52	0.48	0.4
		Whole	0.79	1.38	0.52	0.48	0.4
	CT	Parts	0.79	1.38	0.62	0.62	0.1
		Whole	0.79	1.38	0.57		0.3
M062X	Neutral	Parts	0.85	1.32	0.59	0.50	0.2
		Whole	0.85	1.32	0.69	0.49	0.05
	CT	Parts	0.85	1.32	0.71	0.70	0.04
		Whole	0.85	1.32	0.59		0.6
B3LYP	Neutral	Parts	0.72	1.27	0.43	0.38	1.3
		Whole	0.72	1.27	0.44	0.38	1.3
	CT	Parts	0.72	1.27	0.51	0.50	0.4
		Whole	0.72	1.27	0.48	0.50	0.9

Predicted recombination lifetimes for the TNQ-ZnP_{Ar}-TAPD triad

			ΔE (eV)	λ_{out} (eV)	$\lambda_{\text{in}}^{\text{vib}}$ (eV)	$\lambda_{\text{in}}^{\text{diff}}$ (eV)	Lifetime (ms)
CAMB3LYP	Neutral	Parts	1.01	1.25	0.35	0.31	1475
		Whole	1.01	1.25	0.38	0.31	443
	CT	Parts	1.01	1.25	0.44	0.46	85
		Whole	1.01	1.25	0.38		875
M062X	Neutral	Parts	0.92	1.21	0.40	0.32	278
		Whole	0.92	1.21	0.43	0.31	114
	CT	Parts	0.92	1.21	0.53	0.53	5.5
		Whole	0.92	1.21	0.49		23.3
B3LYP	Neutral	Parts	0.75	1.21	0.27	0.24	2700
		Whole	0.75	1.21	0.28	0.24	1200
	CT	Parts	0.75	1.21	0.34	0.36	255
		Whole	0.75	1.21	0.31		741

10) Analysis of the Influence of Conformational Factors on Electronic Coupling

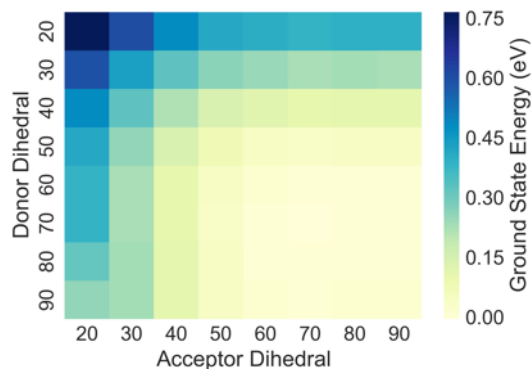


Figure S1. Ground state DFT/B3LYP/6-31G* energy of **TNQ-ZnP_{Ar}-TAPD** as a function of dihedral angle. The more co-planar conformations only occur at a high-energy cost. There is a single overall minimum described with dihedral angles at around 70 degrees.

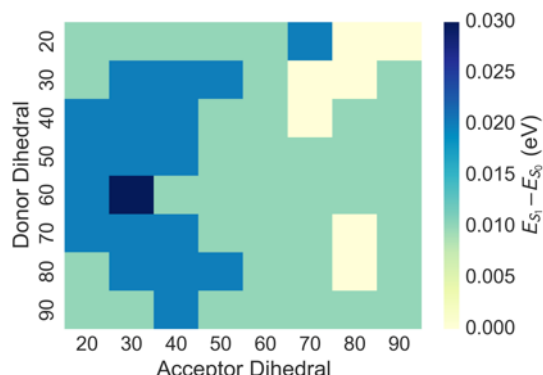


Figure S2. Excitation energy to the CSS₂ charge-transfer state TD-DFT/B3LYP/6-31G* energy of **TNQ-ZnP_{Ar}-TAPD** as a function of dihedral angle, in fluid solution. The energy of the excited state (essentially Coulombic in nature) is hardly affected by the dihedral angle, especially since the π systems remained isolated even in the more planar conformations

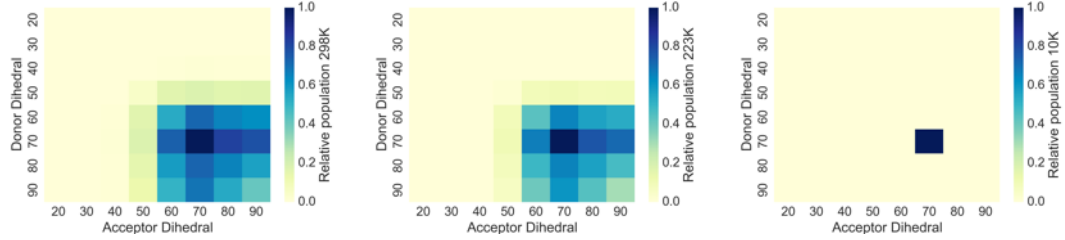


Figure S3. Relative population of **TNQ-ZnP_{Ar}-TAPD**, form the Boltzmann distribution, a) at 298 K and b) at 223 K (melting point of xylene) and c) at 10 K. For slower cooling rates that thermal distribution at which the conformations are effectively frozen is expected to correspond to different temperatures. In all cases the only minimum has a dominating contribution.

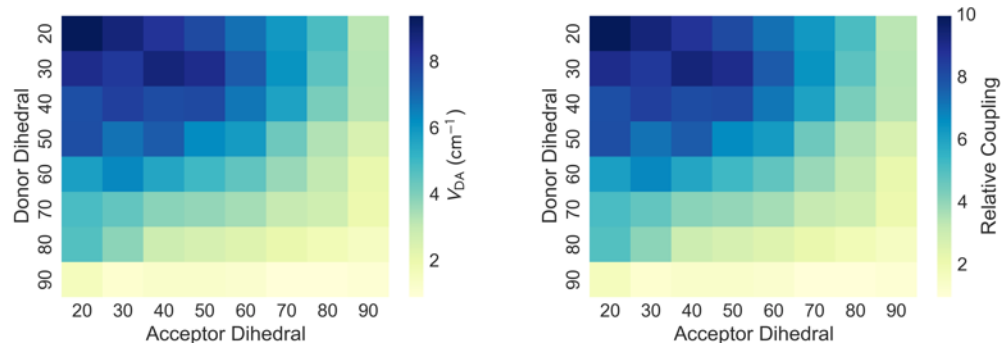
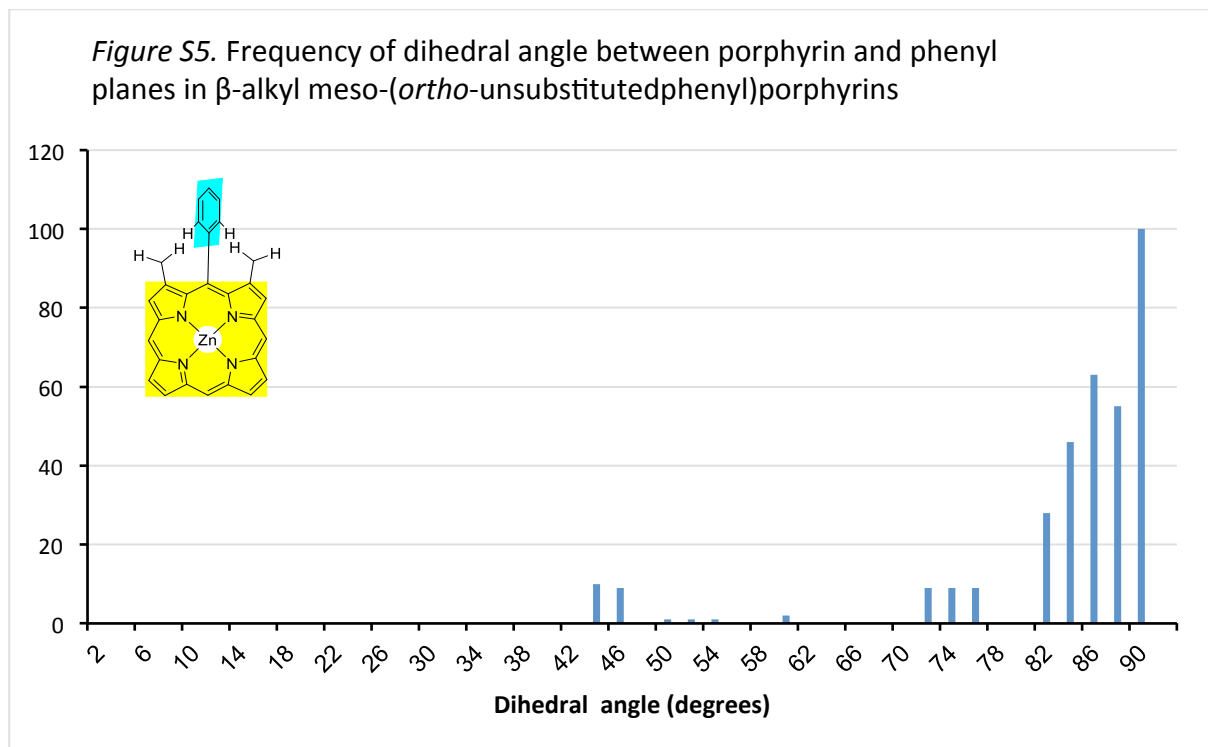


Figure S4. Relative GMH electronic coupling V_{DA} in **TNQ-ZnP_{Ar}-TAPD** as a function of the dihedral angles. As explained by the lack of extended conjugation, the dihedral angle has a modest effect on electronic coupling. Bis-*tert*-butylphenyl groups were removed to reduce the cost of simulation. 10-degree steps were used, for a total of 64 data points. Electronic coupling was calculated as described in the manuscript. The shape of the potential energy surface, in combination with the reduced effect of geometry on the electronic coupling, results in the Boltzmann-weighted electronic coupling being within 5% of the electronic coupling for the minimum-energy conformation.

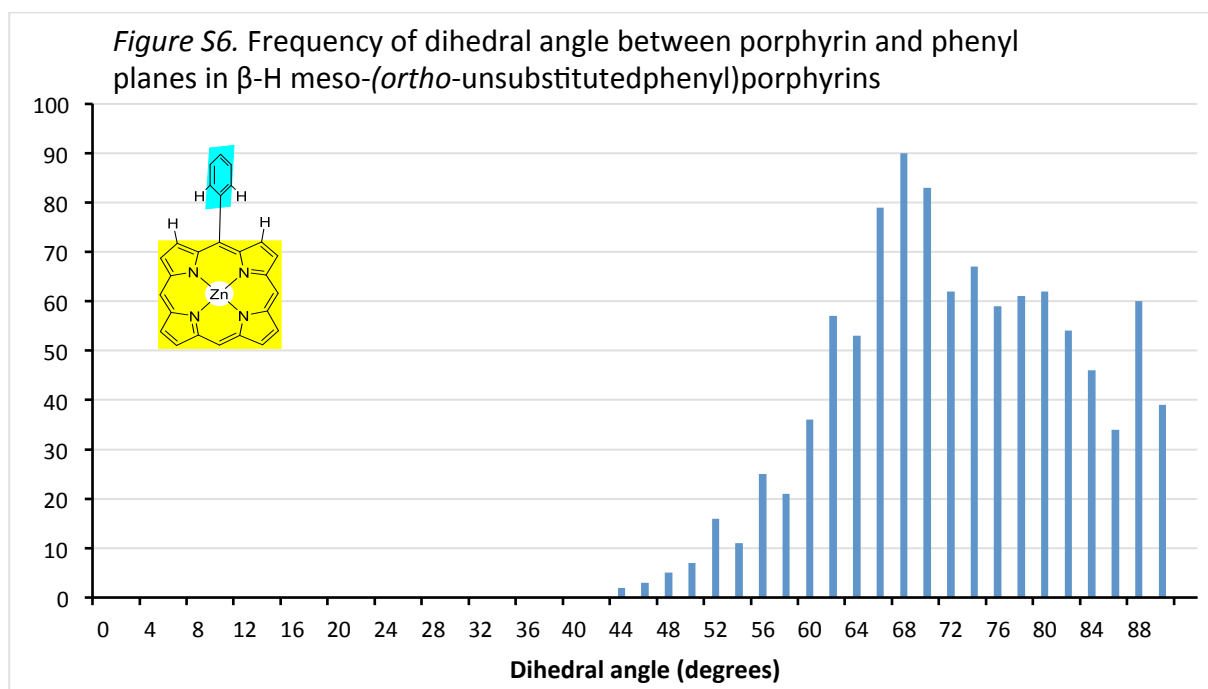
11) Cambridge database analysis of the dihedral angles between meso-phenyls and porphyrin planes.

The following up-to-date Cambridge database search results are consistent with earlier studies.⁵⁴

In β -alkyl substituted porphyrins (bin size of 2° , total number of structures: 343)



In β -unsubstituted porphyrins (bin size of 2° , total number of structures: 1032).



12) Methods and kinetic model fit of the EPR experiments

a. EPR methods:

EPR samples were prepared in 3.8 mm quartz EPR tubes, samples were degassed using several freeze pump thaw cycles and sealed under vacuum. The samples were stored at 77 K in the dark.

EPR experiment were carried out at 10 K on a Bruker ELEXSYS E580 spectrometer operating at X-band equipped with an MD5 dielectric resonator, Oxford Instruments continuous flow cryostat and ITC503 temperature controller. Laser excitation of the samples was provided by a Surelite OPO system, pumped by a Surelite I-20 Q-switched Nd:YAG laser, with a variable repetition rate. The photo-excitation wavelength was around 590 nm with a pulse energy of around 10 mJ per pulse and pulse width of 7 ns. Experiments on **TNQ-ZnP_{Ar}-TAPD**, **ZnTPP**, **C₆₀-ZnP_{Ar}-H** were carried out with the laser repetition rate at 20 Hz, while experiments on **C₆₀-ZnP_{Ar}-TAPD** was carried out with a repetition rate of 1 Hz, due to the long lifetime of the charge separation state.

b. Simulations:

Time resolved EPR spectra were simulated using the EasySpin toolbox^{S5} in MATLAB, simulated spectra were used to determine the zero field splitting parameters (ZFS) and the polarization of the triplet states seen in **TNQ-ZnP_{Ar}-TAPD**, **ZnTPP** and **C₆₀-ZnP_{Ar}-TAPD**.

The time resolved EPR spectrum for both the **TNQ-ZnP_{Ar}-TAPD** triad and the reference sample **ZnTPP**, taken 1 μ s after the laser flash, only showed a porphyrin triplet state. The porphyrin triplet for both EPR spectra was simulated using the same g tensors and relative sublevel populations, ZFS parameters used and relative populations of sublevels are shown in Table 1.

The time resolved EPR spectrum for the **C₆₀-ZnP_{Ar}-TAPD** triad showed a C₆₀ triplet and a spin polarized radical pair signal corresponding to the C₆₀⁻ anion. The C₆₀ triplet signal seen in the spectrum, taken 1.2 μ s after the laser flash, was simulated with the parameters in Table 1. The ZFS parameters and the relative triplet polarization is consistent with literature values for a C₆₀-pyrrolidine mono-adduct, while the negative sign for D is consistent with that of C₆₀, determined by ENDOR.^{S11}

Table 1 D / MHz E / MHz $p_x : p_y : p_z$ $g_x : g_y : g_z$ Ref.

TNQ-³ZnP_{Ar}-TAPD	910 ^a	287 ^b	0.18 : 0.0 : 0.82	2.005 : 2.000 : 2.000	This work
³ZnTPP	928 ^a	295 ^b	0.18 : 0.0 : 0.82	2.005 : 2.000 : 2.000	This work
TNQ -³ZnP- TAPD	1079	327	0.35 : 0.00 : 0.65		S6
³ZnTPP	893	294	0.0 : 0.0 : 1.0		S7
³ZnTPP	888				S8
³C₆₀-ZnP_{Ar}-TAPD	-272 ^c	39	0.28 : 0.72 : 0.00	2.001 : 2.001 : 2.003	This work
³C₆₀-pyrrolidine	-234	30	0.23 : 0.87 : 0.00		S9
³C₆₀-pyrrolidine	270	-42			S10

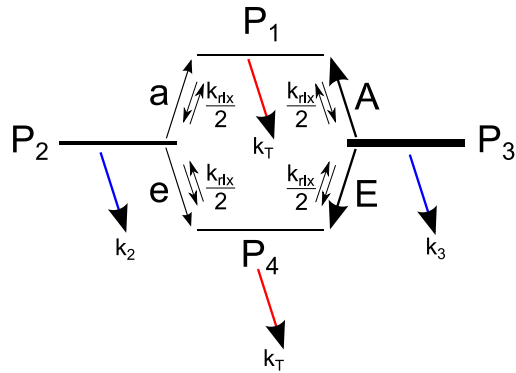
^a Gaussian distribution of D with a FWHM of 70 MHz

^b Gaussian distribution of E with a FWHM of 20 MHz

^c Gaussian distribution of D with a FWHM of 60 MHz.

c. **Flash-delay experiment – kinetic model fit for CSS decay:**

Change in population of sub-levels in 4-level system of Radical Pair:



The time evolution of the radical pair peaks can be calculated using simple rate equations, for each sublevel in the 4-level system, as previously shown by Miura and Wasielewski.^{S12}

$$\frac{dP_1}{dt} = (P_2 + P_3) \frac{k_{rlx}}{2} - P_1(k_{rlx} + k_T)$$

$$\frac{dP_2}{dt} = (P_1 + P_4) \frac{k_{rlx}}{2} - P_2(k_{rlx} + k_2)$$

$$\frac{dP_3}{dt} = (P_1 + P_4) \frac{k_{rlx}}{2} - P_3(k_{rlx} + k_3)$$

$$\frac{dP_4}{dt} = (P_2 + P_3) \frac{k_{rlx}}{2} - P_4(k_{rlx} + k_T)$$

Where

$$k_2 = k_s \cos^2 \theta + k_T \sin^2 \theta$$

$$k_3 = k_s \sin^2 \theta + k_T \cos^2 \theta$$

$$k_{rlx} = \frac{1}{T_1}$$

and k_s and k_T are the singlet and triplet recombination rates respectively.

We assume no recombination from the pure triplet levels (P_1 and P_4) and therefore the fast and slow decay seen experimentally must be due to k_s and k_{rlx} , therefore $k_s \gg k_{rlx}$. Since triplet recombination is not allowed we can say $k_2 \approx k_3 \approx k_s$.

The emission peak intensity is given by $I_{34}(t) = C_{34}(P_4(t) - P_3(t))$ and where C_{34} is the transition probability.

Substituting for $P_4(t)$ and $P_3(t)$ gives:

$$I_{34}(t) = C_{34}(P_4 e^{-(k_{rlx})t} - P_3 e^{-(k_s)t}) \quad (S1)$$

We solve equation (S1) analytically, with the addition of a Gaussian distribution in the rate constants k_{rlx} and k_s , and fit this model to the experimental trace. The fit result gives:

$k_s = k_{fast} = 1.8 \times 10^5 \text{ s}^{-1}$ with one standard deviation of $0.7 \times 10^5 \text{ s}^{-1}$.

$k_{rlx} = k_{slow} = 64 \text{ s}^{-1}$ with one standard deviation of 32 s^{-1} .

d. Spin polarized radical pair signal:

The central emission/absorption peak centered at $g = 1.9999$ can be attributed to the C_{60}^- anion, since the g factor matches those previously reported in literature and also as we do not expect to see the TAPD⁺ cation ($g = 2.0023\text{--}2.0030$), due to hyperfine broadening.^{S6,S13–16}

Magnetic field calibration using ³¹P in ²⁸Si.

e. Estimation of the Quantum Yield for Formation of CSS₂ in C₆₀-ZnP_{Ar}-TAPD:

The quantum yield was estimated from the area of the signal from the charge-separated state (CSS), as a percentage of the total area of the time-resolved EPR spectrum (trEPR).

The central part of the trEPR spectrum was fitted to a 3rd order polynomial and two Gaussians (Gaussian 1, blue: emissive, and Gaussian 2, cyan: absorptive; Figure S7).

The quantum yield was estimated as the sum of the areas of the two Gaussians (Gaussian 1 + Gaussian 2) divided by the total area, giving a value of about 0.1.

This estimate assumes that formation of CSS₂ and the C₆₀ triplet are the dominant decay channels, and that these two species have similar polarizations.

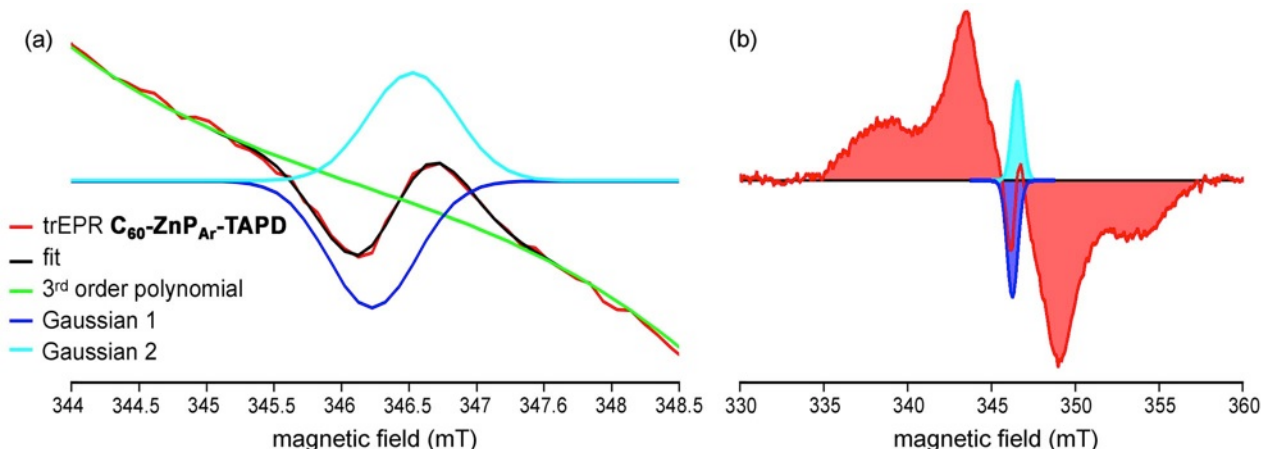


Figure S7. Time-resolved EPR spectrum **C₆₀-ZnP_{Ar}-TAPD**, taken 1.2 μs after laser flash. (a) Central feature, showing experimental data (red), fitting with 3rd order polynomial and two Gaussians (black), 3rd order polynomial (green), Gaussian 1 – emissive peak (blue) and Gaussian 2 – absorptive peak (cyan).

(b) Whole spectrum showing Gaussian 1 – emissive peak (blue line), Gaussian 2 – absorptive peak (cyan line). Absolute area taken of shaded regions.

13) Supporting References

- S1 R. S. Coleman and M. A. Mortensen, *Tetrahedron Letters*, 2003, **44**, 1215.
- S2 J. Plater, S. Aikena and G. Bourhill, *Tetrahedron*, 2002, **58**, 2405.
- S3 N. K. S. Davis, A. L. Thompson and H. L. Anderson, *Org. Lett.*, 2010, **12**, 2124.
- S4 H. L. Anderson, *Chem. Commun.*, 1999, **23**, 2323; H. N. Fonda, J. V. Gilbert, R. A. Cormier, J. R. Sprague, K. Kamioka and J. S. Connolly, *J. Phys. Chem.*, 1993, **97**, 7024.
- S5 S. Stoll and A. J. Schweiger, *Magn. Reson.*, 2006, **178**, 42.
- S6 A. Van Der Est, G. Fuechsle, D. Stehlik and M. R. Wasielewski, *Appl. Magn. Reson.*, 1997, **13**, 317.
- S7 O. Gonen and H. Levanon, *J. Chem. Phys.*, 1986, **84**, 4132.
- S8 B. Kirste, P. Tian, W. Kalisch and H. Kurreck, *J. Chem. Soc. Perkin Trans. 2*, 1995, 2147.
- S9 S. Ceola, L. Franco, M. Maggini and C. Corvaja, *Photochem. Photobiol. Sci.*, 2006, **5**, 1177.
- S10 G. Agostini, C. Corvaja and L. Pasimeni, *Chem. Phys.*, 1996, **202**, 349.
- S11 G. J. B. van den Berg, D. J. van den Heuvel, O. G. Poluektov, I. Holleman, G. Meijer and E. J. J. Groenen, *J. Magn. Reson.*, 1998, **131**, 39.
- S12 T. Miura and M. R. Wasielewski, *J. Am. Chem. Soc.*, 2011, **133**, 2844.
- S13 M. R. Wasielewski, G. L. Gaines, M. P. O'Neil, W. A. Svec and M. P. Niemczyk, *Mol. Cryst. Liq. Cryst.*, 1991, **194**, 201.
- S14 S.-H. Lee, A. G. Larsen, K. Ohkubo, Z.-L. Cai, J. R. Reimers, S. Fukuzumi and M. J. Crossley, *Chem. Sci.*, 2012, **3**, 257.
- S15 M. Di Valentin, A. Bisol, G. Agostini and D. Carbonera, *J. Chem. Inf. Model.*, 2005, **45**, 1580.
- S16 M. Di Valentin, A. Bisol, G. Agostini, P. A. Liddell, G. Kodis, A. L. Moore, T. A. Moore, D. Gust and D. Carbonera, *J. Phys. Chem. B*, 2005, **109**, 14401.